



UNIVERSIDADE FEDERAL FLUMINENSE
DEPARTAMENTO DE GEOLOGIA E FÍSICA
PROGRAMA DE PÓS-GRADUAÇÃO EM DINÂMICA DOS OCEANOS E DA
TERRA - DOT

LUTHIENE ALVES DALANHESE

SOUTH ATLANTIC STORM TRACK ANALYSIS USING BRAZILIAN NAVY
DATA AND ERA5

NITEROI

2021

LUTHIENE ALVES DALANHESE

**SOUTH ATLANTIC STORM TRACK ANALYSIS USING BRAZILIAN NAVY
DATA AND ERA5**

Tese apresentada ao programa de Pós-Graduação em Dinâmica dos Oceanos e da Terra da Universidade Federal Fluminense, como requisito parcial para obtenção do grau de Doutor em Ciências.

Área de concentração: Hidrografia.

ADVISOR: PROF. DR. RER. NAT. ANDRE LUIZ BELEM

CO-ADVISOR: PROF. DR. SHIH-YU SIMON WANG

NITEROI

2021

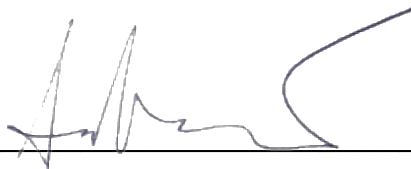
LUTHIENE ALVES DALANHESE

**SOUTH ATLANTIC STORM TRACK ANALYSIS USING BRAZILIAN NAVY
DATA AND ERA5**

Tese apresentada ao programa de Pós-Graduação em Dinâmica dos Oceanos e da Terra da Universidade Federal Fluminense, como requisito parcial para obtenção do grau de Doutor em Ciências.
Área de concentração: Hidrografia.

ADVISOR: PROF. DR.RER.NAT. ANDRE LUIZ BELEM
CO-ADVISOR: PROF. DR. SHIH-YU SIMON WANG

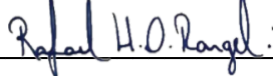
BANCA EXAMINADORA:



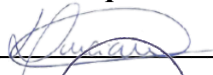
Dr. André Luiz Belém



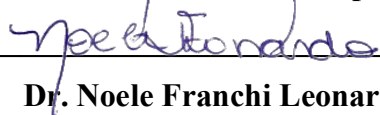
Dr. Shih Yu Simon Wang



Dr. Rafael Henrique Oliveira Rangel



Dr. Luciano Carvalho Rapagña



Dr. Noele Franchi Leonardo

NITEROI

2021

Ficha catalográfica automática - SDC/BIG
Gerada com informações fornecidas pelo autor

A474s Alves dalanhese, Luthiene
South Atlantic Storm Track Analysis Using Brazilian Navy
Data and Era5 / Luthiene Alves dalanhese ; Andre Luis Belem,
orientador ; Shih-Yu Simon Wang, coorientador. Niterói, 2021.
101 f.

Tese (doutorado)-Universidade Federal Fluminense, Niterói,
2021.

DOI: <http://dx.doi.org/10.22409/PPGDOT.2021.d.12150803798>

1. Ciclone Extratropical no Atlantico Sul. 2. Ciclone track.
3. Cartas Sinóticas. 4. Ciclone track no Atlantico Sul. 5.
Produção intelectual. I. Belem, Andre Luis, orientador. II.
Wang, Shih-Yu Simon, coorientador. III. Universidade Federal
Fluminense. Instituto de Geociências. IV. Título.

CDD -

I dedicate this work to Lauro Henrique Dalanhese and Isabelle Dalanhese de Almeida. They are my assurance of a love that lasts for eternity.

ACKNOWLEDGES

"Gratitude is a powerful catalyst for happiness. It's the spark that lights a fire of joy in your soul." – Amy Collette. I had that fire in my soul. And I'm grateful. I thank God for allowing me to fight for my dreams. Thanks to my friends and family. Thanks to Vitor for giving me the support to embark on this dream, full of sacrifices. I thank my mother Luzia and my father Lauro (in memorial) for being proud of me. I thank my brothers for accepting me as this ogress. Also, or grateful to many people who made my fight less lonely. But there are some special ones I would like to thank:

Andre, for having welcomed me in many moments over these six years. Thank you for not letting me freak out when I found out I was pregnant and helping me with my discovery process. Thank you to my old laboratory companies that became friends for life: Thais and Yaci. For all the cafes (and toddy), random roles, and dinners. Thank you, Yaci, for always being by my side (even telling me I'm wrong). I love you so much, even with our crazy time zones.

I would like to thank Luciano, Jaqueline, and Gabriel Rapagña, for being my family and having always been with me, even from another hemisphere.

Thank you, Natalia, for being by my side for so many years, for so many sacrifices. For being a wonderful sister and godmother.

Thanks to Gustavo and Andrea for being more than family. For loving me, loving my Isa that much. Thank you for changing my life.

And talking about changing my life: thanks, Simon. For welcoming me, giving me so much knowledge, patience, and all the laughs. I believe that saying thank you is not enough.

To my lab team: I love you all. You folks always make me feel welcome as a part of your team. You always had patience with my English and my questions. Especially to Jacob and Matthew for dedicating so much time working with me. Thank you so much! And I would like to thank the Climate Center folks for always finding time to explain dynamics, coding logic, places to eat, and parking tips. Thanks for making me feel welcome.

And in those four years, a world happened. A love more extraordinary than the world, losses that broke my heart, Isabelle who came to show me that there is a lot of love in me, and the certainty that love is never lost: no matter the time zone, no matter the distance, it transcends, even life. And I believe him. That's why I move on.

At last but not least: coffee. Without you, nothing would be.

ABSTRACT

Extratropical cyclones are weather phenomena with significant energy transfer between the surface (over the ocean or on land) and the atmosphere. Studies using cyclone tracks in the South Atlantic have proven more difficult, particularly in a localized context. By complementing a first-order observation record with a modern reanalysis dataset, this study reveals the general characteristics of cyclones that develop in the Lee regions of the Andes and those that develop near the Atlantic coast. The resulting comparative climatologies reveal that cyclone development in these separate contexts is driven by topography, local atmospheric circulations, and basin-scale climate oscillations. Through the analysis were noted an inter-decadal variation in the frequencies between lee and coast cyclogenesis, where lee cases seem to have an anticorrelated behavior compared to coastal cases, and cross-basin ocean temperature differences may trigger that behavior. The mechanism causing the lee and coastal cyclogenesis variations is discussed.

Keywords: EXTRATROPICAL CYCLONES, CYCLONE TRACK, SYNOPTIC CHARTS, SOUTH ATLANTIC CYCLONE TRACK, BRAZILIAN NAVY

RESUMO

Ciclones extratropicais são fenômenos climáticos com significativa transferência de energia entre a superfície (sobre o oceano ou na terra) e a atmosfera. Estudos usando rastreamento de ciclones no Atlântico Sul têm se mostrado mais difíceis, particularmente em um contexto localizado. Ao complementar o histórico de observações de primeira ordem com um conjunto de dados de reanálise moderno, este estudo revela as características gerais dos ciclones que se desenvolvem nas regiões a sotavento dos Andes e aqueles que se desenvolvem perto da costa do oceano Atlântico Sul. As climatologias comparativas resultantes revelam que o desenvolvimento de ciclones nesses contextos é impulsionado pela topografia, circulações atmosféricas locais e oscilações climáticas na escala na costa oceânica. Através da análise foi observada uma variação interdecadal nas frequências entre a ciclogênese a sotavento da montanha e litoral, onde os casos a sotavento da montanha parecem ter um comportamento anti correlacionado em comparação com os casos costeiros, e diferenças de temperatura oceânica entre as bacias oceanicas podem desencadear esse comportamento. O mecanismo que causa as variações da ciclogênese costeira e a sotavento é discutido.

Palavras-chave: CICLONES EXTRATROPICAIS, RASTREAMENTO DE CICLONES, CARTAS SINÓTICAS, RASTREAMENTO DE CICLONES DO ATLÂNTICO SUL, MARINHA DO BRASIL

LIST OF FIGURES

FIGURE 1: STUDY AREA LOCATED IN THE WESTERN SECTOR OF THE SOUTH ATLANTIC OCEAN AND THE ANALYZED AREA, HIGHLIGHTED IN BLACK DOTTED LINES. THE DIAGRAM BELOW SHOWS A MAP WITH THE PRESSURE DIFFERENTIAL AT MEDIUM SEA LEVEL USING DATA FROM ERA5 (COPERNICUS CLIMATE CHANGE SERVICE 2017), A SYNOPTIC CHART ISSUED BY THE BRAZILIAN NAVY, AND THE SATELLITE IMAGE USED BY EOSDIS WORLDVIEW (NASA 2020) FOR THE POSITION OF THE STUDY AREA. ALL IMAGES WERE GENERATED FOR JUNE 1, 2020.	8
FIGURE 2: SIMPLIFIED DIAGRAM OF THE GRAPHIC REPRESENTATION OF CURRENTS AND OCEAN CIRCULATION FOR THE WEST SECTOR OF THE SOUTH ATLANTIC, ADAPTED FROM PETERSON & STRAMMA (1991). THE SCHEME WAS STRUCTURED IN AN IMAGE THAT SHOWS THE VARIATION OF THE SEA SURFACE TEMPERATURE IN °C USING DATA FROM ERA5 AND CONSIDERING THE DAY 06/01/2020 AT 6 PM.	10
FIGURE 3: SCHEME PROPOSED BY BJERKNES IN 1919, DESIGNING THE DEVELOPMENT OF A CYCLONE FOR THE NORTHERN HEMISPHERE. SOURCE: BJERKNES (1919).	14
FIGURE 4: CONCEPTUAL MODELS OF THE LIFE CYCLE OF AN EXTRATROPICAL CYCLONE FOR THE SOUTHERN HEMISPHERE, WHERE THE SCHEME CLASSIFIED FROM “A” TO “E” WAS PROPOSED BY BJERKNES & SOLBERG IN 1922, WHILE THE SCHEME FROM “I” TO “IV” WAS PROPOSED BY SHAPIRO & KEYSER IN 1990. ADAPTED FROM BJERKNES & SOLBERG (1922) AND SHAPIRO & KEYSER (1990) BY THE AUTHOR.....	16
FIGURE 5: SYNOPTIC CHART REFERRING TO 1 JUNE 2020 AT MIDNIGHT, ISSUED BY THE BRAZILIAN NAVY AND OBTAINED ON THE HTTPS://WWW.MARINHA.MIL.BR/CHM/DADOS-DO-SMM-CARTAS-SINOTICAS/CARTAS-SINOTICAS (BRASIL 2020A) . LAST ACCESS: 18/07/2020.....	21
FIGURE 6: SYMBOLOGY USED IN THE SYNOPTIC CHARTS ELABORATED BY THE BRAZILIAN NAVY.....	22
FIGURE 7: INTERFACE OF THE TRACKING SCRIPT USING GRADS.....	24
FIGURE 8: GENESIS LOCATIONS (SHOWN IN BLACK DOTS) OF LEE CYCLONES AND STORM TRACKS FROM ERA5 REANALYSIS FOR ALL CYCLONES INCLUDED IN THIS STUDY FOR ANNUAL ANALYSIS.	29
FIGURE 9: GENESIS LOCATIONS (SHOWN IN BLACK DOTS) OF LEE CYCLONES AND STORM TRACKS FROM THE BRAZILIAN NAVY FOR ALL CYCLONES INCLUDED IN THIS STUDY FOR ANNUAL ANALYSIS.....	29
FIGURE 10: GENESIS LOCATIONS (SHOWN IN BLACK DOTS) OF COASTAL EXTRATROPICAL CYCLONES AND STORM TRACKS FROM ERA5 REANALYSIS FOR ALL CYCLONES INCLUDED IN THIS STUDY FOR ANNUAL ANALYSIS.	30
FIGURE 11: GENESIS LOCATIONS (SHOWN IN BLACK DOTS) OF COASTAL EXTRATROPICAL CYCLONES AND STORM TRACKS FROM THE BRAZILIAN NAVY FOR ALL CYCLONES INCLUDED IN THIS STUDY FOR ANNUAL ANALYSIS... ..	30
FIGURE 12: GENESIS LOCATIONS (SHOWN IN BLACK DOTS) OF LEE CYCLONES AND STORM TRACKS FROM ERA5 REANALYSIS FOR ALL CYCLONES INCLUDED IN THIS STUDY FOR WARM PERIOD ANALYSIS.....	31
FIGURE 13: GENESIS LOCATIONS (SHOWN IN BLACK DOTS) OF LEE CYCLONES AND STORM TRACKS FROM BRAZILIAN NAVY REANALYSIS FOR ALL CYCLONES INCLUDED IN THIS STUDY FOR WARM PERIOD ANALYSIS.	32
FIGURE 14: GENESIS LOCATIONS (SHOWN IN BLACK DOTS) OF COASTAL EXTRATROPICAL CYCLONES AND STORM TRACKS FROM ERA5 REANALYSIS FOR ALL CYCLONES INCLUDED IN THIS STUDY FOR WARM PERIOD ANALYSIS.	33

FIGURE 15: GENESIS LOCATIONS (SHOWN IN BLACK DOTS) OF COASTAL EXTRATROPICAL CYCLONES AND STORM TRACKS FROM THE BRAZILIAN NAVY FOR ALL CYCLONES INCLUDED IN THIS STUDY FOR WARM PERIOD ANALYSIS.....	33
FIGURE 16: GENESIS LOCATIONS (SHOWN IN BLACK DOTS) OF LEE CYCLONES AND STORM TRACKS FROM ERA5 REANALYSIS FOR ALL CYCLONES INCLUDED IN THIS STUDY FOR COLD PERIOD ANALYSIS.....	34
FIGURE 17: GENESIS LOCATIONS (SHOWN IN BLACK DOTS) OF LEE CYCLONES AND STORM TRACKS FROM BRAZILIAN NAVY REANALYSIS FOR ALL CYCLONES INCLUDED IN THIS STUDY FOR COLD PERIOD ANALYSIS.	35
FIGURE 18: GENESIS LOCATIONS (SHOWN IN BLACK DOTS) OF COASTAL EXTRATROPICAL CYCLONES AND STORM TRACKS FROM ERA5 REANALYSIS FOR ALL CYCLONES INCLUDED IN THIS STUDY FOR COLD PERIOD ANALYSIS.	35
FIGURE 19: GENESIS LOCATIONS (SHOWN IN BLACK DOTS) OF COASTAL EXTRATROPICAL CYCLONES AND STORM TRACKS FOR THE BRAZILIAN NAVY FOR ALL CYCLONES INCLUDED IN THIS STUDY FOR COLD PERIOD ANALYSIS.	36
FIGURE 20: NUMBERS OF GENESIS EVENTS FOR LEE (A, B) AND COASTAL (C, D) EXTRATROPICAL CYCLONES ALONG WITH STORM TRACKS FOR ERA5 REANALYSIS (A, C) AND FROM THE BRAZILIAN NAVY (B, D) FOR ALL SEASONS, INCLUDING WARM AND COLD PERIOD, AND ANNUAL TOTAL.....	37
FIGURE 21: DISPLACEMENT SPEEDS FOR LEE (A, B) AND COASTAL (C, D) CYCLONES, CALCULATED BY THE DIFFERENCE BETWEEN THE LOCATION OF GENESIS AND THE POSITION OF THE CYCLONE TWELVE HOURS LATER. DISPLACEMENT SPEEDS FOR ERA5 CYCLONES (3A, C) ARE SHOWN IN RELATION TO BRAZIL FOR THE ANNUAL PERIOD.	38
FIGURE 22: DISPLACEMENT SPEEDS FOR LEE (A, B) AND COASTAL (C, D) CYCLONES, CALCULATED BY THE DIFFERENCE BETWEEN THE LOCATION OF GENESIS AND THE POSITION OF THE CYCLONE TWELVE HOURS LATER. DISPLACEMENT SPEEDS FOR ERA5 CYCLONES (3A, C) ARE SHOWN IN RELATION TO BRAZIL FOR NOVEMBER THROUGH MARCH.....	39
FIGURE 23: DISPLACEMENT SPEEDS FOR LEE (A, B) AND COASTAL (C, D) CYCLONES, CALCULATED BY THE DIFFERENCE BETWEEN THE LOCATION OF GENESIS AND THE POSITION OF THE CYCLONE TWELVE HOURS LATER. DISPLACEMENT SPEEDS FOR ERA5 CYCLONES (3A, C) ARE SHOWN IN RELATION TO BRAZIL FOR MAY THROUGH SEPTEMBER.....	40
FIGURE 24: ANNUAL FREQUENCY OF ECs FOR LEE (A), COASTAL NORTH (B), COASTAL CENTRAL (C), AND COASTAL SOUTH (D) CYCLOGENESIS FOR THE ANNUAL PERIOD USING ERA5 DATA (BLUE LINE) AND MB (RED LINE). Y LABELS SHOW CYCLONE GENESIS NUMBERS FOR BOTH DATASETS.....	42
FIGURE 25: ANNUAL FREQUENCY OF ECs FOR LEE (A), COASTAL NORTH (B), COASTAL CENTRAL (C), AND COASTAL SOUTH (D) CYCLOGENESIS FOR NOVEMBER TO MARCH, USING ERA5 DATA (BLUE LINE) AND MB (RED LINE). Y LABELS SHOW CYCLONE GENESIS NUMBERS FOR BOTH DATASETS.....	44
FIGURE 26: ANNUAL FREQUENCY OF ECs FOR LEE (A), COASTAL NORTH (B), COASTAL CENTRAL (C), AND COASTAL SOUTH (D) CYCLOGENESIS FOR MAY TO SEPTEMBER, USING ERA5 DATA (BLUE LINE) AND MB (RED LINE). Y LABELS SHOW CYCLONE GENESIS NUMBERS FOR BOTH DATASETS.....	45
FIGURE 27: ANNUAL, WARM, AND COLD PERIODS OF FREQUENCY OF ECs FOR LEE (RED LINE) AND COASTAL (BLUE LINE) CYCLOGENESIS. Y LABELS SHOW CYCLONE GENESIS NUMBERS FOR BOTH AREAS.	47

FIGURE 28: ANNUAL COMPOSITE STREAM FUNCTION ANOMALIES (CONTOURS) AND SST ANOMALIES (SHADING) FOR YEARS WITH HIGH FREQUENCIES OF LEE CYCLOGENESIS. POSITIVE (NEGATIVE) STREAM FUNCTION VALUES IN THE SOUTHERN HEMISPHERE INDICATE A CYCLONIC (ANTI-CYCLONIC) ANOMALY OR A LOW (HIGH) PRESSURE AREA.	48
FIGURE 29: ANNUAL COMPOSITE STREAM FUNCTION ANOMALIES (CONTOURS) AND SST ANOMALIES (SHADING) FOR YEARS WITH LOW FREQUENCIES OF LEE CYCLOGENESIS. POSITIVE (NEGATIVE) STREAM FUNCTION VALUES IN THE SOUTHERN HEMISPHERE INDICATE A CYCLONIC (ANTI-CYCLONIC) ANOMALY OR A LOW (HIGH) PRESSURE AREA.	49
FIGURE 30: ANNUAL COMPOSITE STREAM FUNCTION ANOMALIES (CONTOURS) AND SST ANOMALIES (SHADING) FOR YEARS WITH HIGH FREQUENCIES OF COASTAL CYCLOGENESIS. POSITIVE (NEGATIVE) STREAM FUNCTION VALUES IN THE SOUTHERN HEMISPHERE INDICATE A CYCLONIC (ANTI-CYCLONIC) ANOMALY OR A LOW (HIGH) PRESSURE AREA.	49
FIGURE 31: ANNUAL COMPOSITE STREAM FUNCTION ANOMALIES (CONTOURS) AND SST ANOMALIES (SHADING) FOR YEARS WITH LOW FREQUENCIES OF COASTAL CYCLOGENESIS. POSITIVE (NEGATIVE) STREAM FUNCTION VALUES IN THE SOUTHERN HEMISPHERE INDICATE A CYCLONIC (ANTI-CYCLONIC) ANOMALY OR A LOW (HIGH) PRESSURE AREA.	50
FIGURE 32: NOVEMBER TO MARCH COMPOSITE STREAM FUNCTION ANOMALIES (CONTOURS) AND SST ANOMALIES (SHADING) FOR YEARS WITH HIGH FREQUENCIES OF LEE CYCLOGENESIS. POSITIVE (NEGATIVE) STREAM FUNCTION VALUES IN THE SOUTHERN HEMISPHERE INDICATE A CYCLONIC (ANTI-CYCLONIC) ANOMALY OR A LOW (HIGH) PRESSURE AREA.	51
FIGURE 33: NOVEMBER TO MARCH COMPOSITE STREAM FUNCTION ANOMALIES (CONTOURS) AND SST ANOMALIES (SHADING) FOR YEARS WITH LOW FREQUENCIES OF LEE CYCLOGENESIS. POSITIVE (NEGATIVE) STREAM FUNCTION VALUES IN THE SOUTHERN HEMISPHERE INDICATE A CYCLONIC (ANTI-CYCLONIC) ANOMALY OR A LOW (HIGH) PRESSURE AREA.	52
FIGURE 34: NOVEMBER TO MARCH COMPOSITE STREAM FUNCTION ANOMALIES (CONTOURS) AND SST ANOMALIES (SHADING) FOR YEARS WITH HIGH FREQUENCIES OF COASTAL CYCLOGENESIS. POSITIVE (NEGATIVE) STREAM FUNCTION VALUES IN THE SOUTHERN HEMISPHERE INDICATE A CYCLONIC (ANTI-CYCLONIC) ANOMALY OR A LOW (HIGH) PRESSURE AREA.	52
FIGURE 35: NOVEMBER TO MARCH COMPOSITE STREAM FUNCTION ANOMALIES (CONTOURS) AND SST ANOMALIES (SHADING) FOR YEARS WITH LOW FREQUENCIES OF COASTAL CYCLOGENESIS. POSITIVE (NEGATIVE) STREAM FUNCTION VALUES IN THE SOUTHERN HEMISPHERE INDICATE A CYCLONIC (ANTI-CYCLONIC) ANOMALY OR A LOW (HIGH) PRESSURE AREA.	53
FIGURE 36: MAY TO SEPTEMBER COMPOSITE STREAM FUNCTION ANOMALIES (CONTOURS) AND SST ANOMALIES (SHADING) FOR YEARS WITH HIGH FREQUENCIES OF LEE CYCLOGENESIS. POSITIVE (NEGATIVE) STREAM FUNCTION VALUES IN THE SOUTHERN HEMISPHERE INDICATE A CYCLONIC (ANTI-CYCLONIC) ANOMALY OR A LOW (HIGH) PRESSURE AREA.	53
FIGURE 37: MAY TO SEPTEMBER COMPOSITE STREAM FUNCTION ANOMALIES (CONTOURS) AND SST ANOMALIES (SHADING) FOR YEARS WITH LOW FREQUENCIES OF LEE CYCLOGENESIS. POSITIVE (NEGATIVE) STREAM FUNCTION VALUES IN THE SOUTHERN HEMISPHERE INDICATE A CYCLONIC (ANTI-CYCLONIC) ANOMALY OR A LOW (HIGH) PRESSURE AREA.	54

FIGURE 38: MAY TO SEPTEMBER COMPOSITE STREAM FUNCTION ANOMALIES (CONTOURS) AND SST ANOMALIES (SHADING) FOR YEARS WITH HIGH FREQUENCIES OF COASTAL CYCLOGENESIS. POSITIVE (NEGATIVE) STREAM FUNCTION VALUES IN THE SOUTHERN HEMISPHERE INDICATE A CYCLONIC (ANTI-CYCLONIC) ANOMALY OR A LOW (HIGH) PRESSURE AREA.....	54
FIGURE 39: MAY TO SEPTEMBER COMPOSITE STREAM FUNCTION ANOMALIES (CONTOURS) AND SST ANOMALIES (SHADING) FOR YEARS WITH LOW FREQUENCIES OF COASTAL CYCLOGENESIS. POSITIVE (NEGATIVE) STREAM FUNCTION VALUES IN THE SOUTHERN HEMISPHERE INDICATE A CYCLONIC (ANTI-CYCLONIC) ANOMALY OR A LOW (HIGH) PRESSURE AREA.....	55
FIGURE 40: ANNUAL ANALYSIS FOR LEE CASES USING VORTICITY ADVECTION AVERAGED FOR THE UPPER TROPOSPHERE (500 hPa) ACROSS 50°S 20°S WITH 500 hPa WIND VECTORS.....	56
FIGURE 41: VORTEX STRETCHING ANALYSIS FOR THE LOWER TROPOSPHERE FROM 850–500 hPa ACROSS 50°S 20°S AND WITH 850 hPa WIND VECTORS FOR LEE CASES CONSIDERING ANNUAL ANALYSIS.....	57
FIGURE 42: ANNUAL ANALYSIS FOR COASTAL CASES USING VORTICITY ADVECTION AVERAGED FOR THE UPPER TROPOSPHERE (500 hPa) ACROSS 55°S 25°S WITH 500 hPa WIND VECTORS.....	58
FIGURE 43: VORTEX STRETCHING ANALYSIS FOR THE LOWER TROPOSPHERE FROM 1000–850 hPa ACROSS 55°S 25°S AND WITH 850 hPa WIND VECTORS FOR COASTAL CASES CONSIDERING ANNUAL ANALYSIS.....	59
FIGURE 44: WARM PERIOD ANALYSIS FOR LEE CASES USING VORTICITY ADVECTION AVERAGED FOR THE UPPER TROPOSPHERE (500 hPa) ACROSS 50°S 20°S WITH 500 hPa WIND VECTORS.....	60
FIGURE 45: VORTEX STRETCHING ANALYSIS FOR THE LOWER TROPOSPHERE FROM 850–500 hPa ACROSS 50°S 20°S AND WITH 850 hPa WIND VECTORS FOR LEE CASES CONSIDERING WARM PERIOD ANALYSIS.....	61
FIGURE 46: WARM PERIOD ANALYSIS FOR COASTAL CASES USING VORTICITY ADVECTION AVERAGED FOR THE UPPER TROPOSPHERE (500 hPa) ACROSS 55°S 25°S WITH 500 hPa WIND VECTORS.....	62
FIGURE 47: VORTEX STRETCHING ANALYSIS FOR THE LOWER TROPOSPHERE FROM 1000–850 hPa ACROSS 55°S 25°S AND WITH 850 hPa WIND VECTORS FOR COASTAL CASES CONSIDERING WARM PERIOD ANALYSIS.	63
FIGURE 48: COLD PERIOD ANALYSIS FOR LEE CASES USING VORTICITY ADVECTION AVERAGED FOR THE UPPER TROPOSPHERE (500 hPa) ACROSS 50°S 20°S WITH 500 hPa WIND VECTORS.....	64
FIGURE 49: VORTEX STRETCHING ANALYSIS FOR THE LOWER TROPOSPHERE FROM 850–500 hPa ACROSS 50°S 20°S AND WITH 850 hPa WIND VECTORS FOR LEE CASES CONSIDERING COLD PERIOD ANALYSIS	65
FIGURE 50: COLD PERIOD ANALYSIS FOR COASTAL CASES USING VORTICITY ADVECTION AVERAGED FOR THE UPPER TROPOSPHERE (500 hPa) ACROSS 55°S 25°S WITH 500 hPa WIND VECTORS.....	66
FIGURE 51: VORTEX STRETCHING ANALYSIS FOR THE LOWER TROPOSPHERE FROM 1000–850 hPa ACROSS 55°S 25°S AND WITH 850 hPa WIND VECTORS FOR COASTAL CASES CONSIDERING COLD PERIOD ANALYSIS.....	67

LIST OF TABLES

TABLE 1: COLLECTED INFORMATION TO BUILD THE TRACKING DATASET.	25
TABLE 2: YEARS INCLUDED IN THE COMPOSITE ANALYSIS FOR DIFFERENT REGIONS AND TYPES OF CYCLOGENESES. AN UP-FACING ARROW IN THE 1ST COLUMN INDICATES YEARS WITH HIGHER NUMBERS OF ECs, WHILE A DOWN-FACING ARROW INDICATES YEARS WITH LOWER NUMBERS OF ECs.	26

LIST OF EQUATIONS

(EQUATION 1).....	15
(EQUATION 2).....	27
(EQUATION 3).....	27
(EQUATION 4).....	28
(EQUATION 5).....	28

LIST OF ACRONYMS

AS - South Atlantic

BC – Brazil Current

BMC - Brazil-Malvinas Confluence

CHM - Centro de Hidrografia da Marinha (Brazilian Navy Hydrographic Center)

CSE - South Equatorial Current

CS3 - Copernicus Climate Change Service

CPTEC - Centro de Previsão de Tempo e Estudos Climáticos (Brazilian Center for Weather Forecasting and Climate Studies)

EC's – Extratropical Cyclone

ECMWF – European Centre for Medium-Range Weather Forecasts

ERA5 - European Centre for Medium-Range Weather Forecasts Reanalysis v5

INPE - Instituto Nacional de Pesquisas Espaciais (Brazilian National Institute for Space Research)

ITCZ - Intertropical Convergence Zone

MB – Marinha do Brasil (Brazilian Navy)

MC – Malvinas Current

MJJAS – May, June, July, August, September

NDJFM – November, December, January, February, March

NHC – National Hurricane Center

NOAA - National Oceanic & Atmospheric Administration (NOAA)

SAA – South Atlantic Anticyclone

SACZ - South Atlantic Convergence Zone

SST – Sea Surface Temperature

UTCV – Upper Tropospheric Cyclonic Vortex

TABLE OF CONTENTS

1. INTRODUCTION.....	1
1.1 PROBLEM CHARACTERIZATION.....	1
1.2 MONITORING SYSTEMS	2
1.3 RISK ASSESSMENT FOR EXTREME CLIMATIC EVENTS	5
1.4 PURPOSE.....	7
2 METHODS AND MATERIALS.....	7
2.1 AREA	7
2.2 OCEANOGRAPHIC AND ATMOSPHERIC CHARACTERISTICS.....	9
2.3 CYCLONES	12
2.3.1 EXTRATROPICAL CYCLONES	13
2.3.2 SUBTROPICAL OR HYBRID CYCLONES.....	18
2.3.3 CYCLOGENESIS AND ASSOCIATED FACTORS	18
2.4 DATA ACQUISITION AND PROCESSING	20
2.4.1 BRAZILIAN NAVY DATA.....	20
2.4.2 ERA5	23
2.5 CATEGORIZATION OF CYCLOGENESIS.....	25
2.6 CYCLOGENESIS MECHANISMS.....	27
3 RESULTS.....	28
3.1 GENERAL CLIMATOLOGY OF SOUTH AMERICA-BORN CYCLONES	28
3.2 CIRCULATION FEATURES ASSOCIATED WITH LEE AND COASTAL CYCLONES 46	
3.3 MECHANISMS DRIVING THE LEE AND COASTAL CYCLOGENESIS VARIATIONS	55
4 DISCUSSION AND CONCLUSIONS	67
REFERENCES.....	70

1. INTRODUCTION

1.1 PROBLEM CHARACTERIZATION

Both the understanding and assessment of the path traveled by a cyclone, which is referred to here as cyclone tracks, has become a usual tool when it comes to analyzing meteorological data due to the deleterious effects that cyclones may cause not only on the human population but also the economy. A cyclone track may create storm propagation areas, as well intense rainfall, thus influencing areas that generate strong winds over the ocean and wave formation, which can result in waves or even storm tides on the coast. On the other hand, anticyclone tracks act directly in situations of atmospheric blockages resulting in changes in the rain regime and drought periods (Rodrigues and Woollings, 2017). Changes in these tracks caused by extreme climatic phenomena have a great influence on regional climate (Blender & Schubert, 2000; Pezza & Ambrizzi, 2000).

South America's climatic regime is intertwined with the interactions between air mass from different properties and its movement. During the Winter season, cold air masses tend to become stronger in higher latitudes due to the decrease in incident solar radiation. Together with atmospheric circulation at medium and high levels, cold air masses may move or not to low latitudes, and these influence the occurrence of adverse weather conditions, such as excessive snow, rain, and south wind (Blender & Schubert, 2000; Fortune & Kousky, 1983; Kousky, 1979).

Fortune & Kousky (1983) and Pezza & Ambrizzi (2000) listed cyclonic behavior and its effects in different regions of Brazil, generally correlating them with precipitation and damage rates on the country's agrarian economy. However, production and transportation of mineral resources, exploitation of fishing resources, as well as tourism are also activities that were affected by adverse conditions. It is crucial to carry out studies related to the adverse climatic conditions and the potential damages to the South American continent. Synoptic analysis such as those of Gan & Rao (1999), Innocentini & Caetano Neto (1996), Reboita et al. (2009), Pianca et al. (2010), and Fuentes et al. (2013), list cyclonic tracks in Brazil with effects on ocean waves but are usually focused on specific events or even in strict areas of the coast.

In addition to the state of the sea, cyclogenesis in the South Atlantic promotes a strong influence on the flow of precipitation on the South American continent, where cyclonic circulation associated with fronts and anticyclonic is the result of the exchange of ocean/atmosphere energy and thus modulate the climate regime on land. Situations of heavy rain (Bernardino et al., 2018; Carvalho et al., 2002; Nielsen et al., 2016) or atmospheric blockages (Pezza & Simmonds, 2005; Pinto et al., 2013; Rodrigues & Woollings, 2017; Sinclair, 1996a; Woollings et al., 2018) are influenced not only by cyclonic circulation but also by a variety of factors associated with it.

Caetano Neto et al. (1996) and Candella (1997) point out in their works that the assessment of climatic interactions in extreme cases is paramount so that we can have a better understanding of events regarding them, and especially when there is loss of life and/or heritage.

1.2 MONITORING SYSTEMS

The general atmospheric circulation is used to determine a basic status of reference of the atmospheric status, therefore being the result of the relationship between mass conservation, pressure forces, and surface thrust, analyzed by means of a rotating reference. Atmospheric observations include *in situ* analysis, which is estimated by satellites, of atmospheric variables such as wind's speed, pressure, temperature, and humidity. However, there is no observation system that can provide said atmospheric variables with the same spatial and temporal coverage (satellite data has 375 to 750 m of resolution). Due to low spatial coverage observations, numerical models are a rather good alternative for the assessment of future behavior (and past) of the dynamics regarding ocean/atmosphere interactions. Andreoli et al. (2008) affirm in their analysis that, whenever there is a consistent set of observations *in situ*, it reflects positively on the quality of the analysis fields and modeled predictions.

The description regarding rotational movements of winds and storms is dated as of 1835 (Redfield, 1841). Bjerknes (1919) described the formation of cyclones whilst in movement, and afterward, Bjerknes and Solberg (1922) described their cycle and structure. McDonald (1935) has described the life cycle of a hurricane in chronological

order, thus collecting information that subsequently was used to predict their behavior and destructive impacts.

Boffi (1949) argued the influence of the Andes Mountains in the atmospheric circulation to the Southern Hemisphere by means of synoptic charts to do so. Afterward, Taljaard (1967) described the frequency and the atmospheric behavior, as well as the preferable route of cyclones and anticyclones also based upon synoptic charts. Until the 1970's, there was little spatial coverage for oceans in the Southern Hemisphere; however, at this time, a digital collection was created. With the evolution of satellite images, broader spatial coverage could be achieved, and statistical analysis of cyclone behavior began to take shape (Troup and Streten, 1972). Such studies originated from the need of understanding cyclonic behavior and were (and are) paramount for the analysis and planning to reduce disasters arising from the passage of such systems (Farber, 1987; Minor, 1983; Morss et al., 2005).

The evolution of climatic analysis and the search to predict cyclonic behavior has progressed in a relatively accelerated way; the broad development of numerical models and statistical schemes has become an essential tool in the understanding of cyclonic behavior for the Southern Hemisphere, as can be seen in the scheme proposed by Murray and Simmonds (1991). The scheme proposed by them involved a comparison of pressures with neighboring points, where the calculation of a minimum means pressure value around the analyzed center allowed to neglect weaker systems, thus guaranteeing the analysis of cyclonic vorticity. However, such a scheme did not present a good response to the South Atlantic because it would not efficiently identify low-pressure systems that originated in the South American continent.

Sinclair (1994) presented a climatology for cyclones in the Southern Hemisphere, adapting automatic schemes such as those of de Murray and Simmonds (1991b) and analyzing not only the minimum internal and external pressure but also the geostrophic vorticity. Hoskins and Hodges (2005) used vorticity, mean pressure at sea level, geopotential height, and surface temperature to adapt the scheme proposed by Hodges (1999, 1995) to the Southern Hemisphere. As far back as 2009, Ulbrich et al. bought 14 models and concluded that some results differ among themselves, even though it used the same set of data, that is due to the variety of approaches, which varies between identification and intensity tracking methods. That is, depending on the perspective and physical parameters that are being used in the analysis, the results may differ among

themselves.

Reboita et al. (2010b) used a model that carried out the analysis in regional scales, adapting the scheme proposed by Sinclair and getting satisfactory results when it came to identifying cyclones. Despite automatic schemes to track cyclones and anticyclones (e.g., Simmonds et al., 2012; Sinclair, 1996b, 1994b; Sinclair et al., 1997) are widely used, such models have shown great uncertainty for pressure values that ranged from 1010 and 1020 hPa, where, in some cases, some models could not differentiate between centers of high or low pressure (Pezza and Ambrizzi, 2003a).

Lionello et al. (2016) compared 14 cyclonic tracking methods for the Mediterranean region, and in such comparison, the schemes devised by Murray and Simmonds (1991) and Sinclair (1994) were included. The results achieved by Lionello et al. (2016) were assertive in relation to the computed position of the system and pressure differential. However, they differed in relation to “weak” and “slow” cyclones, underestimating the totality of events that occur in the Southern Hemisphere, reinforcing the need for care when carrying out the analyzes. Another relevant factor is the spatial resolution of the data used because the higher the resolution, the greater the precision and quality of the analysis.

Gramscianinov et al. (2019) used in their analysis two different reanalysis data applied to the scheme proposed by Hodges (1995) identifying the cyclones using relative vorticity. Like Gramscianinov, (Crespo et al., 2021) reinforce in their analysis the basic climatology related to cyclogenesis in the South Atlantic, identifying as main cyclogenetic regions the southeast and south coastal regions of the continent.

The identification and understanding of cyclones over time are necessary to identify a trend and the influence of climate modulators in their behavior. Cavallo and Noy (2009) published a survey relating the main causes of natural disasters (including the passage of cyclones/hurricanes) to indirect short and long-term impacts on the economy, highlighting the approach addressed by Minor (1983), Farber (1987), and Yuan et al. (2020) and many others: the knowledge about the behavior and demand of extreme events are necessary to prepare for the possible impacts, in addition to reducing the risk of disasters.

1.3 RISK ASSESSMENT FOR EXTREME CLIMATIC EVENTS

Upon analyzing the people's vulnerability in relation to natural disasters, there shall be prioritized efforts to better up the early alerts of extreme weather events (Marengo, 2009). The need for climatic studies, in addition to assessment, monitoring, classification, and forecast of weather adverse conditions, are closely connected to deleterious effects on the people, financial losses, and loss of human lives.

The *National Hurricane Center (NHC)*, a program that is part of the National Oceanic & Atmospheric Administration (NOAA), has created a database¹ with information dated as of 1872, summarizing news and development of analysis regarding the most important events related to tropical cyclones in the United States of America. McDonald (1935), for instance, describes the passage of a hurricane through Florida (USA), its development and intensification, in addition to describing the trail of destruction and losses left not only by its passage but also by the side effects to it. It is worth mentioning that tropical cyclones are more intense and have more diversified characteristics when compared to extratropical cyclones; however, the potentially destructive effect of the latter should not be underestimated (Reboita et al., 2018).

Studies on extreme events are more frequent for regions such as the Northern Hemisphere or Asia, where related effects to it happening is more impactful, destructive, noticeable, and possibly harmful, due to impacts related to loss of life (Frank & Husain, 1971; Rappaport, 2000), in addition to financial impacts (Cinco et al., 2016; Esteban et al., 2010; Irish & Resio, 2010). Mayhorn & McLaughlin (2014) reinforce in their research that the understanding, as well as communication of the risks associated with extreme events, do help to prevent unnecessary damages and losses.

Developing country populations and lower socioeconomic classes are more susceptible to financial impacts after a period/event of extreme events Heinen et al. (2019). And for there to be the identification and application of efficient risk recovery/reduction solutions, it is necessary to invest more in studies that assess impacts resulting from extreme events (Sahani et al., 2019).

In Brazil, cyclones of great intensity are not usual; thus, the attention and

¹NHC - *National Hurricane Center: Monthly Weather Review - Annual Summaries of North Atlantic Storms, 1872-2011* <<https://www.aoml.noaa.gov/general/lib/lib1/nhclib/mwreviews/mwreviews.html>>.

prevention that such events get are not the same as in other countries/continents (McTaggart-Cowan et al., 2006; Pezzi et al., 2016); however, this does mean that such passages do not result in negative impacts (Catto et al., 2019; Pezza a& Simmonds, 2005).

According to WMO (2012), the identification of these events is essential so that effective strategies for risk management can be developed. For this to happen, historical and real-time observations must be available, that is, in addition to information on vulnerability and exposure (Resio and Irish, 2015), past events, and modeling of future conditions. Irish & Resio (2010) state that to assess the impacts caused by a cyclone, a study of the history of events and their effects must be carried out.

It is worth considering that an alert system for the risk of extreme climatic events (intense winds, storm surge, heavy rain, hail, flood, drought, etc.) is an interdisciplinary system, which involves the care with past information, with the language used with the population and with their perception of the risks associated with the events (Morrow et al., 2015; Morss et al., 2008, 2005; Ramón-Valencia et al., 2019).

The magnitude of a disaster is not only dependent on the intensity of an extreme event but also on the effectiveness of mitigating actions. The occurrence of such events may not be prevented, but its impact on the community can be reduced should accurate information be provided to the people in a timely manner (Doong et al., 2012). The evolution in the warning system is directly connected to the reduction in death and damages. However, these warnings must be associated with continuous monitoring, risks analysis, dissemination, and communication to avoid false alarms (Rogers & Tsirkunov, 2010).

In addition to improved communication of events, alert systems, and information that gets to the population, the evolution of climatic monitoring systems has been widely encouraged (Morrow et al., 2015). Morss et al. (2017) highlight that, when well disseminated, such information helps the population in their process of recognizing extreme events and their associated risks, as well as the guide in protective actions.

Climate monitoring in Brazil is carried out by different centers, such as: o Centro de Previsão de Tempo e Estudos Climáticos (CPTEC) (*Brazilian Center for Weather Forecasting and Climate Studies*), which is part of the Instituto Nacional de Pesquisas Espaciais (INPE) (*Brazilian National Institute for Space Research*), and the Centro de Hidrografia da Marinha (CHM) (*Brazilian Navy Hydrographic Center*), of the Marinha

do Brasil (MB) (*Brazilian Navy*). The latter is responsible for monitoring sea and weather conditions and for the dissemination of warnings for such conditions. Despite issued warnings being more directed to the country's shoreline, the MB publishes synoptic charts highlighting cyclones, anticyclones, and any instability in the atmosphere that may affect the country.

1.4 PURPOSE

This study has as its main purpose to analyze the preferred track of cyclones that act on the South Atlantic, considering the difficulty that automatic tracking systems show when it comes to rapidly detect fast and small cyclones.

Specifically, this study aims to perform a statistical analysis of cyclonic events for the South Atlantic using reanalysis data, in addition to synoptic charts issued by the MB, seeking to identify cyclogenetic regions and understand cyclonic genesis behavior over time. To do this, we seek:

- identify cyclonic events that occurred between the period 1979 and 2020.
- recognize similarities between the used datasets.
- point out the preferred area of cyclogenesis of these events.
- distinguish seasonal behavior related to the genesis of such systems.
- distinguish the differences between cyclogenetic areas as an order of time.
- discern the climatic influences on the genesis of such systems

2 METHODS AND MATERIALS

2.1 AREA

This present study was carried out for the South Atlantic region (SA) (Figure 1). Specifically, the chosen area is between the coordinates 10°S and 45°S latitude and 0°W to 90°W longitude since a greater number of transient and semi-stationary cyclones may come to be observed directly interfere in the climatology of Brazil.

It is a wide region that has distinct climatological characteristics and a vast ocean area, which influences the genesis, maintenance, and cyclolysis (or lysis) of cyclones and anticyclones. This region is influenced by the Intertropical Convergence Zone (equatorial region), the Upper Subtropical and polar regions, in addition to the Northwestern Argentinean Low and the Chaco Low (Boffi, 1949; Dereczynski & Menezes, 2015; Kousky & Gan, 1981; Ribeiro et al., 2016). The South American continent has an orography that favors the presence of Low-Level Jets, which influence both the cyclogenesis (Gozzo et al., 2014) and the precipitation regime (Liebmann et al., 2004).

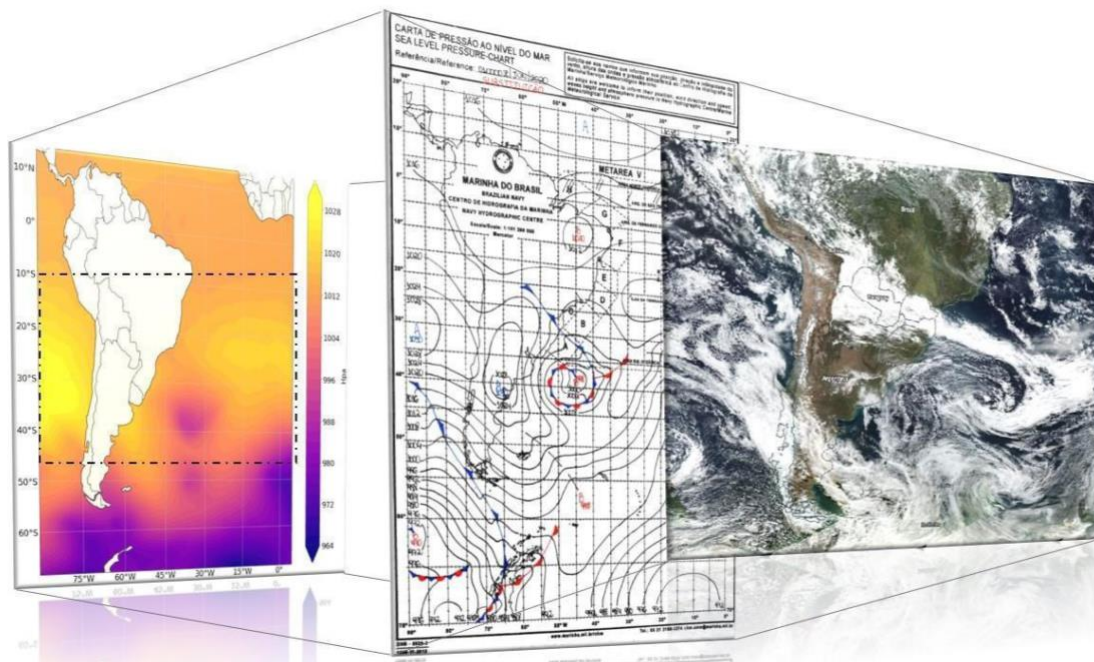


Figure 1: Study area located in the western sector of the South Atlantic Ocean and the analyzed area, highlighted in black dotted lines. The diagram below shows a map with the pressure differential at medium sea level using data from ERA5 (Copernicus Climate Change Service 2017), a synoptic chart issued by the Brazilian Navy, and the satellite image used by EOSDIS Worldview (NASA 2020) for the position of the study area. All images were generated for June 1, 2020.

South America has particularities that make it unique, where a large part of the cyclones formed in its region occurs in a terrestrial environment. Even though the east face of Brazil is “facing” the sea, the western part of the country has a border with the Argentine Northwest, the North of the Paraguay-Bolivian Chaco, and the east of the Andes, which due to its orographic formation presents a vast area prone to low-pressure zones. The South Pacific Anticyclone influences this area. Due to its orography and

proximity to the Andes, it has a higher incidence of transient systems, more evident during the southern summer (Falco et al., 2019; Seluchi & Garreaud, 2012; Seluchi & Saulo, 2012).

Gan & Rao (1994), in their studies, demonstrate the influence of the topography in the mountain range in the pressure field, where the wave flow coming from the Pacific, when “meeting” the mountains, has an anticyclonic behavior at the top due to the geopotential height and temperature, and when descending to the continent, the movement tends to be cyclonic due to the heating of the atmospheric column. Later, Gan & Rao (1996), using synoptic charts, determined that the topography has a favorable effect on cyclogenesis during Spring and Winter if it happens to the leeward of the mountain.

2.2 OCEANOGRAPHIC AND ATMOSPHERIC CHARACTERISTICS

The ocean acts as a climate regulator on the planet due to its ability to redistribute heat across the globe by absorbing part of the solar radiation and releasing that heat through evaporation. Such redistribution depends on different factors for it to occur: heat exchange between the ocean and the atmosphere, the flow of the wind through its surface, the planetary vorticity, in addition to the currents and sub currents associated with different water masses and salinity concentrations (Koszalka & Stramma, 2019; Nobre & Shukla, 1996; Pezzi et al., 2016). This heat exchange affects the sea surface temperature.

Among the factors that contribute to the maintenance of the sea surface temperature (SST) and the interaction (or heat exchange) between the atmosphere and the ocean, it can be highlighted ocean currents and the transport of this heat and mass. Superficially, the maintenance of temperature in the South Atlantic Ocean occurs through ocean-atmosphere interactions, in which the South Atlantic Subtropical Gyre stands out (Silveira et al., 2000).

Specifically, the South Atlantic Ocean (Figure 2) is characterized on its surface by the Subtropical Gyre of the South Atlantic, being maintained concomitantly by the geostrophic circulation and the action of the winds on its surface, being very similar in shape and extension to the subtropical atmospheric gyre that sits on it. The gyre reaches depths of 500 to 100m, with decreasing speeds (Cirano et al., 2006; Garzoli & Simionato,

1990a; Peterson & Stramma, 1991; Silveira et al., 2000).

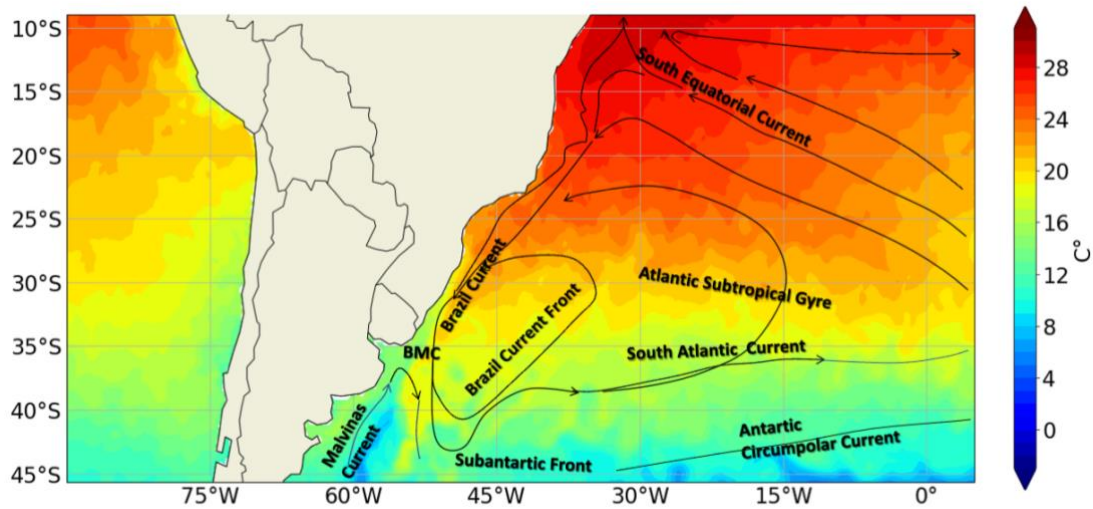


Figure 2: Simplified diagram of the graphic representation of currents and ocean circulation for the West sector of the South Atlantic, adapted from Peterson & Stramma (1991). The scheme was structured in an image that shows the variation of the sea surface temperature in °C using data from ERA5 and considering the day 06/01/2020 at 6 pm.

The South Atlantic Subtropical Gyre is bounded on its western edge by the Brazil Current (BC), a Western Boundary Current originating from the bifurcation of the South Equatorial Current around 10°S, with relatively warm waters that lose heat as it flows South along with the break of Brazil's continental shelf, to the region of the Brazil-Malvinas Confluence (BMC). It is a low-intensity current when compared to other Western Boundary Currents (Campos et al., 2000; Peterson & Stramma, 1991; Silveira et al., 2000). Gozzo et al. (2014) point out in their analysis that the hot water of BC, together with the influence of the Andes, is one of the mechanisms responsible for the cyclogenesis of subtropical cyclones.

In the Southwest of the South Atlantic, a contiguous area to the coast of Argentina, near latitude 38°S, the Brazil-Malvinas Confluence occurs. BMC is positioned in an area where there is an intense passage of storms. It's an area that faces the meet between a warm current (BC) and a cold one (MC) (Stramma 1991). Besides that, this region is an area that interacts with the air mass from the continent, generating temperature instability which results in the induction of fronts, cold and hot air masses, and transient systems that are being conducted from the Southern and Pacific oceans to the South Atlantic Ocean (Campos et al., 1999; Pezzi et al., 2016).

The BMC is considered one of the most energetic regions of the South Atlantic,

being the result of a confluence between the Brazil Current (BC) and the Malvinas Current (MC) (Chelton et al., 1990). On the one hand, BC arises from lower latitudes with temperatures higher than 20°C, on the other hand, the MC arises from higher latitudes, but it is a current with temperatures lower than 16°C, and it becomes less saline with the contribution of the Rio da Prata estuary (Evans & Braun, 2012; Garzoli & Simionato, 1990b). Click or tap here to enter text.

Palmeira et al. (2015), using climate models, show the relationship between the SST and the depth of the oceanic mixture layer, concentrating their analysis close to the coast of Brazil and the BMC. In addition to that, they also observed in their study that the passage of low pressures resulted in a narrowing of the layer and that in these cases, the temperature showed an elevation even if slight. Cataldi et al. (2010) identified the occurrence of positive SST anomalies in the BMC region that result in the intensification of transient low-pressure systems.

Dong et al. (2011) suggest in their work that the convergence of heat occurs through interoceanic exchanges, where the heat supply of the Indian Ocean is about twice that of the Pacific Ocean, playing a unique role in transporting heat to the South Atlantic Ocean. Forget, and Ferreira (2019) reinforces that the Atlantic Ocean, as well as the Pacific Ocean, play a unique role in the distribution of heat across the equator despite the lack of symmetry between the Northern and Southern hemispheres where the South Atlantic Ocean has a larger oceanic area.

The presence of the wind changes the origin of the heat that flows into the Atlantic, thus establishing a heat transport connection between the Atlantic and the Indo-Pacific around the southernmost portion of Africa. Without the wind as a force, heat transport flows to the Atlantic from the circumpolar channel along the East Coast of South America (Corell et al., 2008).

Sterl & Hazeleger (2003) concluded that SST anomalies are generated through the interaction between atypical winds and atmospheric pressure, where changes in the latent heat flow are caused by changes in wind speed and abnormal advection of atmospheric heat. Reboita et al. (2019) identified that the heating of SST contributes to both the formation and intensification of cyclones due to the increase in turbulent heat flows from the sea to the atmosphere. Chan et al. (2001) claim that in addition to ocean conditions, the atmosphere is a determining factor in the generation and intensification of cyclones and that oceanographic and atmospheric factors may not be independent of each

other.

Studies as presented by (Venegas et al., 1996), Pezza and Ambrizzi (2003), Pezza et al. (2007), and Bombardi et al. (2014) suggested in their work a close relationship between SST anomalies and cyclone intensity and frequency occurrences.

The atmosphere is highly sensitive to interactions with the sea surface, and its movement is directly connected to its response to atmospheric pressure due to the heat exchange between the surface and atmosphere, whether it be aquatic or continental. The air tends to move from regions of higher pressure to regions of lower pressure in search of homogeneity. The SST, evaporation rate, planetary vorticity (Coriolis Force), among others, are influencing factors in this movement Lutgens and Tarbuck (2016).

The South Atlantic is bordered in its Western portion by South America, in the Eastern portion by the African continent, and flanked by the Pacific, Indian, and Antarctic Oceans. In addition, it receives influences from said areas in its currents and heat transport, as well as ocean-atmosphere interactions, thus making SST anomalies observed in these regions capable of modulating not only a large part of the interannual climate variability but also the cyclogenetic processes acting on it (Corell et al., 2008; Nobre & Srukla, 1996; Pezzi et al., 2016; Rehbein et al., 2018).

The variability of SST has been the focus of several studies, mainly SST anomalies for the Pacific and Equatorial Atlantic regions (whether positive or negative) tend to influence atmospheric dynamics, moisture supply, and consequently, rains in sensitive agricultural regions of southern Brazil. Strong SST gradients, including intense positive flows of sensitive and latent heat, in addition to moisture from the ocean surface to the atmosphere, contribute to the intensification of cyclogenesis (Dal Piva et al., 2008; Gan and Rao, 1991; Holland et al., 1987; Sinclair, 1994b; Sutil et al., 2019).

2.3 CYCLONES

Cyclones, or low-pressure systems, are characterized by an area in the atmosphere whose pressure is lower when compared to other areas in its surroundings at a height gradient equivalent (Jones & Simmonds, 1993). Despite their genesis and development in situations of temperature instability associated with strong winds, their existence aims at atmospheric stability and homogeneity (Orlanski & Katzfey, 1991;

Robertson & Smith, 1980). During the life cycle of a system, several forces tend to act on it: the Coriolis force, which is responsible for the direction of circulation (clockwise in the Southern Hemisphere); the pressure gradient, which promotes the displacement of the system; and the frictional force, a force that acts as an energy sink, decreasing the intensity of the winds.

Studies with the goal of determining cyclone climatology, identifying their positions and trajectories have been carried out since the 1950s (Fujita, 1955). These studies were carried out using everything from synoptic pressure charts to the surface (Taljaard, 1967) to automatic schemes, which use data of surface pressure, geopotential height, relative vorticity, or surface temperature (Hodges, 1995; Murray & Simmonds, 1991; Reboita et al., 2010; Sinclair, 1994).

Cyclone classification is associated with the regions of their genesis and performance, in addition to the energy source that maintains them, being then classified as extratropical, subtropical, and tropical (Pezza et al., 2007; Reboita et al., 2010; Sinclair, 1994). In this work, extratropical cyclones and their characteristics are presented.

2.3.1 EXTRATROPICAL CYCLONES

Extratropical cyclones (EC's), as the name implies, form in regions far from the tropics and are generally associated with frontal systems that have an intense temperature gradient (Bjerknes, 1919; Bjerknes & Solberg, 1922). They are low-pressure systems that have a hot and humid ascending air center that, when in contact with the cooler air layers, gain speed and descend, generating a large shear of winds moving across the ocean surface, as can be seen in Figure 3.

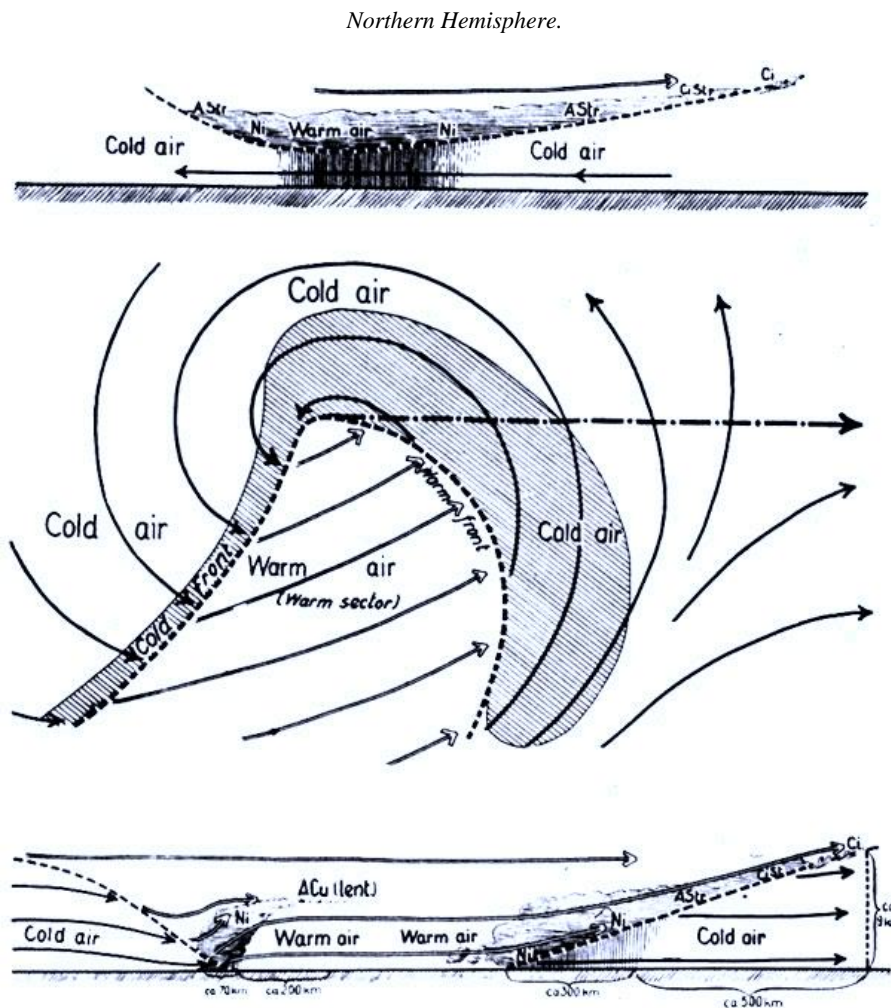


Figure 3: Scheme proposed by Bjerknes in 1919, designing the development of a cyclone for the Northern Hemisphere. Source: Bjerknes (1919).

The scheme proposed by Bjerknes & Solberg (1922), also called Norwegian School Theory, shows that a cyclone undergoes several changes in its life cycle from its genesis to its lysis, with defined stages where two distinct air masses, the polar and tropical, interact with each other (Figure 4). The scheme proposes that the dense polar air is moving to the West, while a current of hot air from the tropics moves to the East. Furthermore, it determines that if there is rising hot air, the cyclone still has the potential energy to develop (from **a** to **e**). However, when it becomes a vortex with homogeneous air temperature, there will be no potential energy available to be converted into kinetics, hence the cyclone tends to weaken and disappear.

Bjerknes & Holmboe (1944) showed how the divergence pattern at higher levels promotes changes in pressure at the sea surface level. Such analysis can be evidenced

through the equation of the surface pressure trend (Equation 1).

$$\frac{\partial p_s}{\partial t} = -g \int_0^{\infty} \nabla \cdot (\rho \mathbf{V}) dz$$

(Equation 1)

where, $\nabla \cdot (\rho \mathbf{V})$ represents the wind's horizontal divergence, g represents gravity acceleration, and ρ air density.

Sutcliffe (1947) established equations describing cyclones' development for a quasi-geostrophic system, considering the variation in surface pressure. His study proposed the combination of the temporal variation of the absolute vorticity at the level of 1000 hPa (indicating the presence of cyclones or anticyclones) with different factors: the vorticity advection at 500 hPa, the temperature advection in the layer between 1000 hPa and 500 hPa; with variation by vertical movement and adiabatic heat sources.

Petterssen et al. (1955), continuing with the research carried out by Sutcliffe (1947), revised the equation for the development of cyclones and anticyclones, including the effect of adiabatic heating and cooling. They determined in their work that the development of cyclones occurs where and when the advection of absolute cyclonic vorticity - this being proportional to the mass divergence - in 500 hPa is superimposed on a baroclinic zone at low levels.

Petterssen and Smebye (1971) classified cyclones according to their development, dividing them into type A: a frontal wave that has its genesis resulting from a baroclinic instability and initially does not have an associated front; and type B: its genesis is associated with a pre-existing upper air cavity, with strong vorticity advection and little heated advection, which may or may not be associated with a front. The classification of type C cyclones was carried out later by Radinovic (1986), where its genesis associated with the effects of orographic blockages, which in its turn is associated with increased baroclinicity, also known as cyclones to the leeward of mountains.

The advancement in numerical modeling and meteorological observations allowed Shapiro and Keyser (1990) to deepen the analysis in the model proposed by Bjerknes and Solberg (1922), describing a model for the development of extratropical cyclones that present slight differences from the one proposed in 1922. Although its genesis is similar, its development and lysis have different characteristics: in the model proposed by Shapiro and Keyser (1990), whose scheme can be seen in image 5, the cold front remains perpendicular to the hot front (III and IV in the scheme), while the cold

front in the scheme proposed by Bjerknes and Solberg (1922) is longer and “coils” around the warm front. Another difference is that hot seclusion in cyclones like Bjerknes and Solberg (1922) occurs at the beginning of cyclogenesis, whereas in cyclones like Shapiro and Keyser (1990), it occurs more towards the end of the cyclone's life cycle.

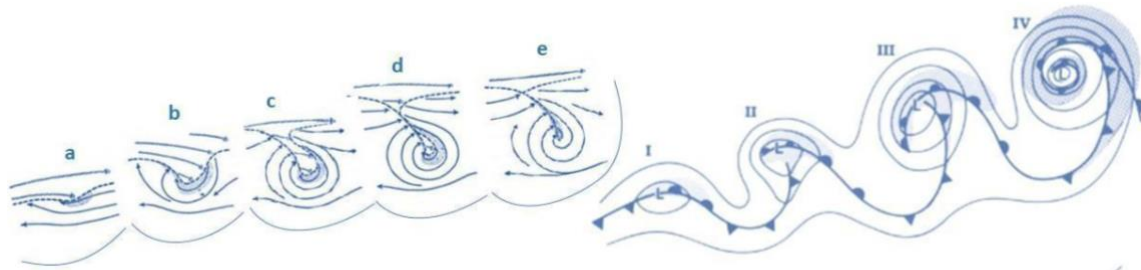


Figure 4: Conceptual models of the life cycle of an extratropical cyclone for the Southern Hemisphere, where the scheme classified from “a” to “e” was proposed by Bjerknes & Solberg in 1922, while the scheme from “I” to “IV” was proposed by Shapiro & Keyser in 1990. Adapted from Bjerknes & Solberg (1922) and Shapiro & Keyser (1990) by the author.

Although they describe different schemes for cyclogenesis and extratropical cyclones, the schemes proposed by Bjerknes and Solberg and by Shapiro and Keyser do not cancel each other out. Reboita et al. (2018) carried out a survey in case studies where they presented the synoptic characteristics described by both authors, then extratropical cyclones of the type Bjerknes and Solberg (1922) and cyclones of the type of Shapiro and Keyser (1990) were identified.

Extratropical cyclones play an important role in the transport and distribution of heat and humidity in the atmosphere, thus contributing to the maintenance of the global climate. Gan and Rao (1994) found evidence that cyclogenesis in SA is more (less) intense during Winter (Summer), and afterward, Gan (1992) identified that the spatial distribution of cyclones in SA, their trajectories and frequency are the result of the orographic influence at the area of the Andes (where there is a displacement of a trough in the middle troposphere) and its contrast in relation to the ocean and the continent.

Another influencing factor in extratropical cyclones is jet currents, characterized as a concentrated and irregular band of wind that tends to influence meteorological systems on the surface. Hurrell and Deser (2009) identify that the changes of the jets interfere in the intensity of storms, as well as in their traced "path". Such currents influence the formation of cyclones, with zones of low pressure in their troughs and zones

of high pressure in their crests. They are the Subtropical Jet, the Polar Jet, and the Low-level Jets. These jet currents at the upper levels are associated with intense horizontal temperature gradients at medium and higher latitudes.

The Subtropical Jet flows between latitudes 20°S to 40°S and has a certain constancy in its position, with predominance in seasonal medium wind fields. Its positioning and intensity are conditioning factors for the displacement of frontal systems, where the persistent presence of high-pressure systems associated with the deviation of the jet current constitutes the occurrence of an atmospheric blockage (Rodrigues & Woollings, 2017). Woollings et al. (2018) point out in their study that in relation to HS, less intense (and slower) subtropical jets have a greater latitudinal amplitude, being able to point more to the North or South, while more intense (and faster) jets, tend to concentrate more in the center of its range, close to the jet's climatological position. In addition, they conclude that this range is greater during the Winter season.

The Polar Jet has its position quite variable over a wide range of mid-latitudes, between 30°S and 70°S, and is associated with a strong temperature gradient. Both the Subtropical Jet and the Polar Jet have seasonal variation, distancing themselves (approaching themselves) more from the equator during Summer (Winter). Physick (1981) associates polar jet currents with cyclogenetic regions for the South Atlantic, and later, Trenberth (1991) identified an increase in the number of storm trails associated with polar jets during Winter.

The Low-level Jet flows East of the Andes, extending from the Amazon region to the Rio da Prata Basin and can be observed throughout the year, has greater intensity during the Southern Summer, and its existence is associated with the topography of the continent. During winter, the Low-level Jets are usually associated with the position and intensity of the ASAS (Marengo et al., 2004).

In addition, the presence and position of the Low-level Jets help to modulate the ZCAS during the Southern Winter, when the jets are located further south, merging with the ZCAS, intensifying them (Marengo, 2002; Seluchi & Marengo, 2000). Ferreira et al. (2003) has concluded that in the event of ZCAS events, the Low-level Jets flow to Southeastern Brazil, and in their absence, they tend to flow towards the Rio da Prata basin. Hoskins and Hodges (2005) identified that Low-Level Jets that are present in the Andes tend to influence cyclogenesis in South America.

2.3.2 SUBTROPICAL OR HYBRID CYCLONES

Subtropical or hybrid cyclones are those that can have their genesis as a subtropical system throughout their life cycle or change from tropical to extratropical and vice versa, therefore presenting a hybrid phase. They are categorized as hybrid systems because they have both the characteristics of tropical and extratropical. They have a cold core at high levels like extratropical cyclones and hot at low levels like tropical ones without having an associated front (Evans & Braun, 2012; Gozzo et al., 2014).

Subtropical or hybrid cyclones are systems considered to be of less intensity, whereas they do not have a closed low-pressure center. They were not detected by (Gan and Rao, 1991). Hoskins & Hodges (2005) identified the development of “weaker” casualties, and later, Reboita et al. (2010) confirmed the presence of "superficial" casualties on the Southeastern coast of Brazil. Reboita et al. (2018), using the subtropical systems identified by the Brazilian Navy, analyzed through a case study, from the genesis to the lysis of a subtropical cyclone, confirming its hybrid characteristics by presenting tropical cyclone characteristics (local, latent, and sensitive heat sources) with a hot inner core and extratropical (cold core at higher levels).

In general, studies indicate that subtropical cyclones are formed associated with the presence of a trough or an Upper Tropospheric Cyclonic Vortex (UTCV). Gozzo et al. (2014) showed in their analysis that among the main characteristics associated with subtropical cyclones in the Southwest of the South Atlantic Ocean is the presence of a dipole-type blocking pattern, that is, there is a crest or a rise on the polar side of the UTCV. It is worth mentioning that subtropical cyclones have a hot core that is shallower than the tropical ones, thus preventing the system from being maintained only by the feedback mechanism between the circulation and the heat flows of the ocean (Gozzo et al., 2017; Reboita et al., 2018).

2.3.3 CYCLOGENESIS AND ASSOCIATED FACTORS

Cyclones are usually classified according to their genesis conditions as Tropical, Subtropical, and Extratropical. This simplified definition is given following the idea that

zones between the same latitude vary around the globe correspond to an environment of similar genesis (Reboita et al., 2018).

The term cyclogenesis is used to characterize the change in atmospheric surface pressure that results in the formation of cyclonic (or anticyclonic) circulation. The genesis stage includes the development of the atmosphere for the formation of the cyclone, evolving from the tropical disturbance stage to the tropical depression stage. Once the tropical depression stage has been reached, the genesis processes are finished, and any further development is considered an intensification of the cyclone Gray (1982) considers that for cyclogenesis to occur, an external process must act on an area or system. However, when analyzing stages of intensification, the internal processes of movement and advection of energy are dominant.

Among the genesis processes of a system that may originate a cyclone, baroclinic instability stands out, is considered the primary mechanism for the development of an extratropical cyclone Bjerknes & Solberg (1922). Baroclinic instability is responsible for converting potential energy into kinetic energy. Directly, the differential heating of the equator associated with the potential energy available and the vertical shear of the wind promote the necessary instability for the generation of a system. Charney (1947) and Eady (1949) demonstrated in their research that a vertically sheared zonal flow ranges from unstable to small disturbances, correlating the development of the mid-latitude cyclone to baroclinic instability.

In the Rio da Prata basin region, at approximately 35°S, the cyclogenesis itself results from the baroclinic instability associated with the presence of the jet (polar or subtropical, depending on the time of year), in addition to being influenced by the orography since it is located to the leeward of the Andes Mountains (Rocha et al., 2016). Gan et al. (2020) show that the baroclinic effect was considered one of the most important contributors to the development of cyclones.

As the South/Southeast coast of Brazil is bathed by the warm waters of the Current of Brazil, the transfer of latent and sensitive heat from the sea to the atmosphere often acts as an additional adiabatic source in cyclogenesis Reboita (2009). Evans & Braun (2012) determine that 75% of the genesis of the cyclones analyzed occurred in a region with a higher temperature of BC. Reboita (2008), in her analysis, reinforces that in the absence of these latent and sensitive heat flows, cyclones tend to be weaker.

As previously discussed, there are numerous factors that contribute to and influence the genesis and route of a cyclone. The results for identifying the influencing factor depend on the data set and physical parameters observed in the analysis (Pinto et al., 2016). Despite this, the passage of cyclones and anticyclones on the globe is a climate modulator/regulator, and that short- and long-term climate changes tend to influence extreme events, reinforcing the need for understanding about cyclone genesis and behavior.

2.4 DATA ACQUISITION AND PROCESSING

2.4.1 BRAZILIAN NAVY DATA

The Brazilian Navy releases a synoptic chart (Figure 5) twice a day determining the position of cyclones and anticyclones present in the South Atlantic, in addition to the present and associated fronts, convergence zones, troughs, and any other instability pointed out by the models and/or observations made by meteorologists involved in the elaboration of the chart (Brasil, 2018). These synoptic charts cover latitudes ranging from 20°N to 70°S and from 90°W to 0°W, comprising the Caribbean Sea and South Atlantic. Included in this vast area is the geographical sea region known as METAREA V, which begins on the Brazilian coastline (north at the border with French Guiana and south at the border with Uruguay) and ends at 20°W.

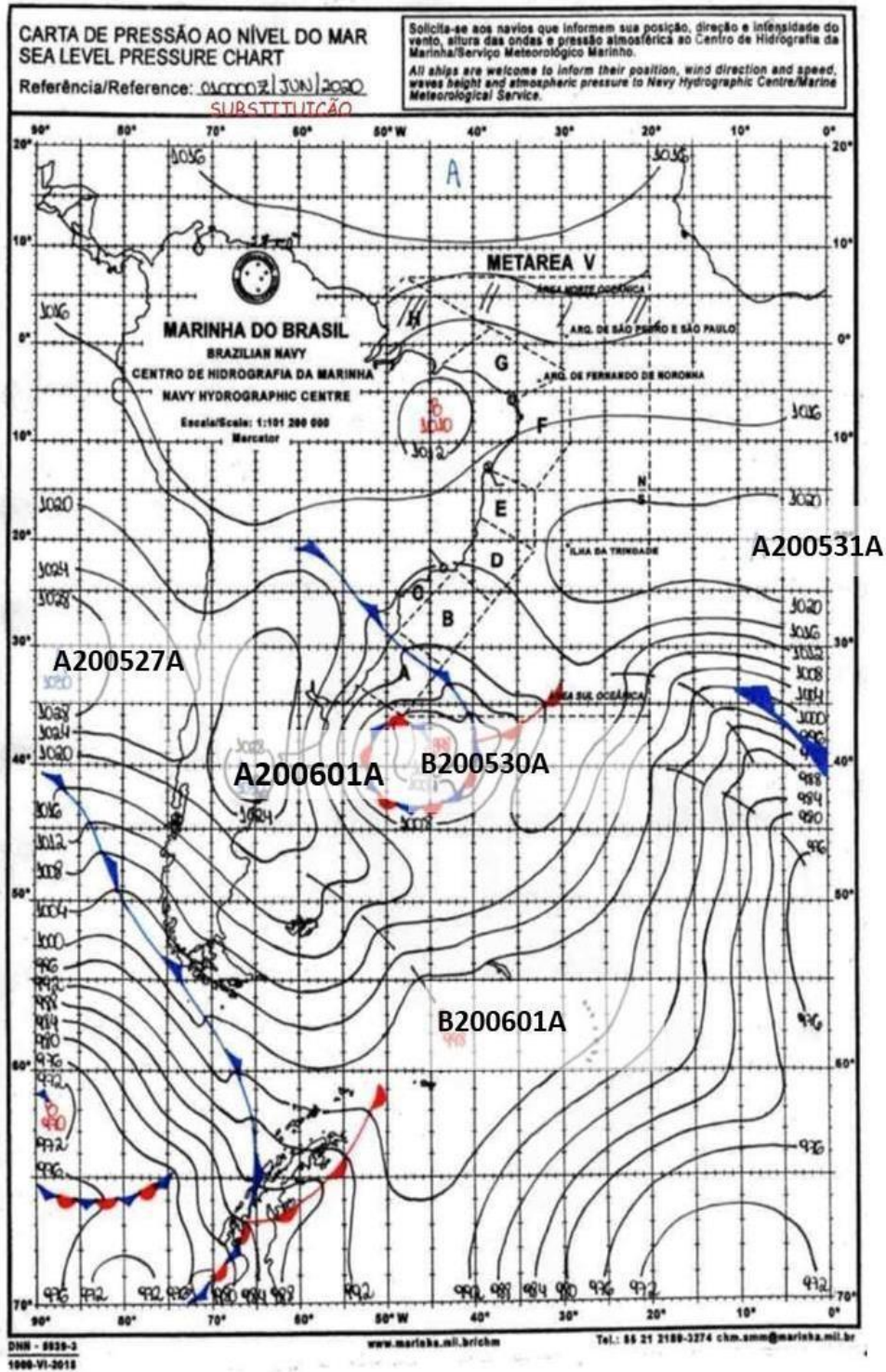


Figure 5: Synoptic chart referring to 1 June 2020 at Midnight, issued by the Brazilian Navy and obtained on the <https://www.marinha.mil.br/chm/dados-do-smm-cartas-sinoticas/cartas-sinoticas> (Brasil 2020a). Last access: 18/07/2020.

In the synoptic charts, isobaric lines are observed - lines of the same atmospheric pressure - where the pressure is the reduced value for sea level. The symbology present in the synoptic charts is described from some letters and symbols, as shown in image 8 (Brasil, 2020). The letter A corresponds to a region of high pressure (anticyclonic area),

and the letter B corresponds to a region of low pressure (cyclonic area). In addition to the letters, there are some symbols that indicate the presence of fronts and others that indicate areas of instability.

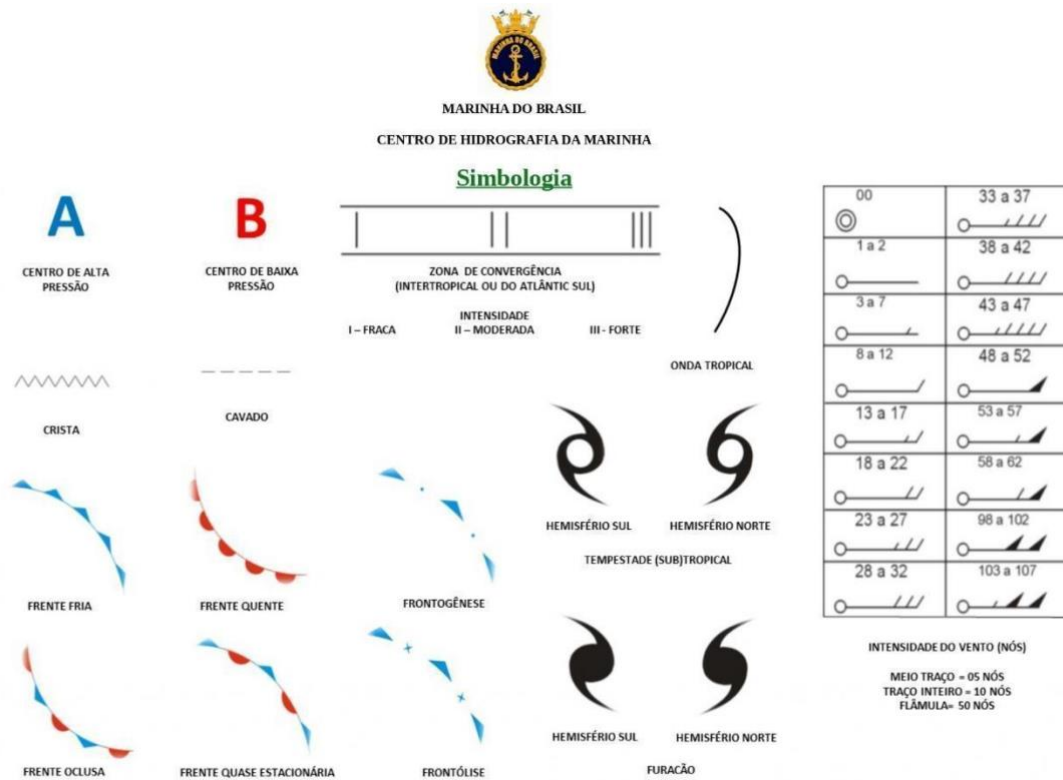


Figure 6: Symboly used in the synoptic charts elaborated by the Brazilian Navy.

The historical data of the synoptic charts used for the analysis of this work was partly provided by the Brazilian Navy, and another part was obtained from a script to automatically collect the letters made available by the Brazilian Navy Hydrographic Center (CHM) available through the website of the Brazilian Navy².

The charts include isobars and a symbological system of letters and symbols in which "B" corresponds to an area of low pressure, the level of which is also noted on each chart. To identify the life cycle of individual cyclones, a single designator was created for each cyclone in which the letter B was followed by the year, month, day, and time of the initial occurrence of each event. This designator was maintained on subsequent charts

²Synoptic charts of the Hydrographic Center of the Brazilian Navy (CHM) are available at the Brazilian Navy website: <https://www.marinha.mil.br/chm/dados-do-smm-cartas-sinoticas/cartas-sinoticas>.

through cyclolysis. The region marked on the chart by the MB was identified as the center of the cyclonic region, and latitudinal and longitudinal positions and changes in pressure were recorded for each time step. Since the charts are in graphic format (rather than the digital/gridded form), the only way to track cyclones from the MB synoptic charts is manual documentation, i.e., by visually identifying and hand-inputting the coordinates after viewing the total of 8,000+ such charts.

Aiming for objective identification of the cyclone's life cycle in the interval between the years 2010 and 2020, simple markings were made on the synoptic charts using the PowerPoint software, where it was also possible to monitor the occurrence of fronts. A single nomenclature was used for each cyclone and anticyclone in the chart, in addition to methods for classifying the characteristics observed considering only those that appeared between latitudes 10°S and 60°S, and longitude 90°W to 0°W, where:

- For system nomenclature, the letters B were used for low-pressure regions and A for high-pressure regions, followed by the year, month, day, and time of the letter's emission, in addition to a letter indicating the cyclone's genesis order. Ex.: B200530A (low-pressure region identified).
- If the cyclone remained in the following synoptic charts, the nomenclature received was maintained until its moment of lysis (disappearance of the system).
- The region marked on the chart by the Brazilian Navy was identified as the center of the cyclonic region, which was then marked as the latitude and longitude position of the cyclonic center.
- Next to the cyclonic center identified by the Brazilian Navy, there is also the pressure value in that region, identified as the internal pressure of the system.

2.4.2 ERA5

European Centre for Medium-Range Weather Forecasts (ECMWF) Reanalysis v5 (ERA5) is the most recent reanalysis produced by ECMWF, available from the Copernicus Climate Change Service (CS3) (Hersbach et al., 2020). The atmospheric variables used in this work are on a horizontal grid of 31 km (0.25° x 0.25°), the highest resolution of its kind. While different timesteps are available, 12-hour outputs were used to best align with the MB's synoptic charts, while a longer time series, from 1 January

1979 to 31 December 2020, was employed. Thus, ERA5 significantly extends the period of record of the MB archive.

The variables used for the identification of low-pressure centers at sea level were mean sea level pressure, U wind, and V wind. Streamlines were used to guide the identification of the center of each system, which was recorded in longitude and latitude along with the associated pressure. To be consistent with the MB case tracking, cyclones were also identified manually with a graphic interface enabled by the software *GrADS* (Figure 7).

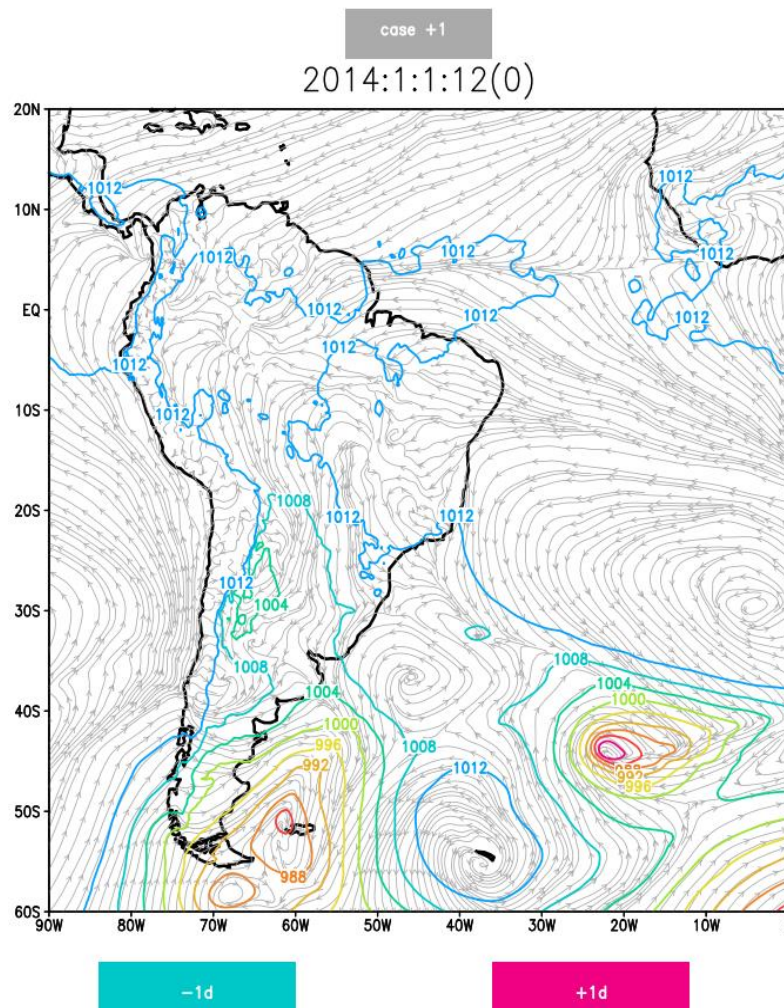


Figure 7: Interface of the tracking script using *GrADS*.

Looking to objectively identify the systems, a few criteria were used: have a closed isobar and continue in a logical path. Additionally, for the ERA5-identified events, any system that did not last for 48 hours and reach the coast was excluded. The resulting dataset included the longitude and latitude position, internal pressure, displacement velocity,

wind max around the center (which was not used in this analysis) of each individual system at 12-hour intervals across its lifespan.

Quantitative statistical analysis using software *MATLAB* was performed, seeking to evaluate the numbers related to the occurrence of cyclones over time and days for their lifetime. Monthly and annual averages were taken to evaluate the occurrence of cyclones, frequency histograms to raise the frequency of cyclonic occurrences, in addition to the calculation of the displacement velocity of the cyclonic center. In addition to statistical analyses using GrADS, climatological analyzes and variability related to cyclonic genesis were carried out to identify which components contribute to the genesis of cyclones for the South Atlantic. The information collected is shown in Table 1.

Table 1: Collected information to build the tracking dataset.

LABEL	MB	ERA
Date and hour o	(YYYY+MM+DD+hh)	(YYYY+MM+DD+hh)
Cyclone Identification	(B + yymmdd + genesis order) e.g.: <u>B200527A</u>	Case Number, e.g., <u>79125</u>
Latitude (S)	Latitude position of the marked center by Brazilian Navy as B	Latitude position of the center indicated by streamlines (fig 8)
Longitude (W)	Longitude position of the marked center by Brazilian Navy as B	Longitude position of the center indicated by streamlines (fig 8)

To identify the cyclone displacement speed, the distance covered by the cyclone was analyzed, considering its initial latitude/longitude and its position in the following period. This distance was calculated in degrees and later converted into kilometers and divided by 12 hours (the total hours of coverage of a synoptic chart issued by the Brazilian Navy and chosen for tracking) to obtain a result in kilometers displaced by hour.

2.5 CATEGORIZATION OF CYCLOGENESIS

Coastal events were categorized as such if they were generated over the Atlantic or nearly 2 degrees of longitude from the continental coastline. Cyclonic events that generated beyond 2 degrees to the west of the coastline were classified as lee cases. This was a subjective decision based on the irregularity of South America coastal line. Given

the vast latitudinal range of the South America coastline and the Andes, events were further classified by latitude. Northern events were those that formed between 10°S and 30°S; central events formed between 30°S and 45°S; southern events formed between 45°S and 55°S, as previously described in other studies (Crespo et al., 2021; Gramscianinov et al., 2019; Reboita et al., 2018). However, southern lee cyclones were excluded from the composite analyses because Pacific transient waves that are common at similar latitudes can make it difficult to distinguish cyclogenesis events from passage ones. Coastal north cyclones were excluded from the analysis due to low numbers and variability over time, indicating no changes through the seasons.

To better understand the climatology and variability of these systems over time, monthly average data from ERA5 was additionally utilized. The variables to depict the climate mean states included sea surface temperature (*SST*) and U wind and V wind reanalysis estimates at 200, 500, 700, 850, 925, and 1000 hPa. To create a composite data picture, the years with the highest and lowest genesis event values were selected for each of four locations: lee (north and central) and coastal (central and south).

To understand seasonal variability, the data was spread into warm (Nov-Mar or NDJFM) and cold (May-Sep or MJJAS) periods based on austral seasons: Summer (December, January, and February), Autumn (March, April, and May), Winter (June, July, and August) and Spring (September, October, and November). For annual composites, a July-June year was used. To identify wind anomalies, the average of selected years was subtracted from the climatology (Table 2).

Table 2: Years included in the composite analysis for different regions and types of cyclogenesis. An up-facing arrow in the 1st column indicates years with higher numbers of ECs, while a down-facing arrow indicates years with lower numbers of ECs.

	LEE	COASTAL
ANNUAL ↑	2000, 2002, 2003.	1981, 1982, 1983, 1984, 1985, 1992,1993,1994,1995, 2016, 2017, 2018, 2019, 2020.
ANNUAL ↓	1980,1981,1994, 2015, 2016.	1989, 1992, 1997, 2004, 2005, 2007, 2010.
NDJFM ↑	2000, 2001, 2002, 2003, 2004, 2005.	1981, 1982, 1983, 1991, 1992, 1993, 2018, 2019, 2020.
NDJFM ↓	1980, 1983, 1985, 1995, 2001, 2016, 2020.	1980, 1990, 1993, 2002, 2007, 2010, 2012, 2017.

MJJAS ↑	2002, 2003, 2004.	1984, 1985, 1986, 1987, 1995, 1996, 1997, 2018, 2019, 2020.
MJJAS ↓	1981, 1994, 1995, 1996, 2013, 2016.	1989, 1991, 1996, 2003, 2004, 2006, 2009.

The stream function (Equation 2) was calculated to demonstrate the potential of relative vorticity (ζ) for the period analyzed to depict the large-scale circulation features.

$$(\psi = \nabla^{-2}\zeta)$$

(Equation 2)

2.6 CYCLOGENESIS MECHANISMS

To help identify the mechanisms driving cyclogenesis that led to Andes's lee and coastal cyclogenesis, parts of the vorticity budget were calculated for both areas. The vertical vorticity within a mesoscale convective vortex is originated from the combination of some terms: (a) horizontal advection of absolute vorticity, (b) vertical advection of relative vorticity, (c) convergence of absolute vorticity, (d) tilting of horizontal vorticity by horizontally varying vertical wind, and (e) horizontal baroclinity. The vorticity budget equation can be observed at (Equation 3, where:

$$\begin{aligned} \frac{\partial \zeta}{\partial t} = & \underbrace{-[V \cdot \nabla(\zeta + f)]}_{(a)} - \underbrace{\left(w \frac{\partial \zeta}{\partial z}\right)}_{(b)} - \underbrace{[(\zeta + f)\nabla \cdot V]}_{(c)} \\ & + \underbrace{\left(\xi \frac{\partial w}{\partial x} + \eta \frac{\partial w}{\partial y}\right)}_{(d)} + \underbrace{[J_{xy}(p, \alpha)]}_{(e)} \end{aligned}$$

(Equation 3)

Where ζ (ξ , η , ζ) is relative vorticity, V (u , v) is horizontal wind, w is vertical wind, f is the Coriolis parameter, and $J_{xy}(p, \alpha)$ is the two-dimensional Jacobian of pressure, p , and specific volume, α .

Some of those terms were used to analyze the mechanism that leads to cyclogenesis. The vorticity generation due to horizontal vorticity advection (Equation 4) was calculated using the 500 hPa wind, where f is the Coriolis parameter and V represents the vector wind.

$$\Delta [V, -V \cdot \nabla (f + \zeta)]$$

(Equation 4)

To account for the differences in elevation where lee and coastal events were generated, the vorticity generation due to vortex stretching (Equation 5) was computed using the integration of wind at 500 hPa, 700hPa, and 850 hPa for lee cases and 850 hPa, 925 hPa and 1000 hPa for coastal cases.

$$\Delta [V, -f \nabla \cdot V]$$

(Equation 5)

3 RESULTS

3.1 GENERAL CLIMATOLOGY OF SOUTH AMERICA-BORN CYCLONES

The spatial distribution and trajectories of extratropical cyclones identified in the ERA5 reanalysis are shown in figure 8 for lee cases and figure 10 for coastal annual cases, along with the MB's annual tracking data in figure 9 and figure 11. The two climatologies are broadly aligned in that event origins, shown in black dots, suggest that favorable conditions for instability are quite localized between 20°S and 45°S. Both datasets also agree that whether lee or coastal in origin, these storms customarily move southeast toward and across the South Atlantic Ocean.

ERA Tracking “Annual” – Lee Area

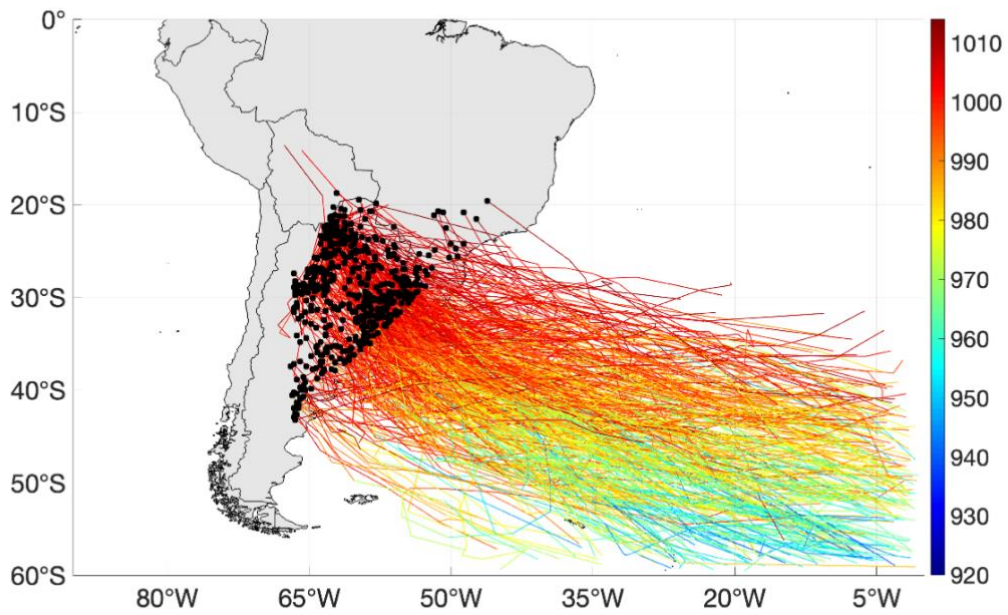


Figure 8: Genesis locations (shown in black dots) of lee cyclones and storm tracks from ERA5 reanalysis for all cyclones included in this study for Annual analysis.

MB Tracking “Annual” – Lee Area

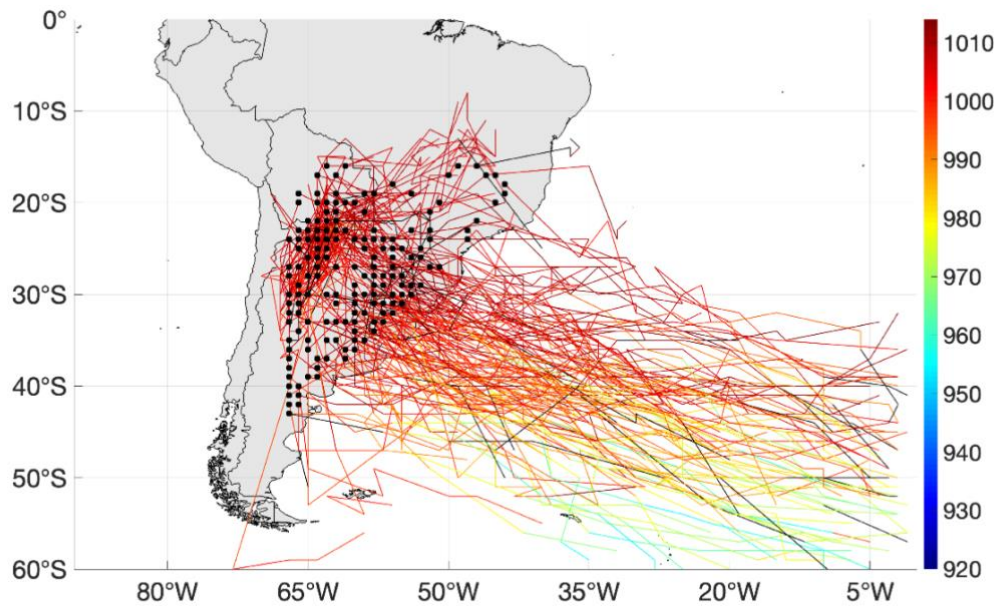


Figure 9: Genesis locations (shown in black dots) of lee cyclones and storm tracks from the Brazilian Navy for all cyclones included in this study for Annual analysis.

ERA Tracking “Annual” – Coastal Area

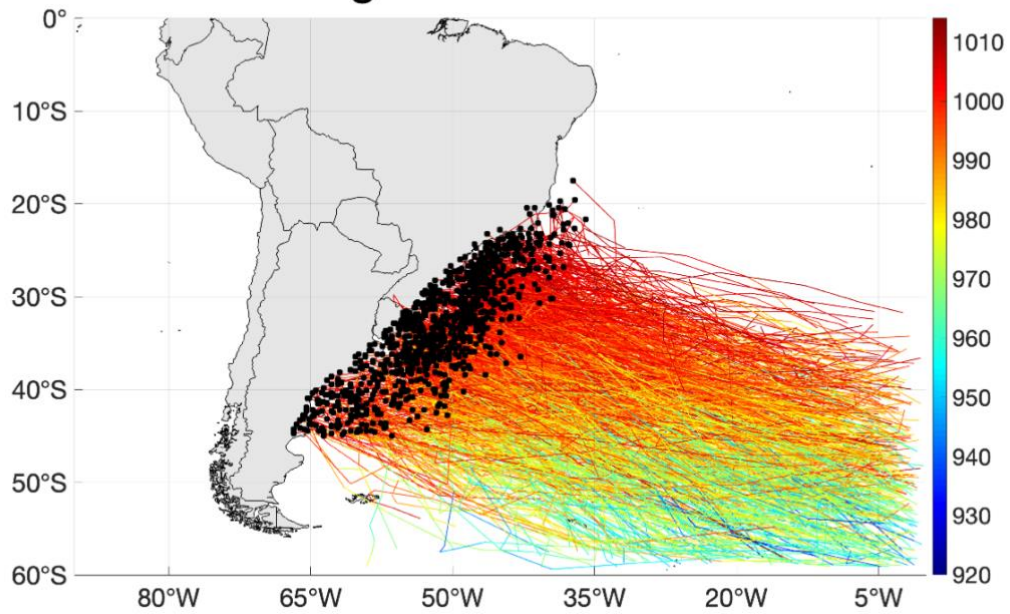


Figure 10: Genesis locations (shown in black dots) of coastal extratropical cyclones and storm tracks from ERA5 reanalysis for all cyclones included in this study for Annual analysis.

MB Tracking “Annual” – Coastal Area

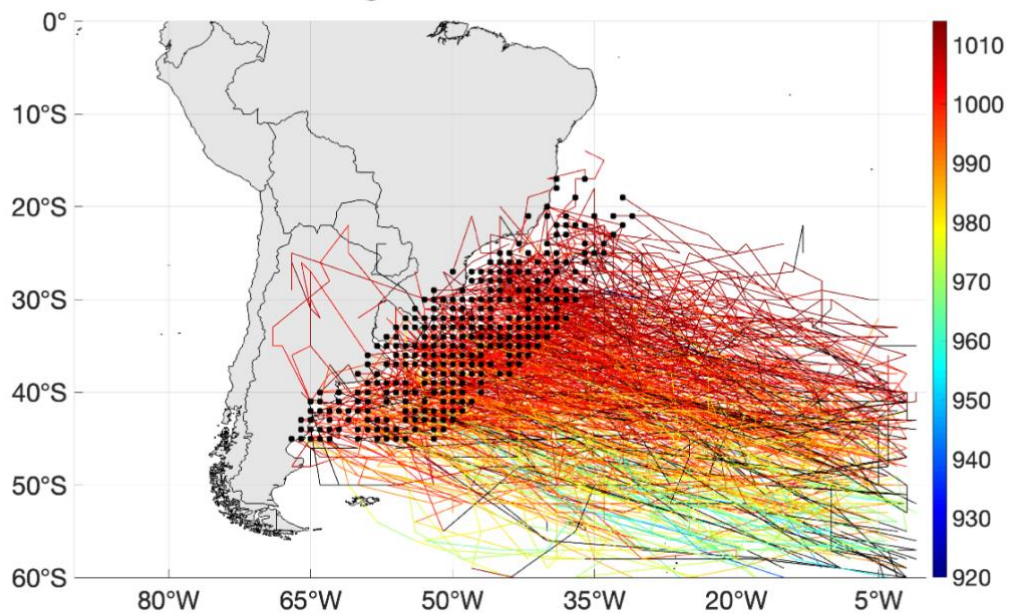


Figure 11: Genesis locations (shown in black dots) of coastal extratropical cyclones and storm tracks from the Brazilian Navy for all cyclones included in this study for Annual analysis.

Moreover, both datasets agree on the spatial distribution of cyclone intensity for all periods analyzed, with more intense cyclones (noted by lower values of mean sea level

pressure) found at lower latitudes. As interannual variability, like the Antarctic Oscillation, can have a strong influence on the strength and location of the polar jet stream and regional baroclinicity (Gan et al., 2020), the longer record of tracking in ERA5 provides a better climatological perspective. The path of the systems seems to follow south-west directions, and how much near to the coast, higher the internal pressure of those systems seems to be, deepening internal pressure when the system moves away from the mainland. This behavior is shared by the systems identified in both datasets.

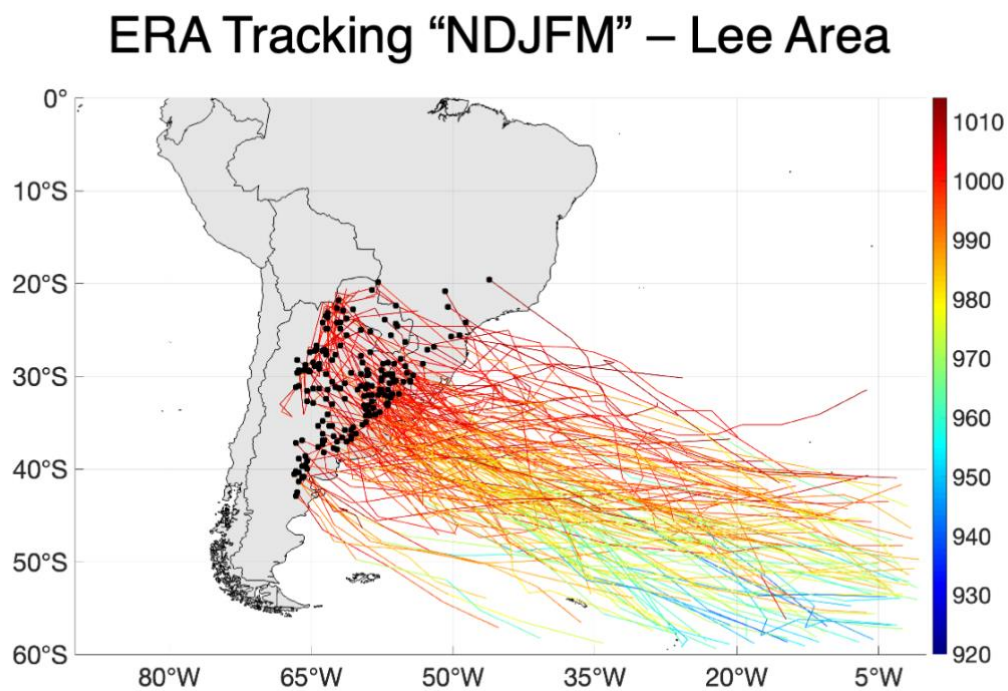


Figure 12: Genesis locations (shown in black dots) of lee cyclones and storm tracks from ERA5 reanalysis for all cyclones included in this study for warm period analysis.

MB Tracking “NDJFM” – Lee Area

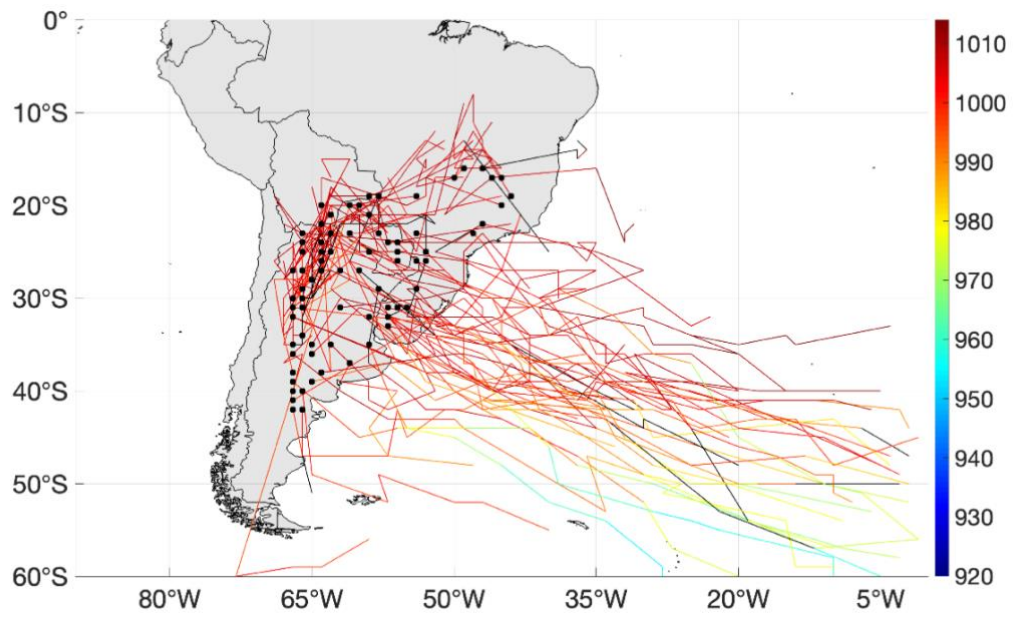


Figure 13: Genesis locations (shown in black dots) of lee cyclones and storm tracks from Brazilian Navy reanalysis for all cyclones included in this study for warm period analysis.

ERA Tracking “NDJFM” – Coastal Area

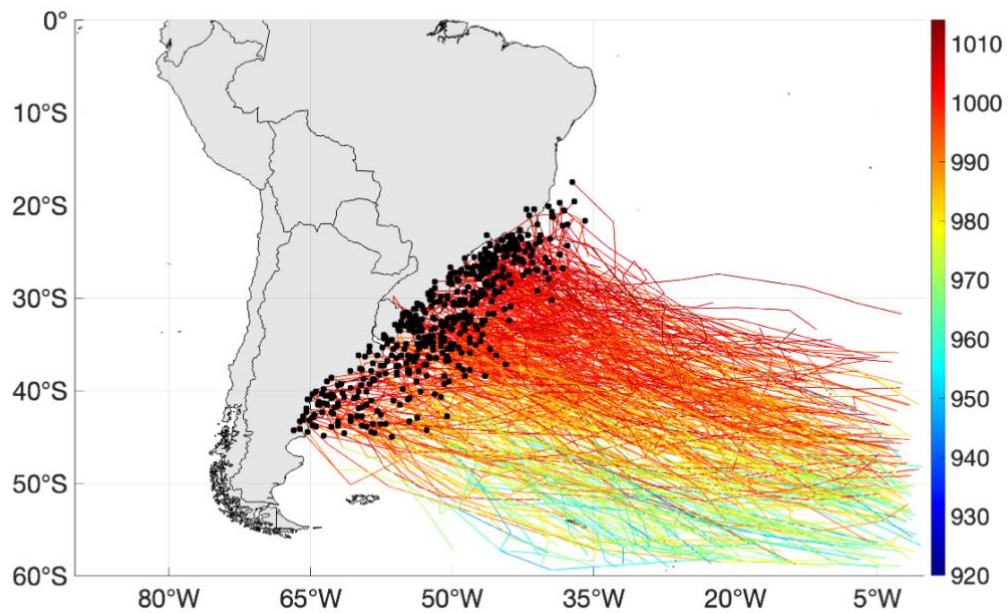


Figure 14: Genesis locations (shown in black dots) of coastal extratropical cyclones and storm tracks from ERA5 reanalysis for all cyclones included in this study for warm period analysis.

MB Tracking “NDJFM” – Coastal Area

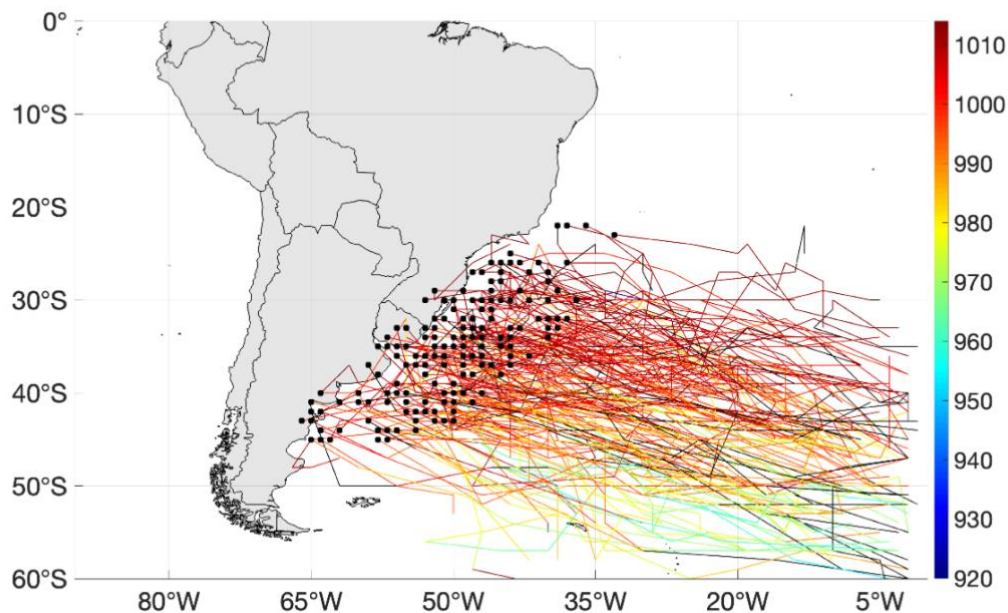


Figure 15: Genesis locations (shown in black dots) of coastal extratropical cyclones and storm tracks from the Brazilian Navy for all cyclones included in this study for warm period analysis.

The ERA5 and the MB datasets disagree on the total number of cyclonic events, with the ERA5 analysis suggesting about 38 events per year (across 42 years of data) and

the MB records indicating about 81 events per year (across 11 years) (Figure 20 a, c vs. Figure 20 b, d). These data also disagree on which meteorological season results in the largest number of lee cyclones, with disparate findings in both the three-month seasons and the five-month warm and cold periods. The difference was expected due to the difference in temporal resolution and methodologies of systems identification. Comparing warm to cold periods, the warm period seems to present fewer lee genesis events, shown in figure 12 and more coastal events (Figure 14). An opposite behavior can be seen during cold period analysis (Figure 16) where lee cyclogenesis seems more expressive when compared to coastal cases (Figure 18). This is reinforced by the genesis numbers in figure 20.

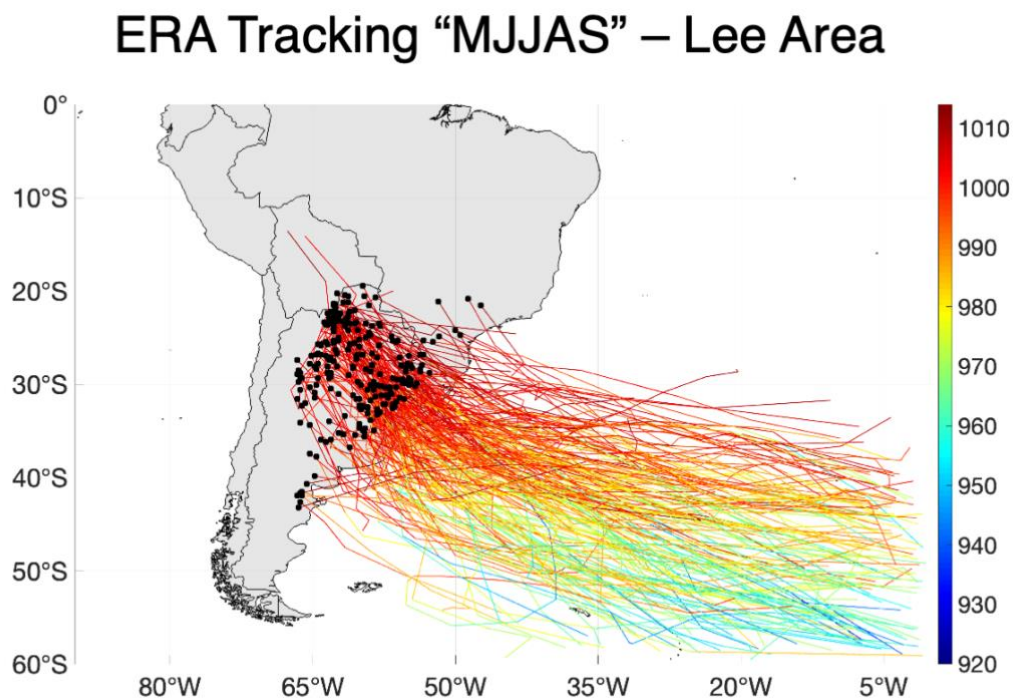


Figure 16: Genesis locations (shown in black dots) of lee cyclones and storm tracks from ERA5 reanalysis for all cyclones included in this study for cold period analysis.

MB Tracking “MJJAS” – Lee Area

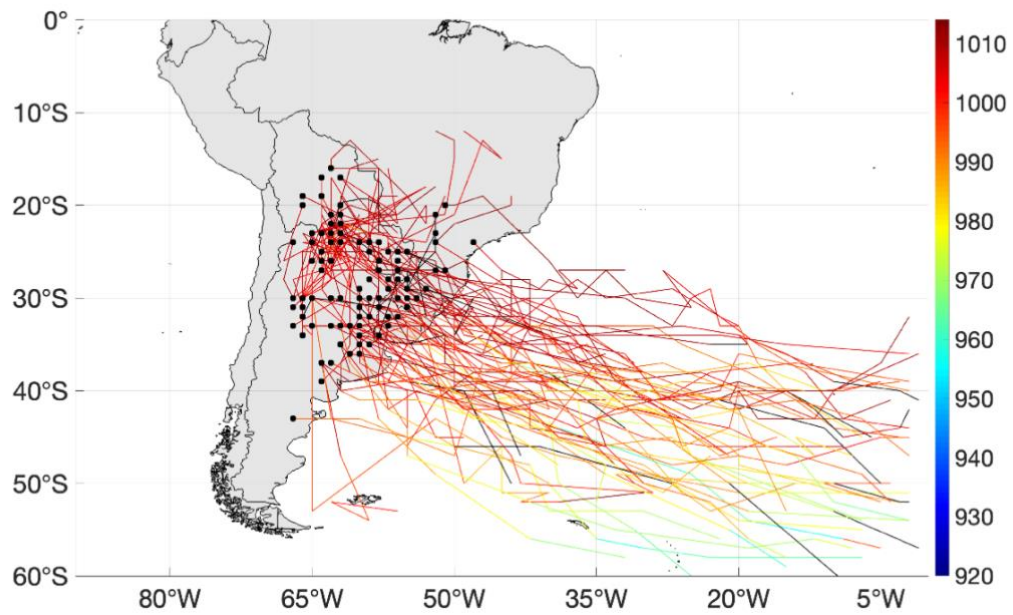


Figure 17: Genesis locations (shown in black dots) of lee cyclones and storm tracks from Brazilian Navy reanalysis for all cyclones included in this study for cold period analysis.

ERA Tracking “MJJAS” – Coastal Area

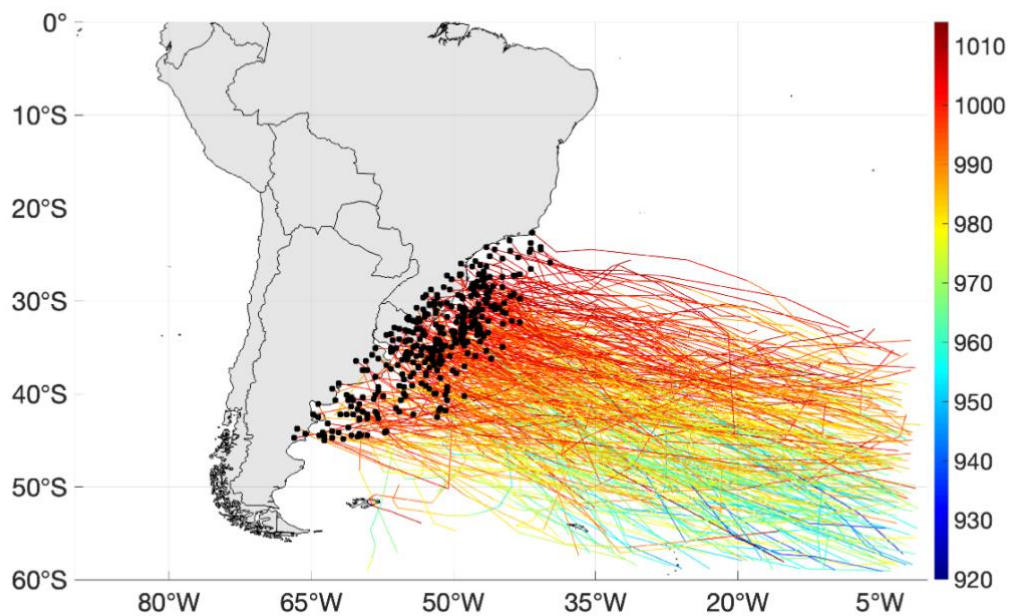


Figure 18: Genesis locations (shown in black dots) of coastal extratropical cyclones and storm tracks from ERA5 reanalysis for all cyclones included in this study for cold period analysis.

MB Tracking “MJJAS” – Coastal Area

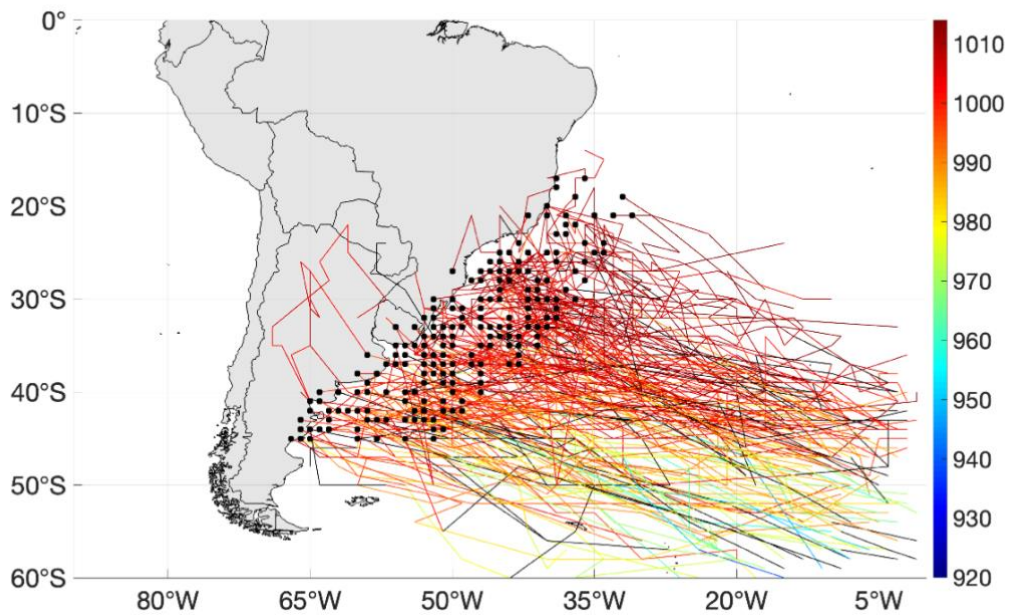


Figure 19: Genesis locations (shown in black dots) of coastal extratropical cyclones and storm tracks for the Brazilian Navy for all cyclones included in this study for cold period analysis.

These discrepancies might also stem from methodological approaches in tracking, as we applied to the ERA5 data a requirement for an EC to persist for at least 48 hours and translate from the land surface to the ocean. Besides that, both datasets agree in genesis location and cyclone path, showing the same concentrated area independent of the analyzed period.

The MB track picked up more disturbances that didn't meet this threshold, potentially resulting in different frequency distributions. This discrepancy is expected because of several non-scientific reasons: I) the officers who analyzed the daily weather were not the same day-by-day causing discontinuation of weaker cases, and II) coarse station readings led to imprecise interpolation of pressure analysis when hand-drawing the charts. Nonetheless, the overall climatologies among the two data sources are in good agreement.

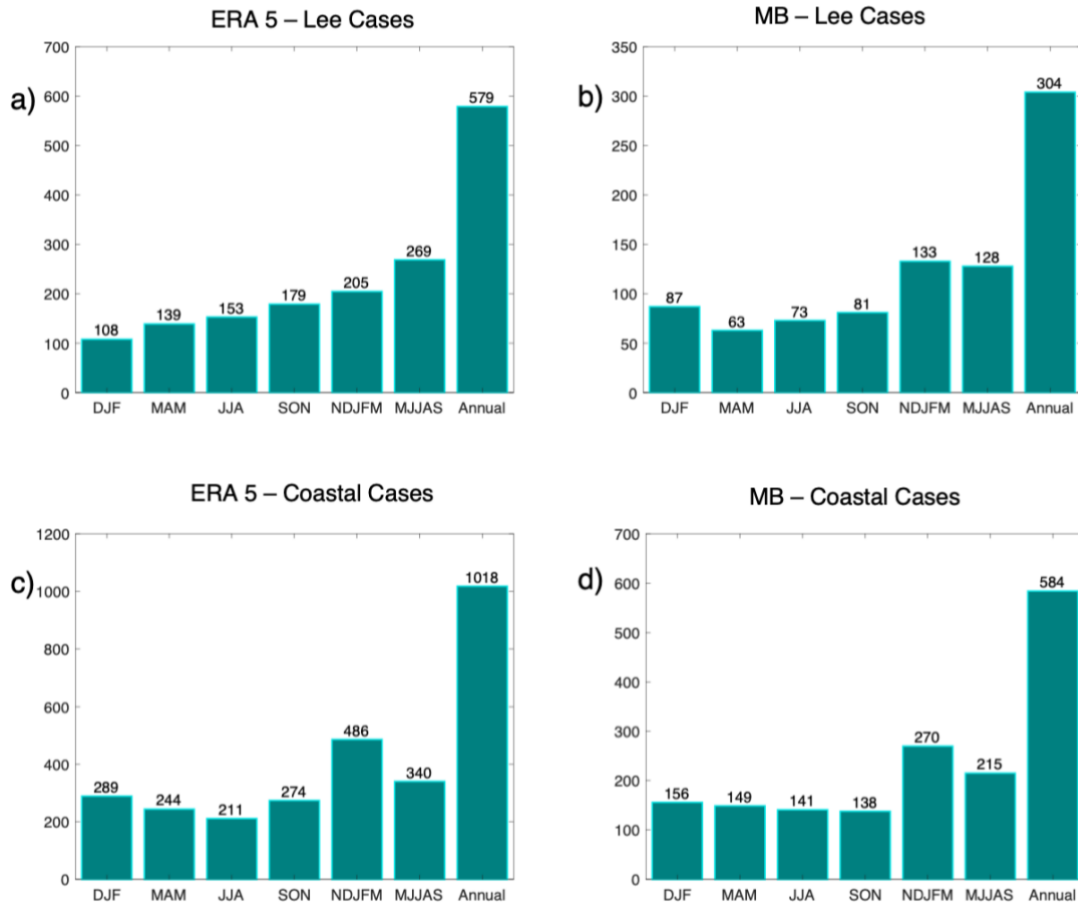


Figure 20: Numbers of genesis events for lee (a, b) and coastal (c, d) extratropical cyclones along with storm tracks for ERA5 reanalysis (a, c) and from the Brazilian Navy (b, d) for all seasons, including warm and cold period, and annual total.

In the case of coastal cyclones, the seasonal relationships are more consistent between the two datasets. Both tracking methods agree that more ECs occur in December through February than in other seasons. Coastal ECs are also much more frequent than lee ECs in both the ERA5 and MB records. Other studies have highlighted the lack of a prominent seasonal cycle in South American cyclogenesis (Mendes et al., 2007; Satyamurty et al., 1990) and have even shown higher cyclone frequencies for the cold season, but these efforts have tracked cyclones over a relatively short time period (~10 years) (Gan & Rao, 1991). The lack of a prominent seasonal cycle may be associated with transient waves, which are prominently featured in the precipitation field for austral summer (Garreaud & Wallace, 1998).

The pace at which a cyclone moves across the Earth's surface, known as displacement speed, is important for forecasting the weather impacts associated with developing ECs and for describing general cyclone behavior. For ECs captured in the

ERA5 analysis, displacement speeds generally ranged between 20 and 50 km/h but, in some cases, exceeded 150 km/h, which is considered explosive cyclogenesis. In general, these speeds closely match the Brazilian Navy tracks, which helps validate the ERA5 tracking method and supports the relatively short MB-based climatology.

Annual

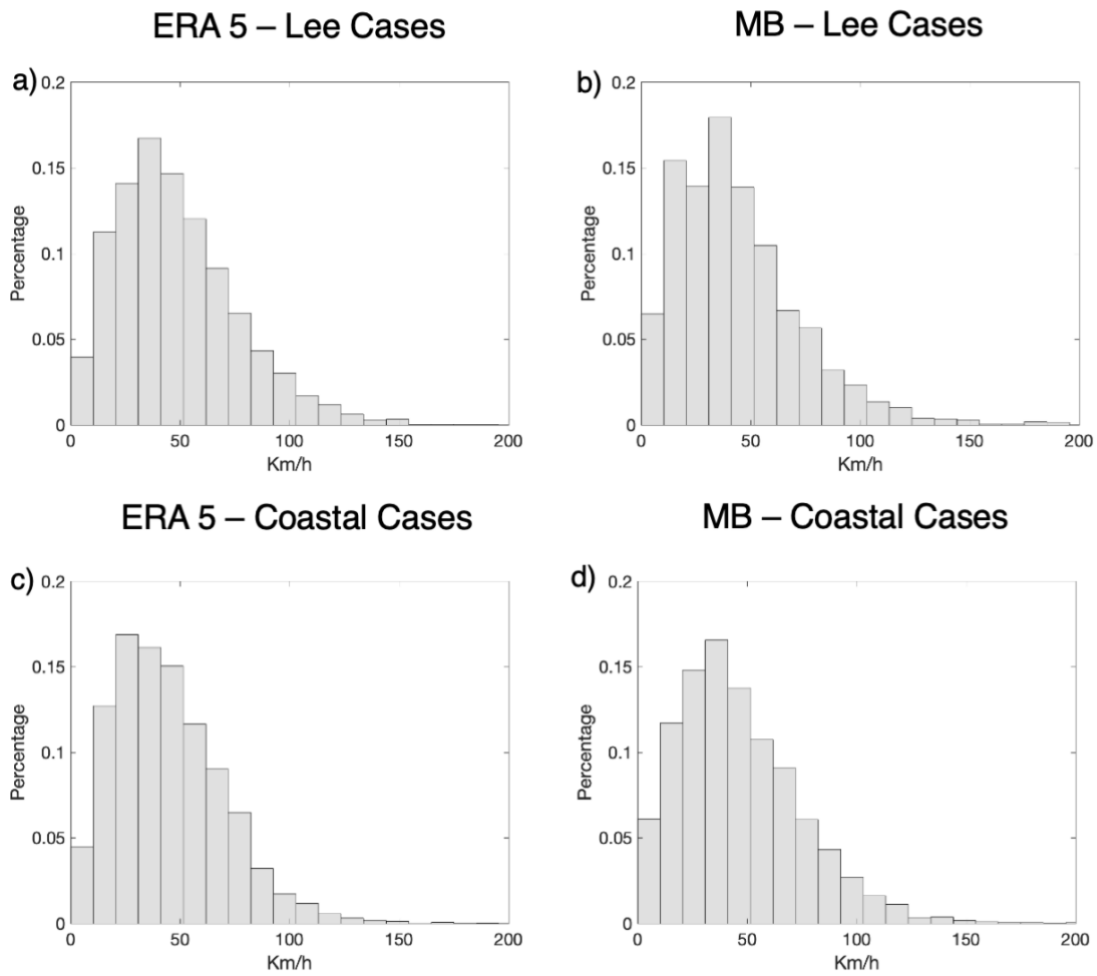


Figure 21: Displacement speeds for lee (a, b) and coastal (c, d) cyclones, calculated by the difference between the location of genesis and the position of the cyclone twelve hours later. Displacement speeds for ERA5 cyclones (3a, c) are shown in relation to Brazil for the annual period.

NDJFM

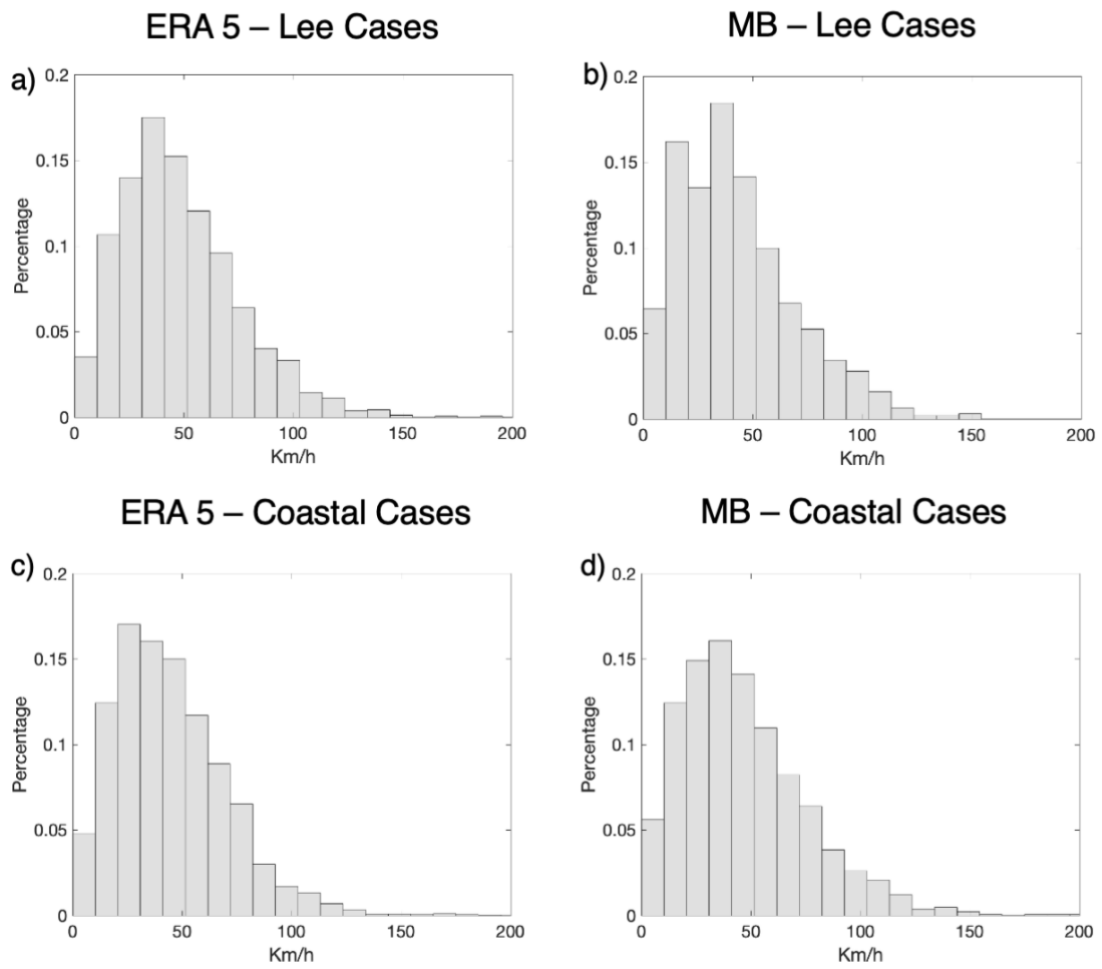


Figure 22: Displacement speeds for lee (a, b) and coastal (c, d) cyclones, calculated by the difference between the location of genesis and the position of the cyclone twelve hours later. Displacement speeds for ERA5 cyclones (3a, c) are shown in relation to Brazil for November through March.

MJJAS

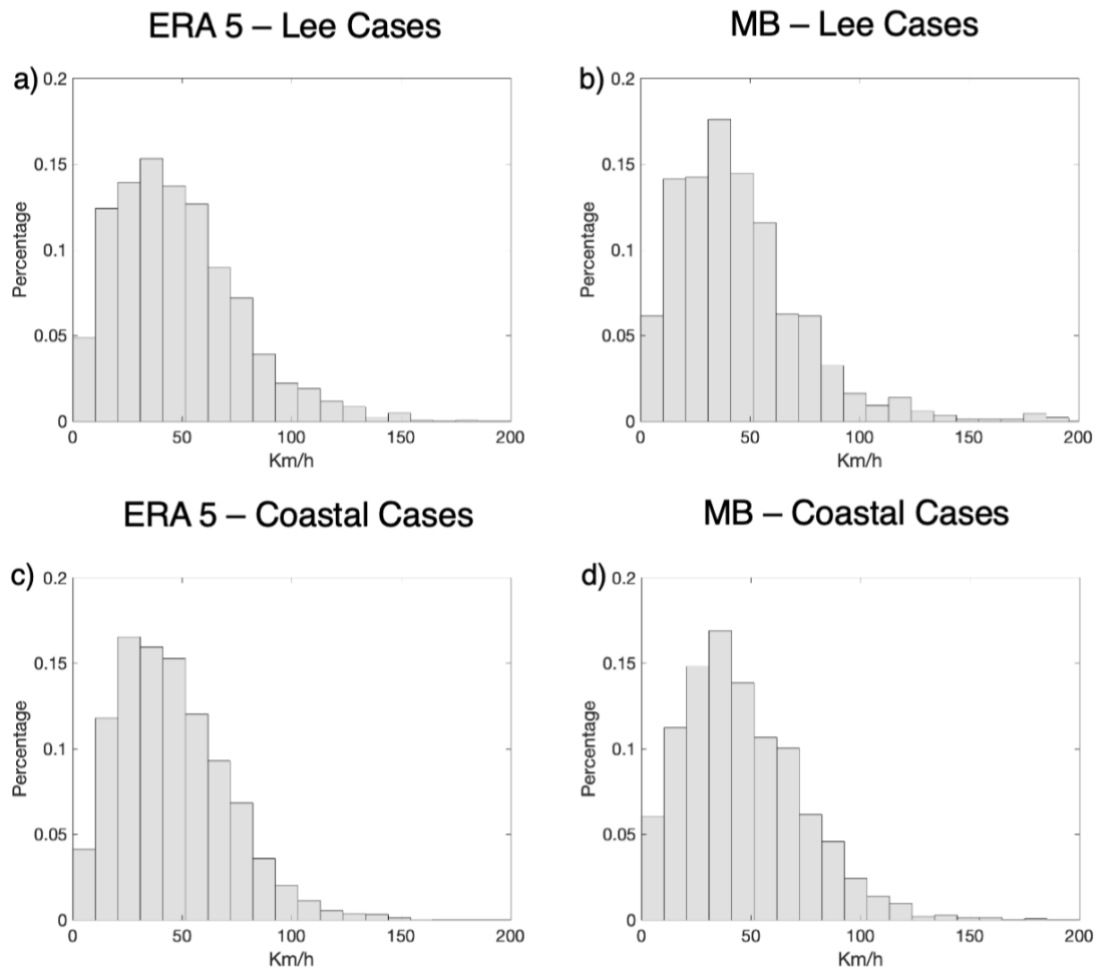


Figure 23: Displacement speeds for lee (a, b) and coastal (c, d) cyclones, calculated by the difference between the location of genesis and the position of the cyclone twelve hours later. Displacement speeds for ERA5 cyclones (3a, c) are shown in relation to Brazil for May through September.

To examine whether regionality impacted the alignment of ERA5 and MB data, we grouped the coastal cyclones into different sub-regions, following the regions identified by Reboita et al. (2010, 2017), Graciannov et al. (2020), and Crespo et al. (2021). While an agreement is higher for certain locations, we still see differing frequency characteristics between the two datasets, notably in coastal North and coastal south cases. However, the spatial distribution of storm tracks, displacement speeds, and seasonality of our tracked storms provide a consensus on the behavior of extratropical cyclones in these sub-regions. With this climatological record of ECs, we can analyze the general circulation features associated with anomalously high numbers or low numbers of storms for a given year.

The ~40-year history of cyclone frequency is shown in figures 24, 25, and 26. While the inter-annual variability during the overlapping period of MB and ERA5 appears agreeable, there are no discernible trends in the ERA5 records. This is also true for the subregions of coastal cyclogenesis, which have prominent variability in frequency but lack a distinct long-term trend, underscoring the need to better understand the impact of natural climate variability on cyclogenesis in the region.

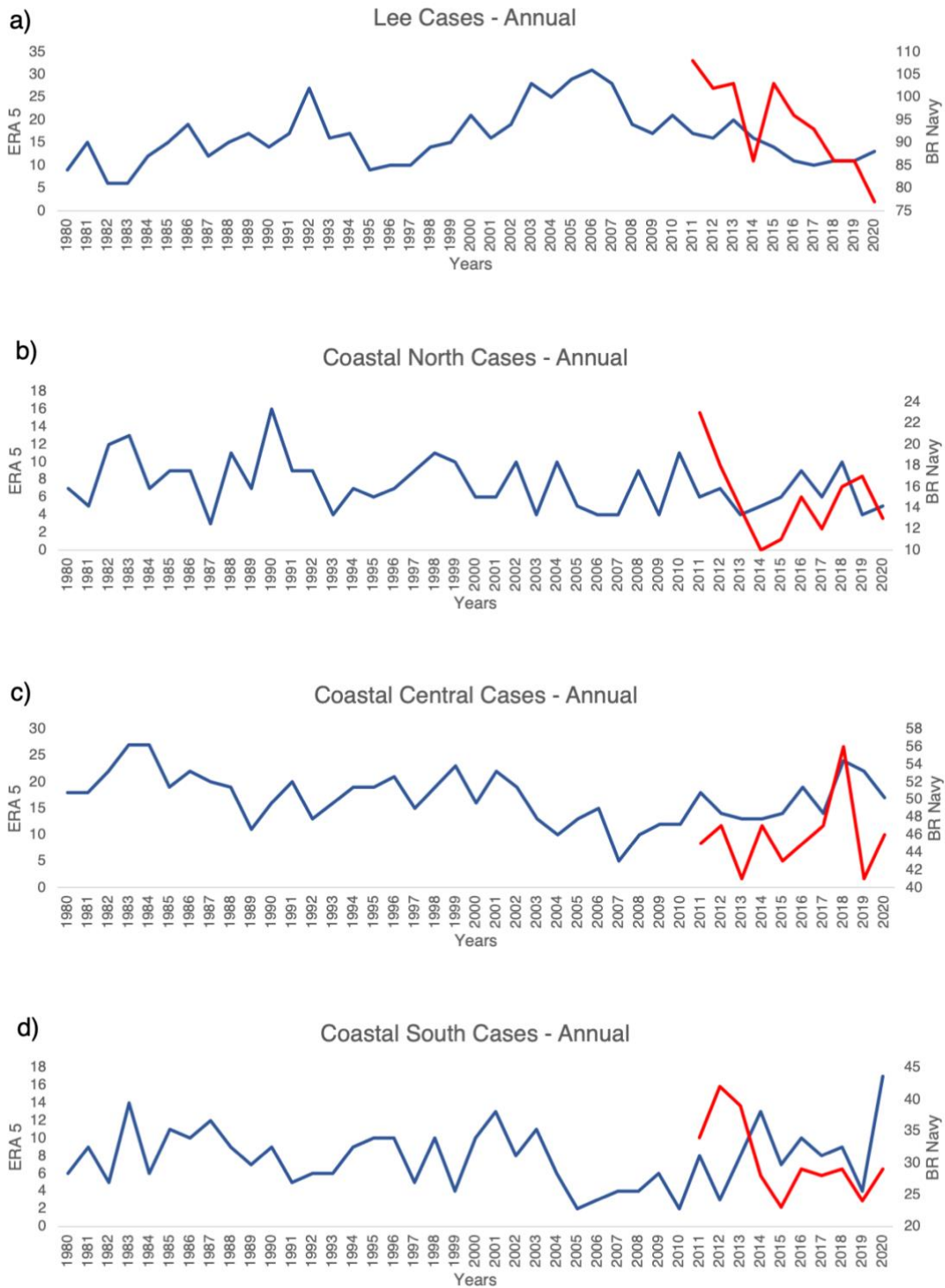


Figure 24: Annual frequency of ECs for lee (a), coastal north (b), coastal central (c), and coastal south (d) cyclogenesis for the annual period using ERA5 data (blue line) and MB (red line). Y labels show cyclone genesis numbers for both datasets.

For the warm (Figure 25) period, we find an anticorrelated relationship for lee cases and part of coastal central cases, but well correlated for coastal north and south,

reinforcing what was previously analyzed for annual mean. The colder period (Figure 26) shows a better-correlated relationship, even if MB presents a larger number of cases. In all analysis, coastal south present the same pattern.

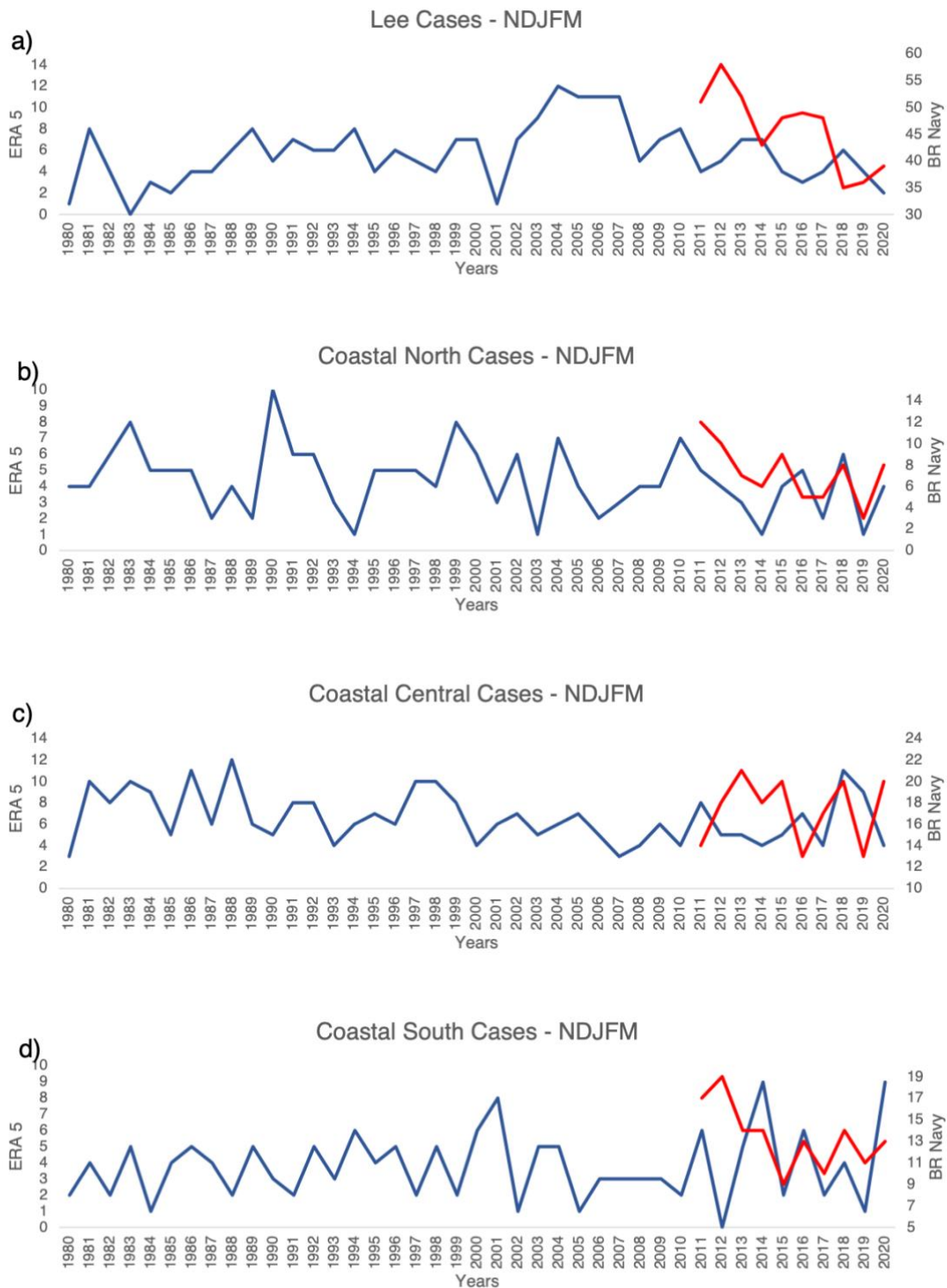


Figure 25: Annual frequency of ECs for lee (a), coastal north (b), coastal central (c), and coastal south (d) cyclogenesis for November to March, using ERA5 data (blue line) and MB (red line). Y labels show cyclone genesis numbers for both datasets.

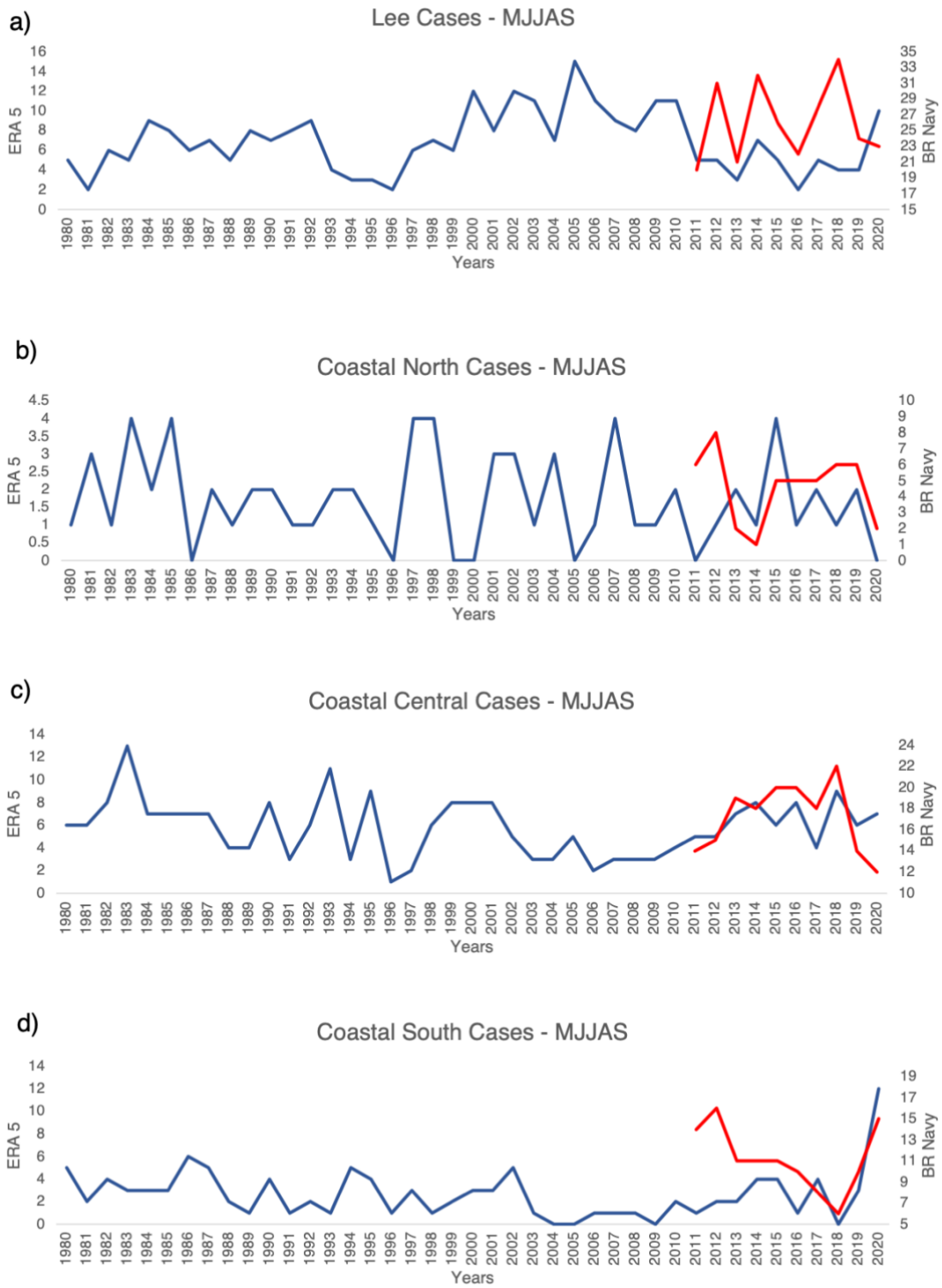


Figure 26: Annual frequency of ECs for lee (a), coastal north (b), coastal central (c), and coastal south (d) cyclogenesis for May to September, using ERA5 data (blue line) and MB (red line). Y labels show cyclone genesis numbers for both datasets.

3.2 CIRCULATION FEATURES ASSOCIATED WITH LEE AND COASTAL CYCLONES

Figure 27 shows the frequency for all analyzed periods in both areas: coastal and lee ECs per the ERA5 analysis, indicating a seemingly anticorrelated relationship between the two regions. Lee cyclogenesis is characterized by a smoother distribution suggestive of a low-frequency climate modulation. The interannual correlation between the two is -0.6, significant at $p < 0.01$. For the warmer period, the correlation between the two is -0.3, significant at $p < 0.01$, and for the colder period, the correlation between the two is -0.2. While coastal cyclogenesis is generally more frequent, there are periods where lee events are more common than coastal events. The fact that the two regions of cyclogenesis act in an opposite manner for all periods analyzed in terms of the low-frequency (decadal-scale) variation is interesting, for it reflects the large-scale oceanic and atmospheric co-variability known to affect Brazil's precipitation and low-level circulation (Grimm, 2003).

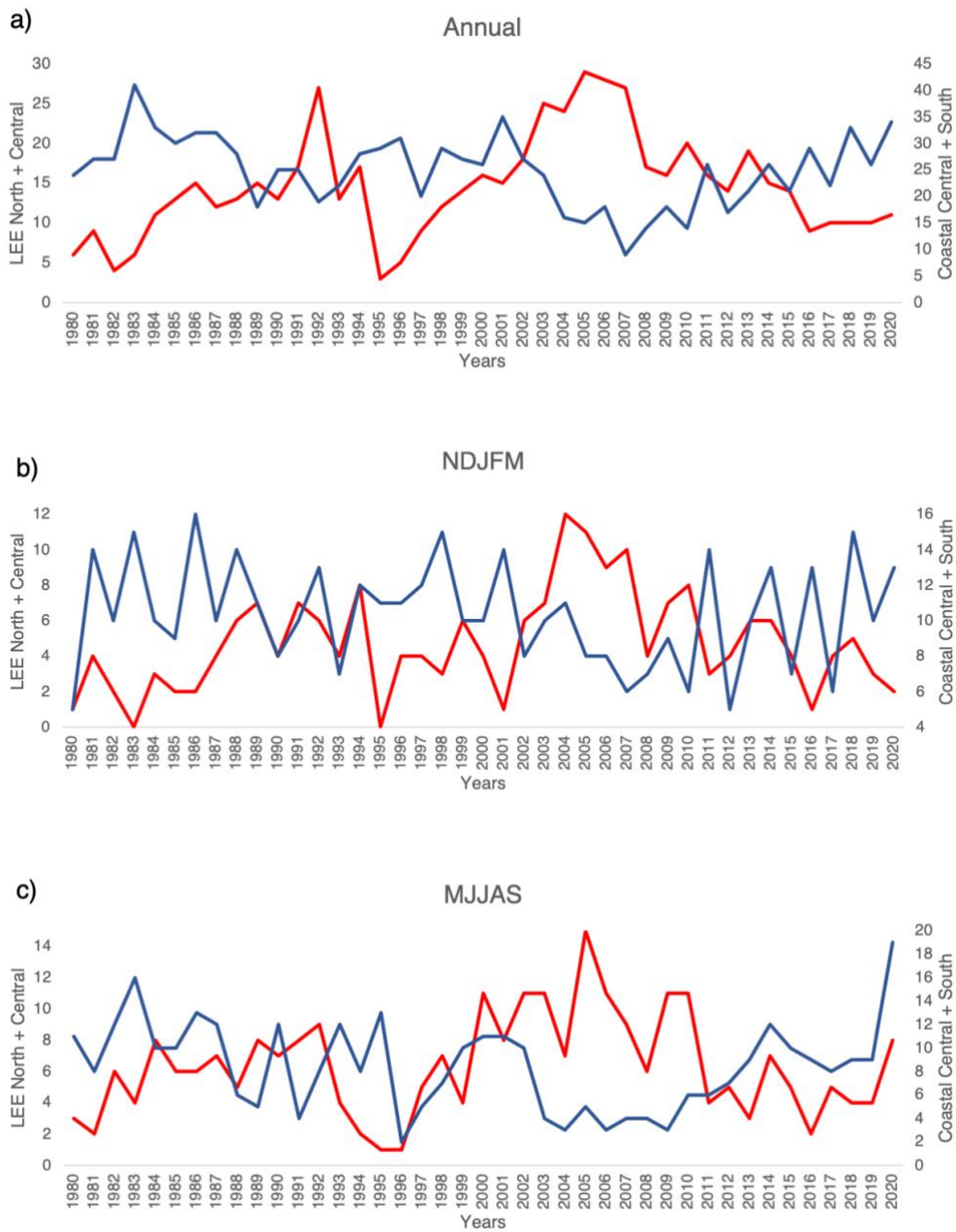


Figure 27: Annual, Warm, and Cold periods of frequency of ECs for lee (red line) and coastal (blue line) cyclogenesis. Y labels show cyclone genesis numbers for both areas.

To diagnose the atmospheric and SST features that are important for the frequency of ECs, we made a composite analysis of upper-level (200hPa) stream function and SST for the annual period (July-June), warm period (November-March), and cold period (May-September). With stream function being proportional to geopotential height and better at depicting tropical circulations, we can identify whether semi-stationary ridge and trough configurations might facilitate or hinder cyclogenesis while simultaneously

analyzing the forcing source of the atmospheric circulation anomalies. Table 2 shows the grouping of years used in our composite analysis for the different cyclogenesis regions and for annual cyclones, along with the warm (NDJFM) and cold (MJJAS) periods; these years were determined based on the time series in figure 27.

The SST and stream function composites for the lee higher-number years depict a weak La Niña feature in years with more frequent lee ECs (Figure 28) and an El Niño-like pattern in years with lower numbers of lee ECs (Figure 29). Associated with SST, atmospheric circulation for lee cyclones depicts a cyclonic anomaly over the west coast of South America, with a frontal zone centered over the Andes figure 28. This frontal boundary along the mountains results in strong directional wind shear along the terrain and localized instability. Vorticity generation over terrain has been attributed to vortex stretching (i.e., the lengthening of an air column along with directional wind shear), a likely driver of instability for most cases of lee cyclogenesis (explored in the next section). This suggests that local atmospheric circulation associated with La Niña facilitates more orographic instability rather than coastal instability.

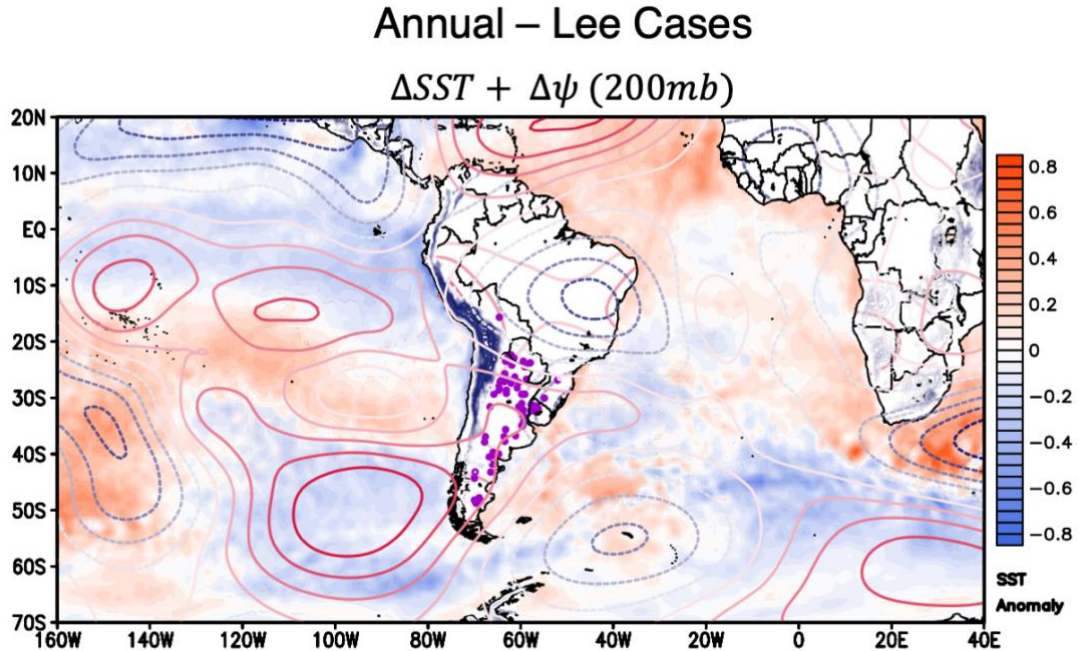


Figure 28: Annual composite stream function anomalies (contours) and SST anomalies (shading) for years with high frequencies of lee cyclogenesis. Positive (negative) stream function values in the southern hemisphere indicate a cyclonic (anti-cyclonic) anomaly or a low (high) pressure area.

Annual – Lee Low Cases

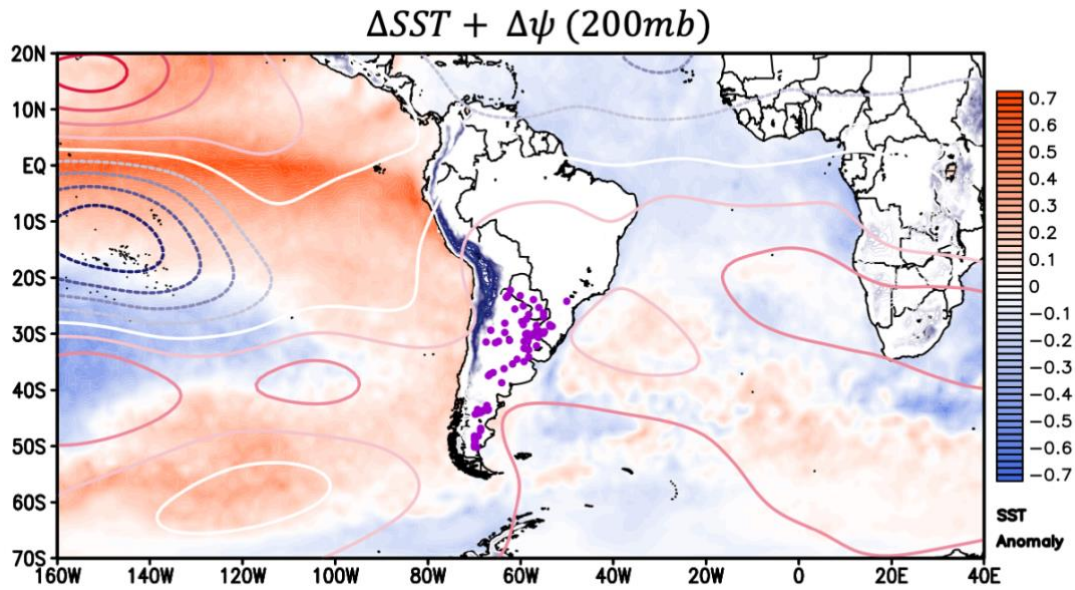


Figure 29: Annual composite stream function anomalies (contours) and SST anomalies (shading) for years with low frequencies of lee cyclogenesis. Positive (negative) stream function values in the southern hemisphere indicate a cyclonic (anti-cyclonic) anomaly or a low (high) pressure area.

Annual – Coastal Cases

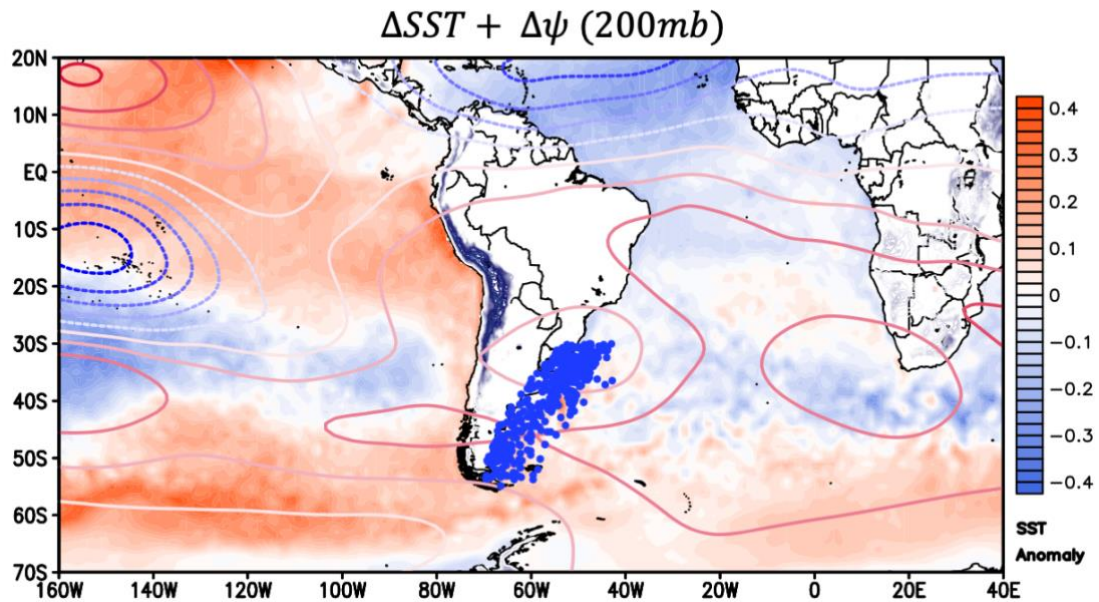


Figure 30: Annual composite stream function anomalies (contours) and SST anomalies (shading) for years with high frequencies of coastal cyclogenesis. Positive (negative) stream function values in the southern hemisphere indicate a cyclonic (anti-cyclonic) anomaly or a low (high) pressure area.

Annual – Coastal Low Cases

$\Delta SST + \Delta \psi (200mb)$

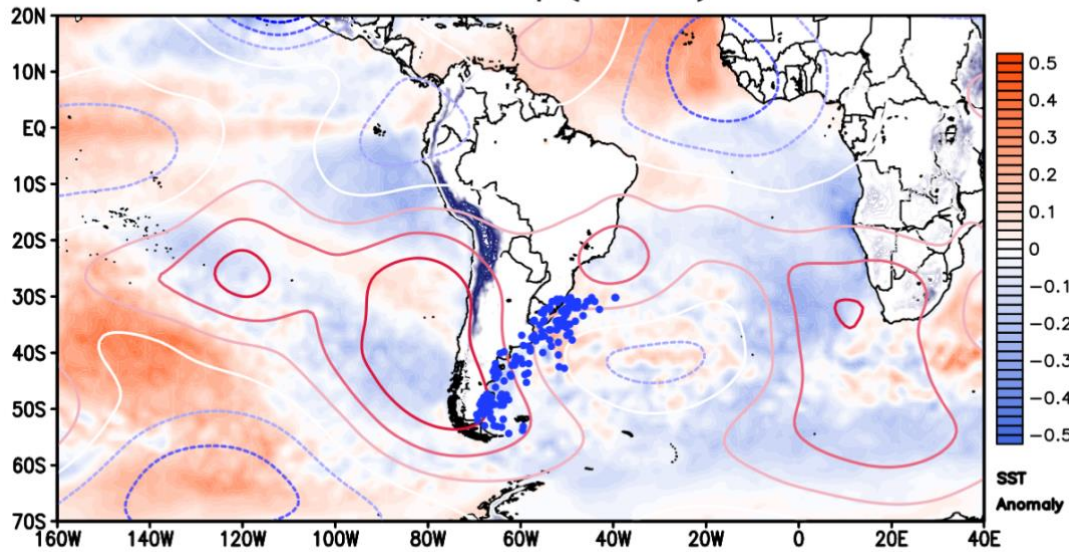


Figure 31: Annual composite stream function anomalies (contours) and SST anomalies (shading) for years with low frequencies of coastal cyclogenesis. Positive (negative) stream function values in the southern hemisphere indicate a cyclonic (anti-cyclonic) anomaly or a low (high) pressure area.

The lower-number composite for lee ECs (Figure 28) suggests El Niño-related circulations induce a less amplified frontal zone over the Andes range. Figure 33 suggests a different pattern for warm period analysis: a strong La Nina event in lee low cases, different from observed from the annual analysis. The low number of geneses may be associated with little difference in sst values between the Pacific coast when compared to the Atlantic Ocean coast, and that also explains the lack of number of geneses on lee annual analysis. Even when are analyzed coastal low cases (Figure 35) show a negative anomaly associated with La Niña events, the lack of sst difference between the Pacific coast of South America and the Atlantic coast of South America may explain the lower number of geneses. Nonetheless, it's presenting a cold portion of water on the Brazilian coast (between 5°S and 30°S), indicating no temperature gradient strong enough between Pacific and Atlantic areas to lead instability.

We also note an intriguing feature, that is, the apparent SST anomaly seesaw between the south Pacific and south Atlantic oceans. By combining the major SST features from figures 28, and 36 to figures 31, 35, and 39, one can infer that a colder Pacific and warmer Atlantic SST anomaly setting is associated with

more lee cases and fewer coastal cases, and vice versa. It is arguable that such an SST seesaw sandwiching South America may directly force the regional circulation change more so than the tropical feature of ENSO does. In the ensuing analysis, we will focus on the annual numbers due to the lack of seasonality in EC frequencies and the apparent inter-decadal modulation.

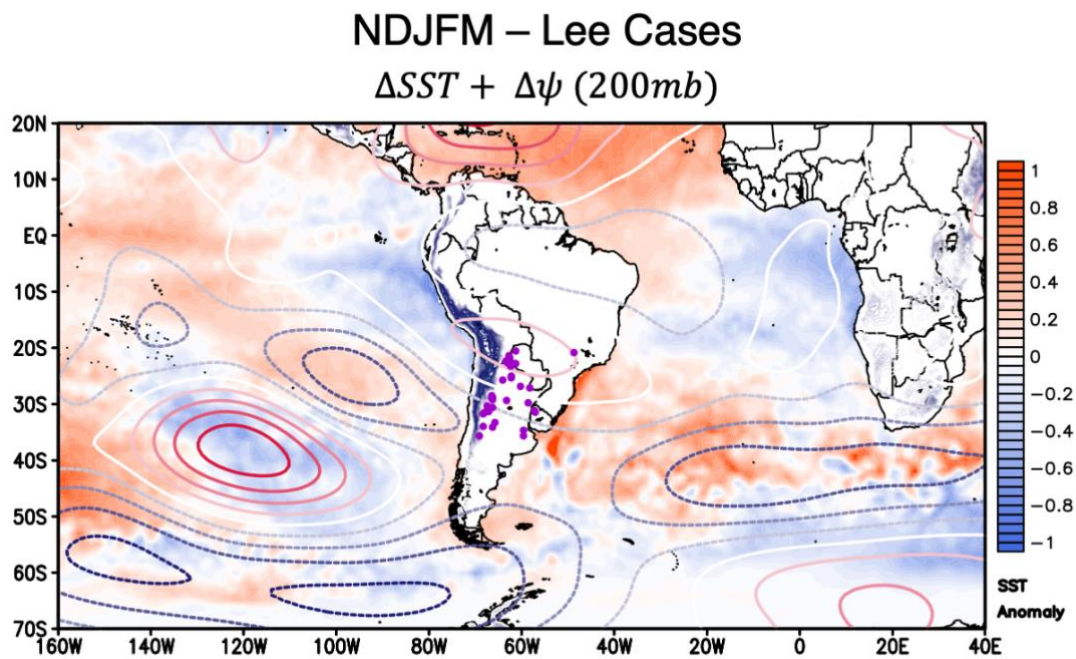


Figure 32: November to March composite stream function anomalies (contours) and SST anomalies (shading) for years with high frequencies of lee cyclogenesis. Positive (negative) stream function values in the southern hemisphere indicate a cyclonic (anti-cyclonic) anomaly or a low (high) pressure area.

NDJFM – Lee Low Cases $\Delta SST + \Delta\psi$ (200mb)

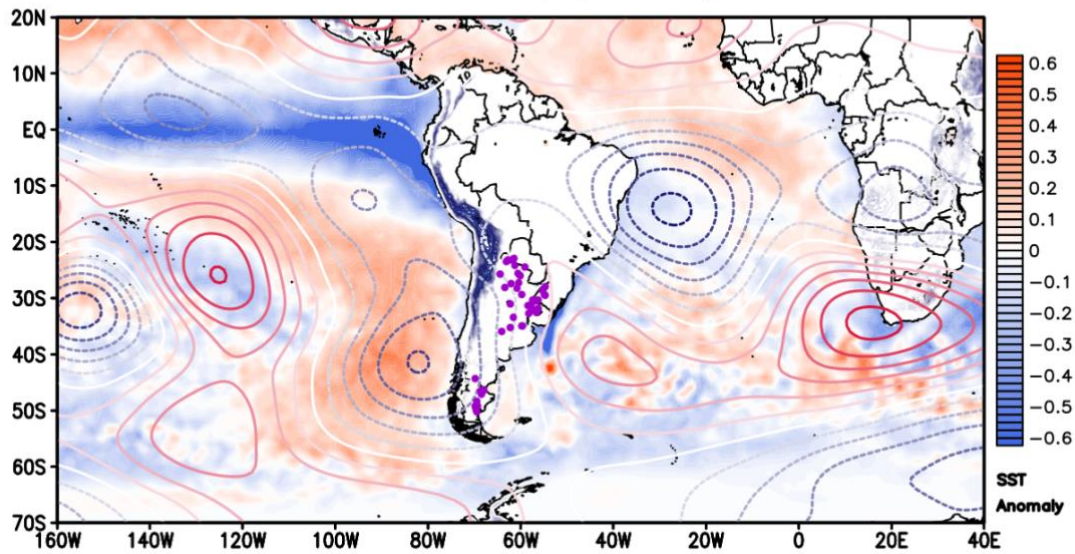


Figure 33: November to March composite stream function anomalies (contours) and SST anomalies (shading) for years with low frequencies of lee cyclogenesis. Positive (negative) stream function values in the southern hemisphere indicate a cyclonic (anti-cyclonic) anomaly or a low (high) pressure area.

NDJFM – Coastal Cases $\Delta SST + \Delta\psi$ (200mb)

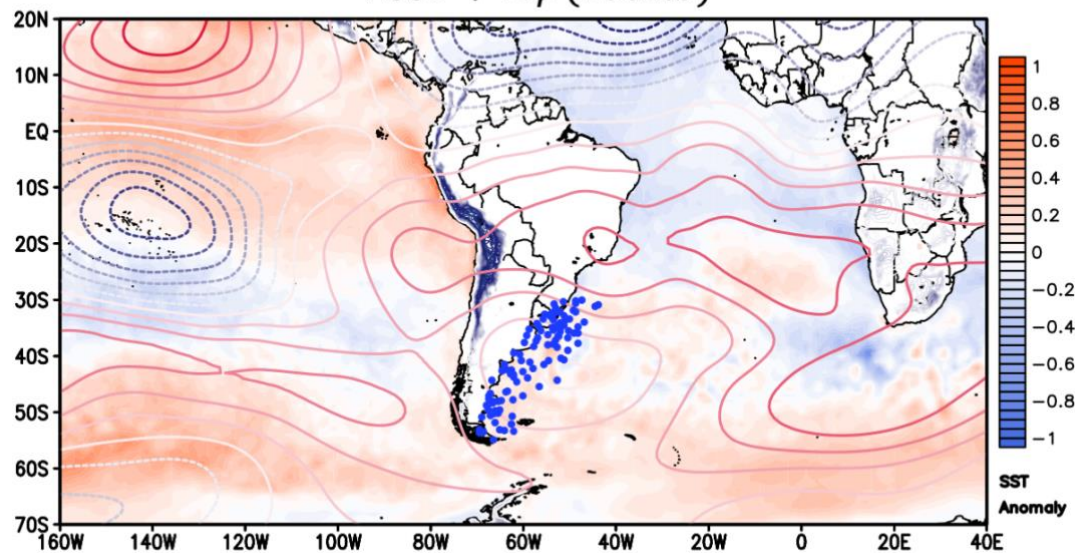


Figure 34: November to March composite stream function anomalies (contours) and SST anomalies (shading) for years with high frequencies of coastal cyclogenesis. Positive (negative) stream function values in the southern hemisphere indicate a cyclonic (anti-cyclonic) anomaly or a low (high) pressure area.

NDJFM – Coastal Low Cases

$\Delta SST + \Delta \psi$ (200mb)

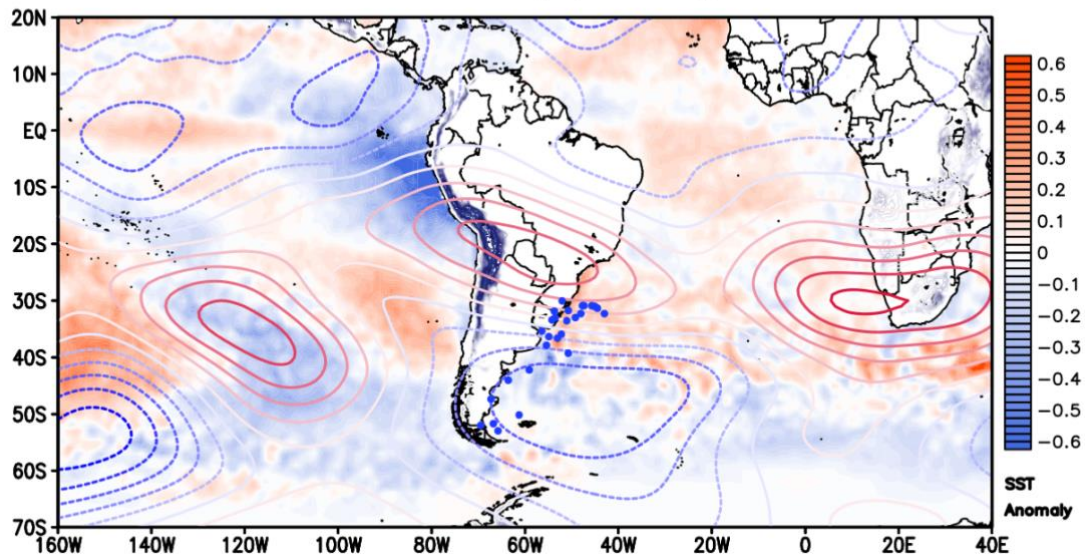


Figure 35: November to March composite stream function anomalies (contours) and SST anomalies (shading) for years with low frequencies of coastal cyclogenesis. Positive (negative) stream function values in the southern hemisphere indicate a cyclonic (anti-cyclonic) anomaly or a low (high) pressure area.

MJJAS – Lee Cases

$\Delta SST + \Delta \psi$ (200mb)

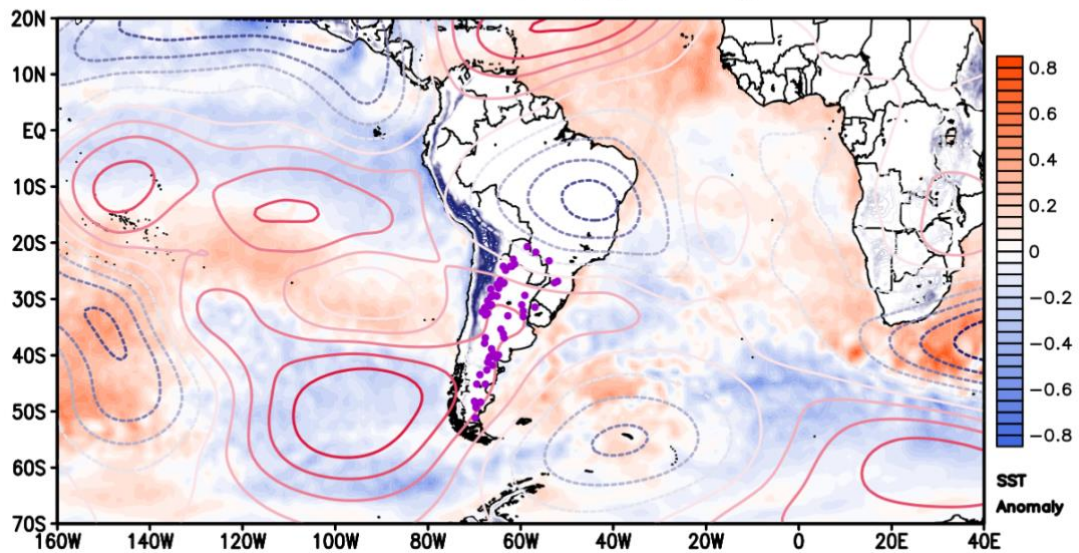


Figure 36: May to September composite stream function anomalies (contours) and SST anomalies (shading) for years with high frequencies of lee cyclogenesis. Positive (negative) stream function values in the southern hemisphere indicate a cyclonic (anti-cyclonic) anomaly or a low (high) pressure area.

MJJAS – Lee Low Cases

$\Delta SST + \Delta \psi$ (200mb)

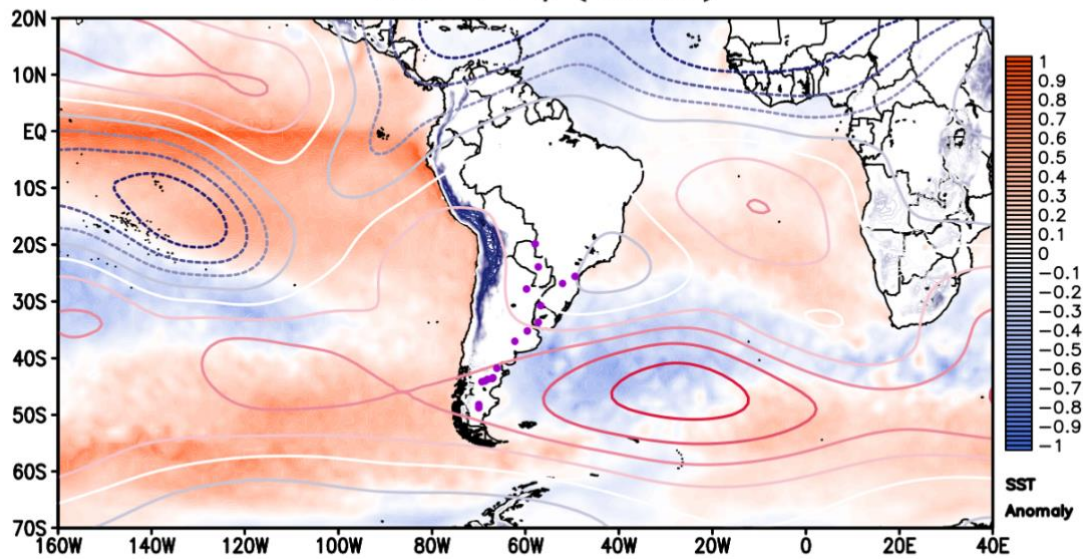


Figure 37: May to September composite stream function anomalies (contours) and SST anomalies (shading) for years with low frequencies of lee cyclogenesis. Positive (negative) stream function values in the southern hemisphere indicate a cyclonic (anti-cyclonic) anomaly or a low (high) pressure area.

MJJAS – Coastal Cases

$\Delta SST + \Delta \psi$ (200mb)

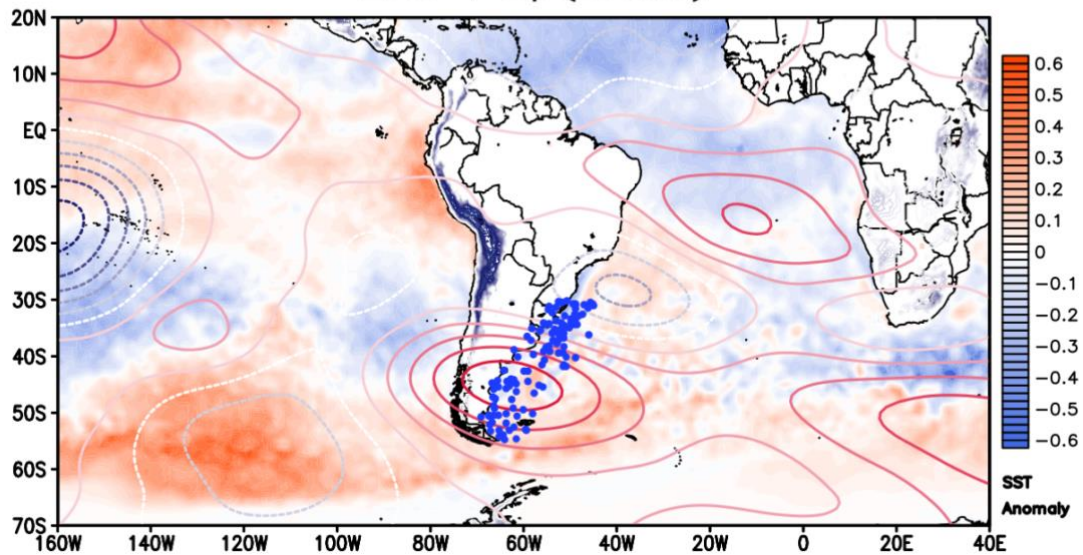


Figure 38: May to September composite stream function anomalies (contours) and SST anomalies (shading) for years with high frequencies of coastal cyclogenesis. Positive (negative) stream function values in the southern hemisphere indicate a cyclonic (anti-cyclonic) anomaly or a low (high) pressure area.

MJJAS – Coastal Low Cases

$\Delta SST + \Delta \psi$ (200mb)

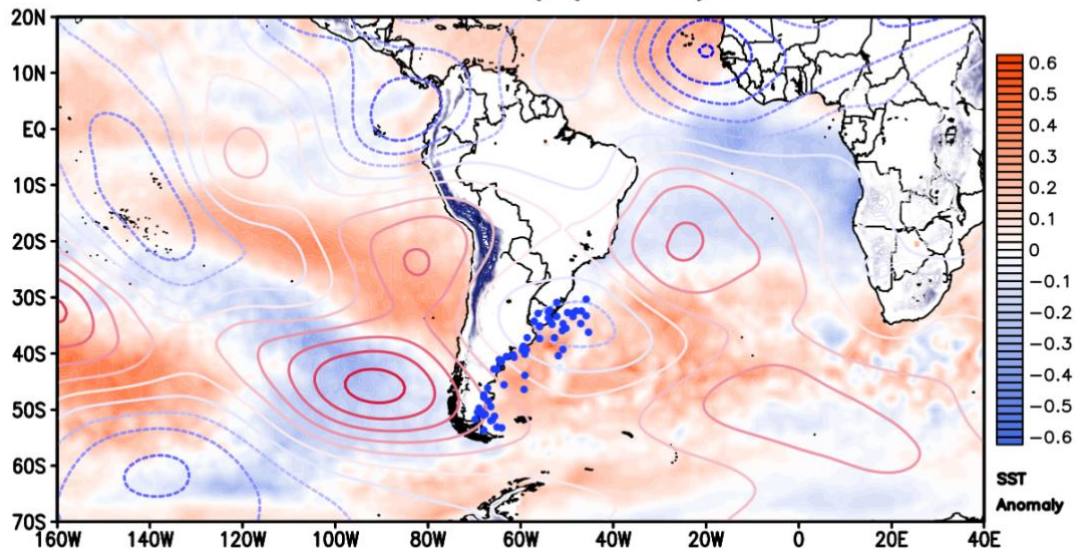


Figure 39: May to September composite stream function anomalies (contours) and SST anomalies (shading) for years with low frequencies of coastal cyclogenesis. Positive (negative) stream function values in the southern hemisphere indicate a cyclonic (anti-cyclonic) anomaly or a low (high) pressure area.

3.3 MECHANISMS DRIVING THE LEE AND COASTAL CYCLOGENESIS VARIATIONS

The composite analysis of stream function and SST anomalies indicates that an amplified pressure gradient centered over the Andes is commonly associated with more frequent lee cyclogenesis, while a more elongated cyclonic circulation anomaly is associated with coastal cyclogenesis. To affirm that the general circulation features from Figure 6 are indeed resulting in different cyclogenesis mechanisms, we evaluate the vorticity budget for the same grouping of years from the previous composites. Vorticity advection (Equation 4) is an important contributor to developing cyclones and is associated with convective activity, often driven by thermal contrast or diurnal heating alongside large mountains (Banta, 1986, 1984; Wang et al., 2011). The vortex stretching component of the vorticity generation process (Equation 5) is effective for showing topographical impacts on the generation of atmospheric disturbances, as airflow over a mountain can result in positive vorticity generation due to the lengthening of the air

column (Gan & Rao, 1994; Wang et al., 2011). It has also been shown that westerly flow over terrain can generate lee-side vorticity generation when directional wind shear is present (Wang et al., 2011), a feature that can be seen in figures 40, 44, and 48 due to the frontal boundary over the Andes.

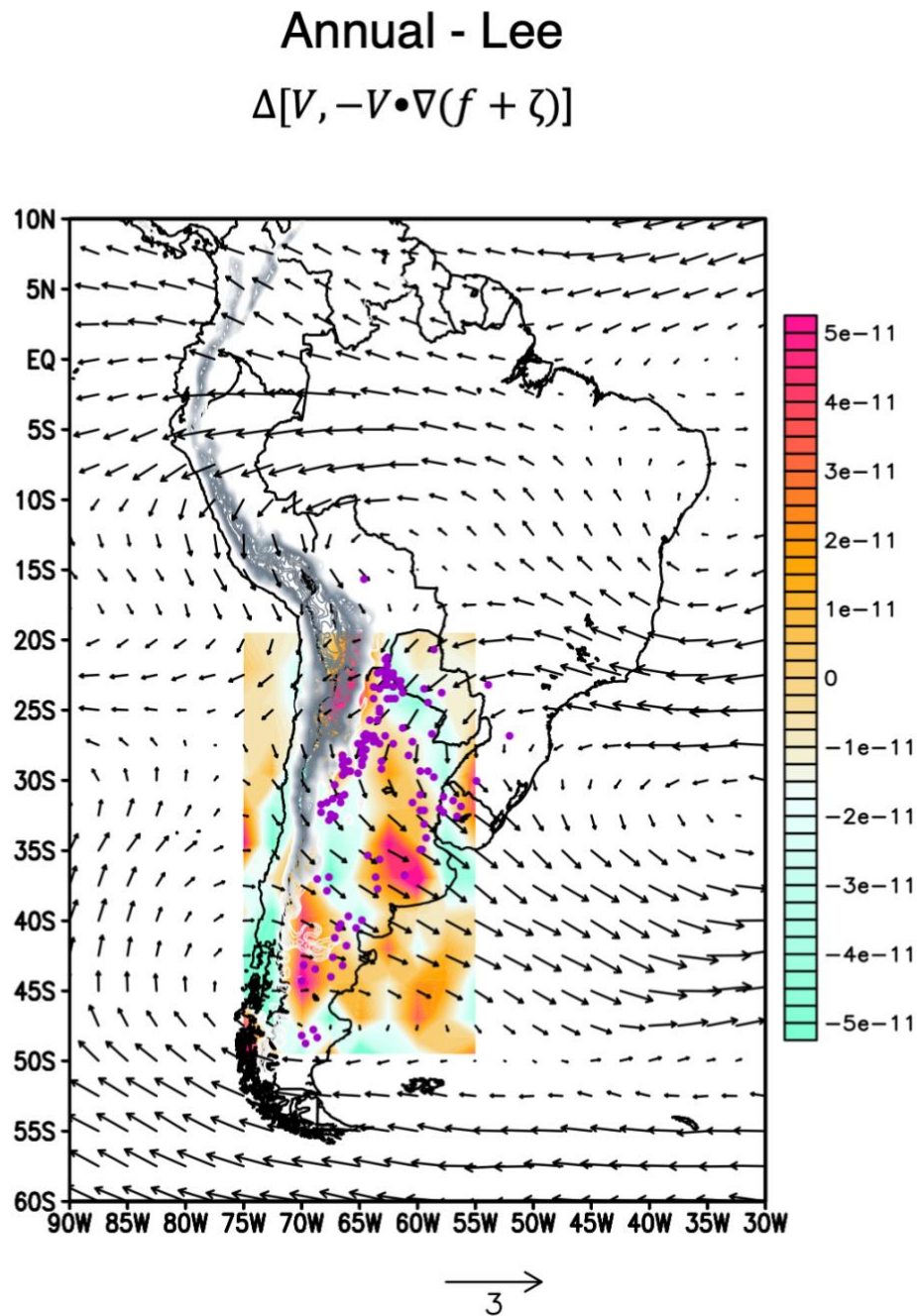


Figure 40: Annual analysis for lee cases using vorticity advection averaged for the upper troposphere (500 hPa) across 50°S 20°S with 500 hPa wind vectors.

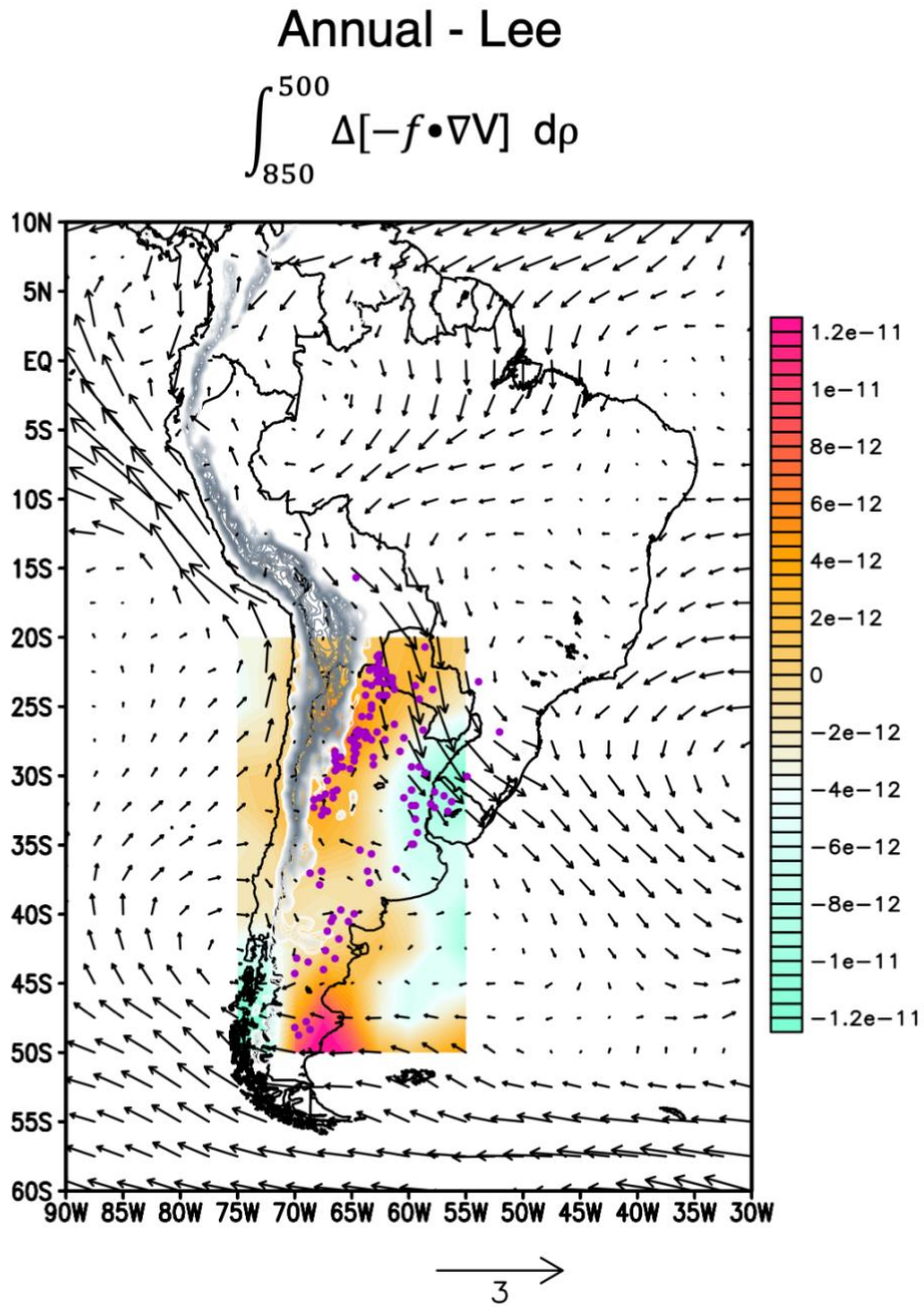


Figure 41: Vortex stretching analysis for the lower troposphere from 850–500 hPa across 50°S–20°S and with 850 hPa wind vectors for lee cases considering annual analysis.

Annual - Coastal

$$\Delta[V, -V \cdot \nabla(f + \zeta)]$$

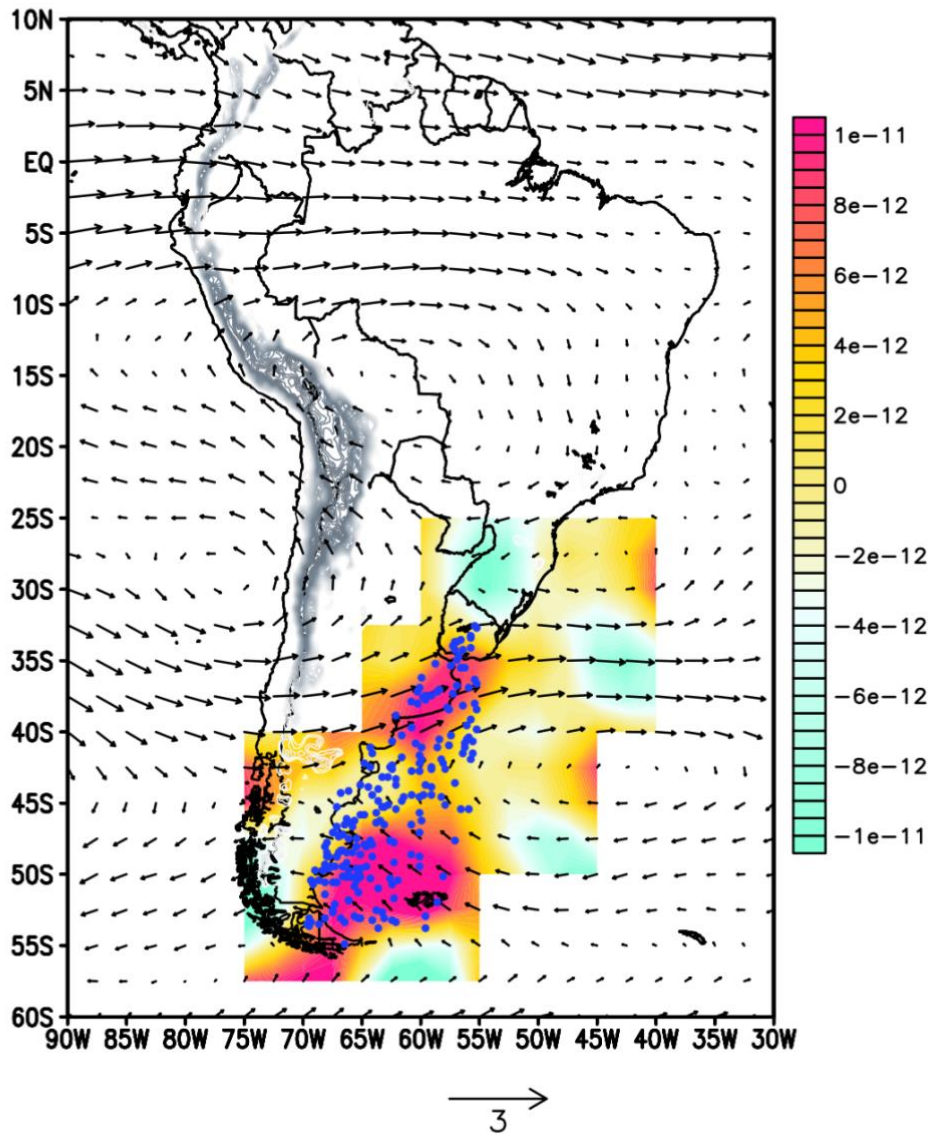


Figure 42: Annual analysis for coastal cases using vorticity advection averaged for the upper troposphere (500 hPa) across 55°S 25°S with 500 hPa wind vectors.

Annual - Coastal

$$\int_{1000}^{850} \Delta[-f \cdot \nabla V] \, d\rho$$

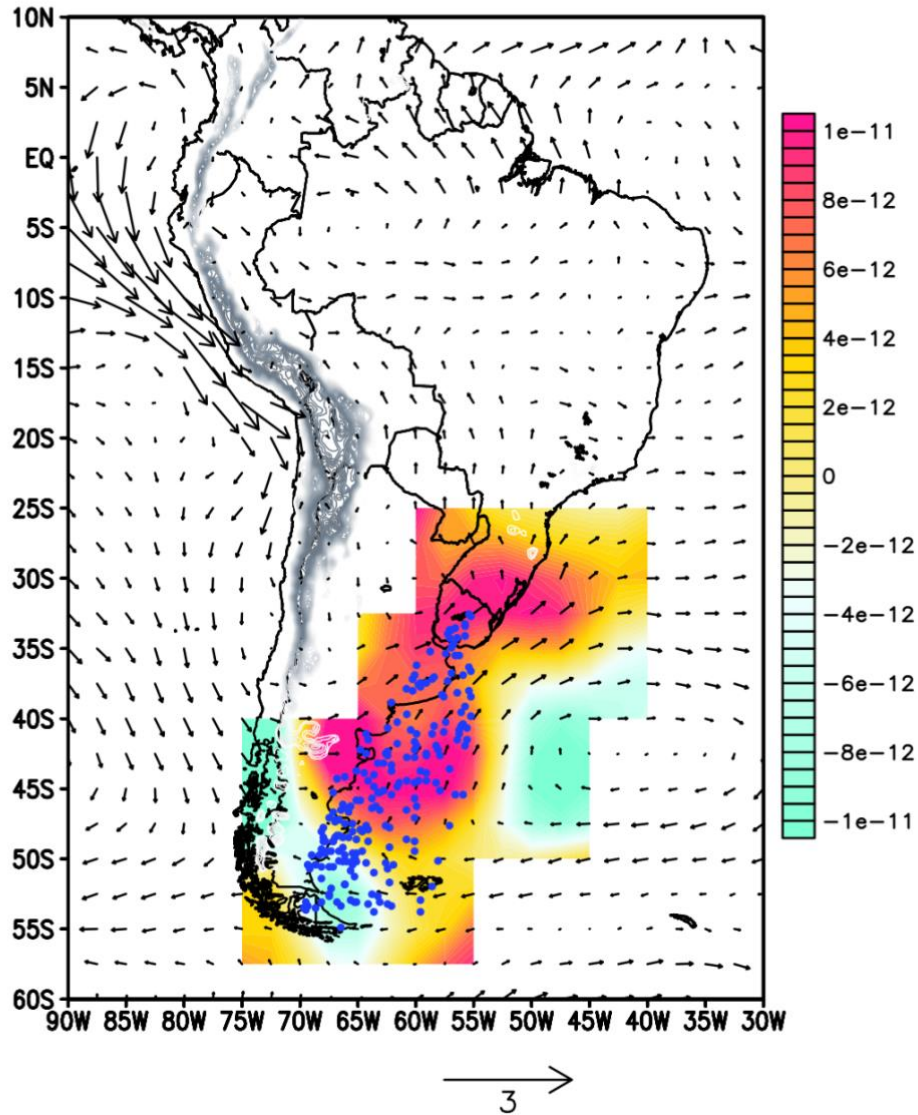


Figure 43: Vortex stretching analysis for the lower troposphere from 1000–850 hPa across 55°S–25°S and with 850 hPa wind vectors for coastal cases considering annual analysis.

For the lee cyclones, instability in the cyclogenesis locations (shown in purple dots) on in annual period is generated mostly by vortex stretching as positive vortex stretching values adjacent to cyclogenesis regions are seen more prominently in (Figure 41) than the effect of vorticity advection in (Figure 40). However, the coastal composites depict a stronger contribution from vorticity advection (Figure 42) than is present in the lee composites (Figure 40), with more positive values of vorticity located around

cyclogenesis regions (Figure 42). Noteworthy, for warm (Figure 44) and cold periods (Figure 48), lee cyclogenesis seems to have a stronger response in vortex stretching when compared to the annual mean, even stronger during the warm period. Vortex stretching is still prominently featured in the coastal regions, showing that both mechanisms play an important role in coastal flow instability, showing a stronger contribution in annual mean valuation.

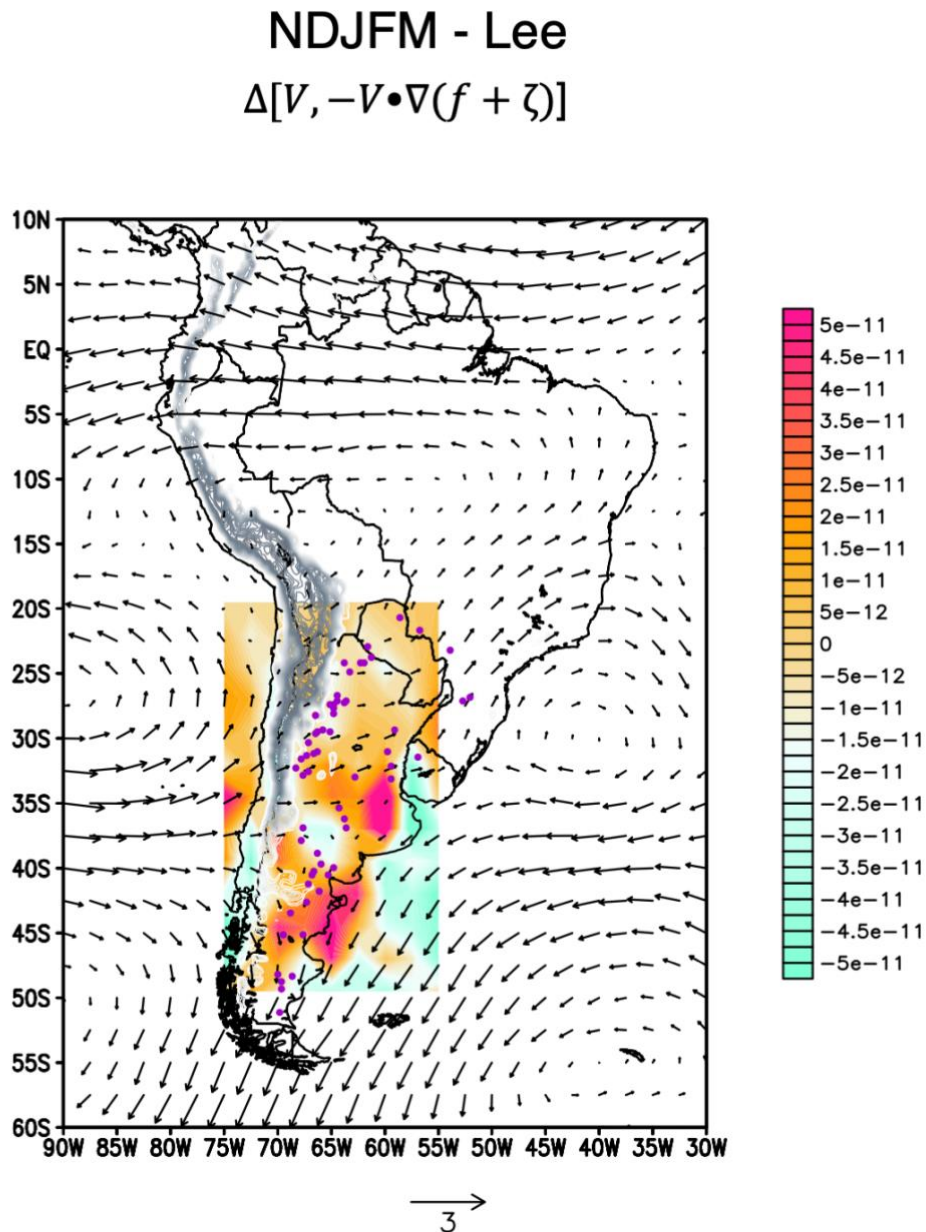


Figure 44: Warm period analysis for lee cases using vorticity advection averaged for the upper troposphere (500 hPa) across 50°S 20°S with 500 hPa wind vectors.

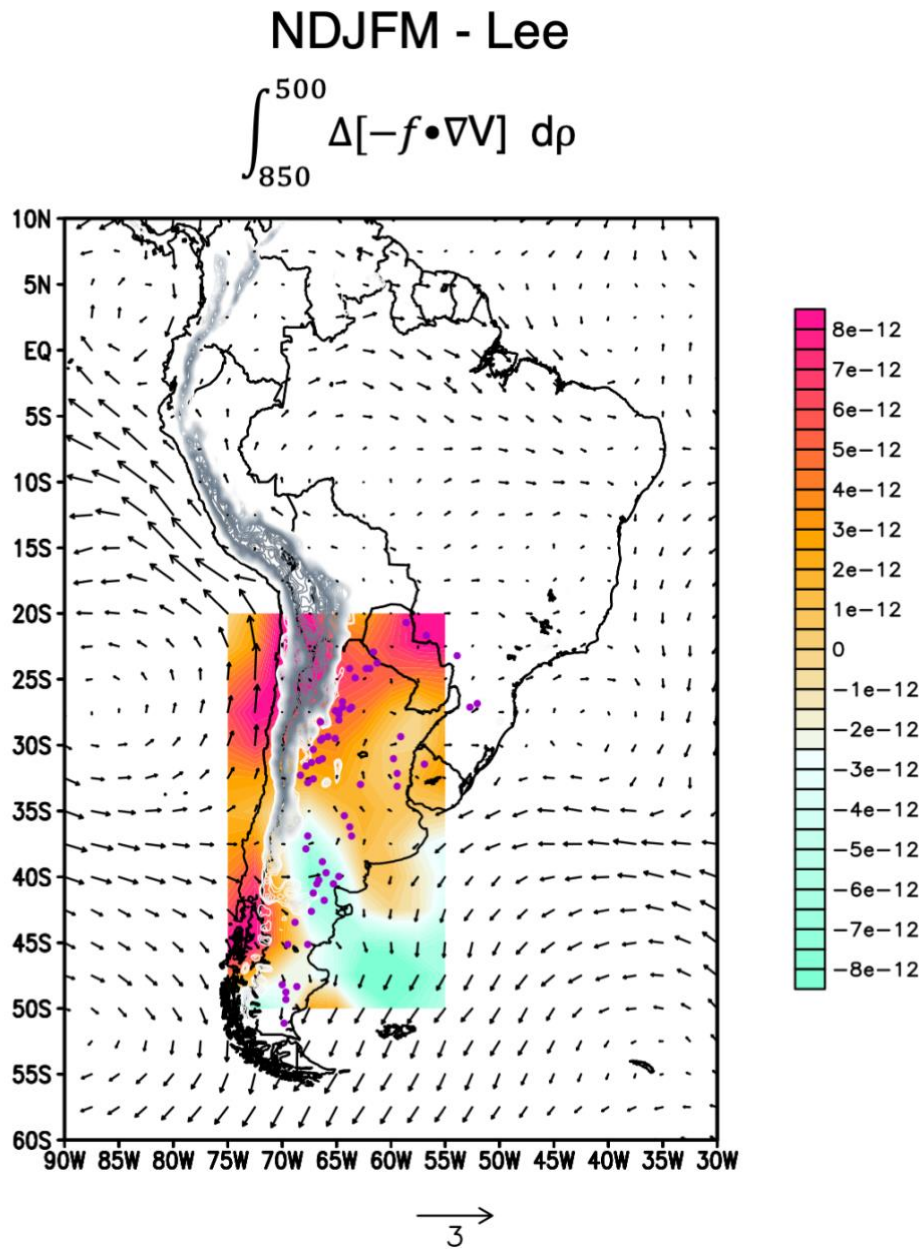


Figure 45: Vortex stretching analysis for the lower troposphere from 850–500 hPa across 50°S 20°S and with 850 hPa wind vectors for lee cases considering warm period analysis.

NDJFM - Coastal

$$\Delta[V, -V \cdot \nabla(f + \zeta)]$$

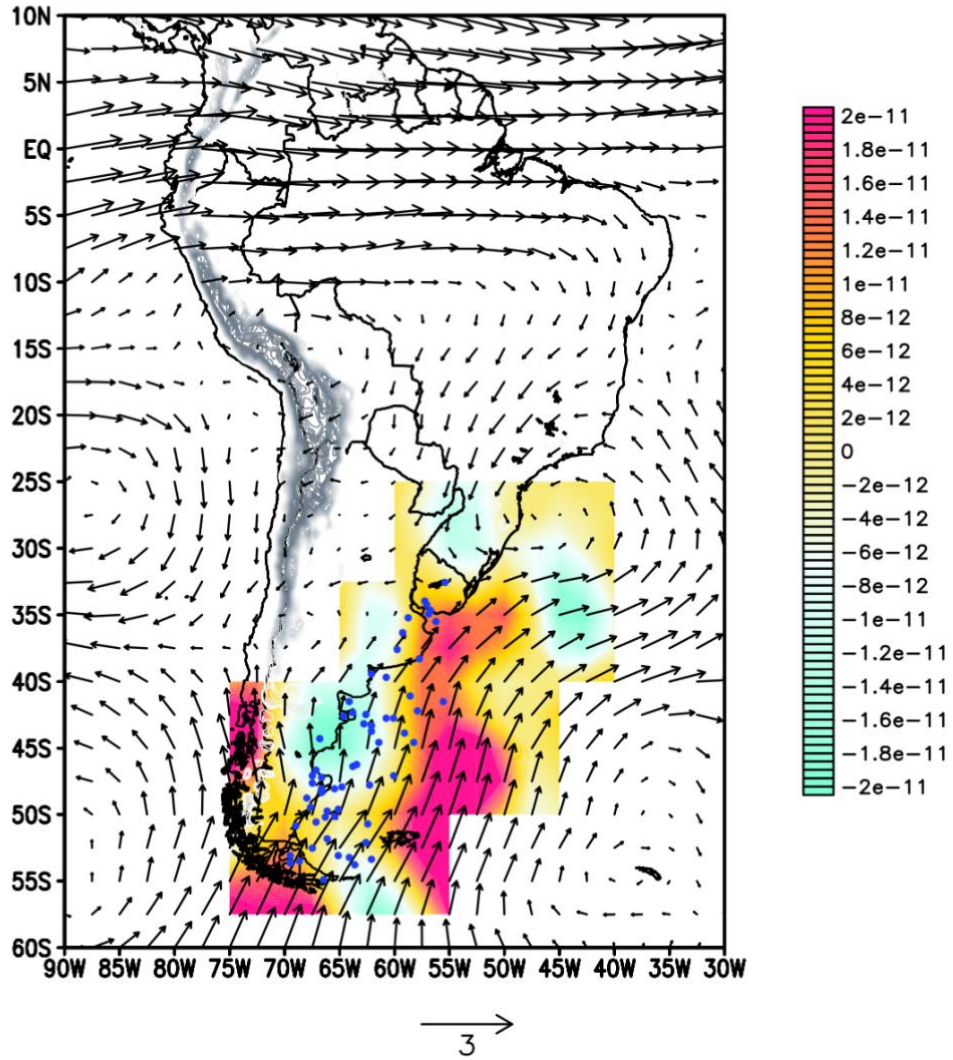


Figure 46: Warm period analysis for coastal cases using vorticity advection averaged for the upper troposphere (500 hPa) across 55°S 25°S with 500 hPa wind vectors.

NDJFM - Coastal

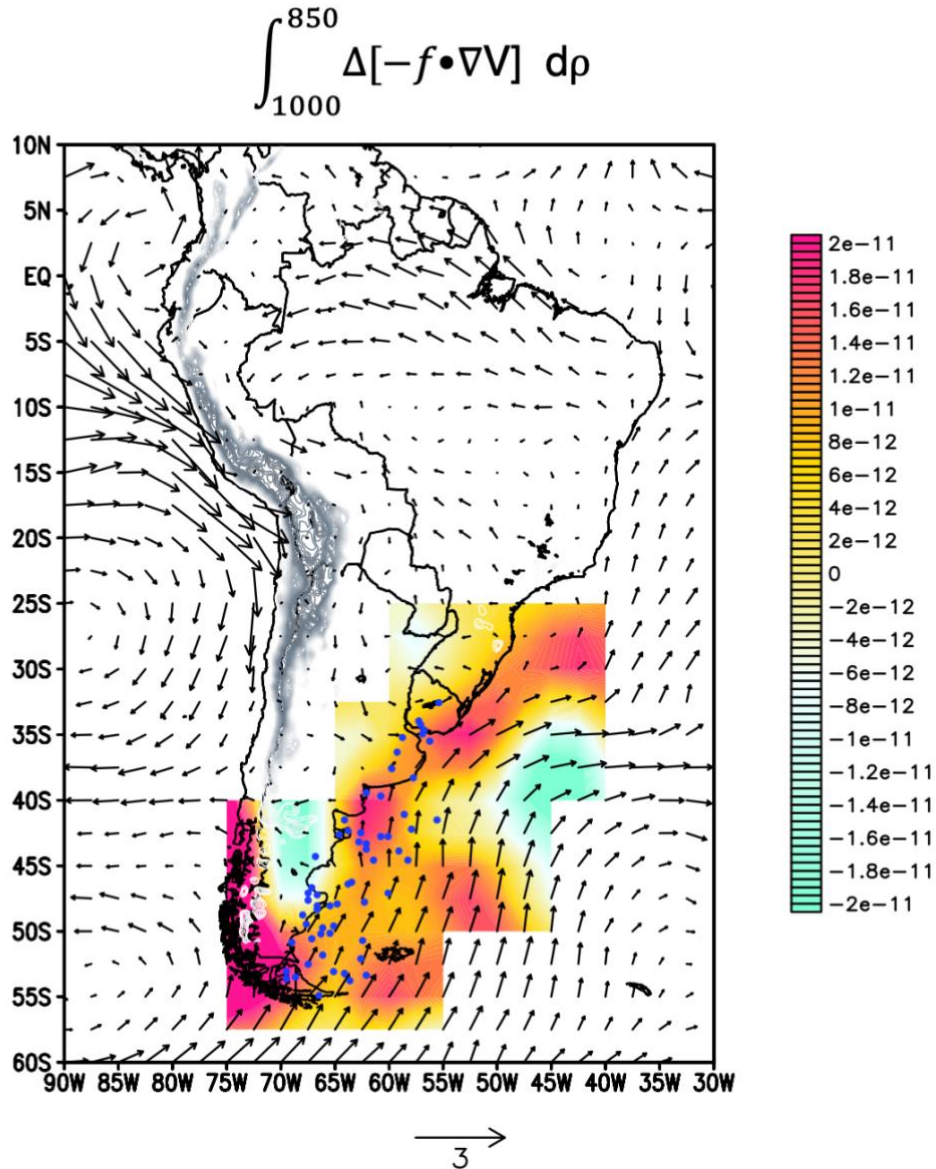


Figure 47: Vortex stretching analysis for the lower troposphere from 1000–850 hPa across 55°S 25°S and with 850 hPa wind vectors for coastal cases considering warm period analysis.

The prevalence of both positive vortex stretching and positive vorticity advection at the coast may explain why coastal cyclogenesis is more frequently relative to lee cyclogenesis. The proximity of the coast and warm western boundary currents to the Andes range allows for coastal cyclones to generate from vortex stretching from terrain influences and from vorticity advection due to thermal gradients.

MJJAS - Lee

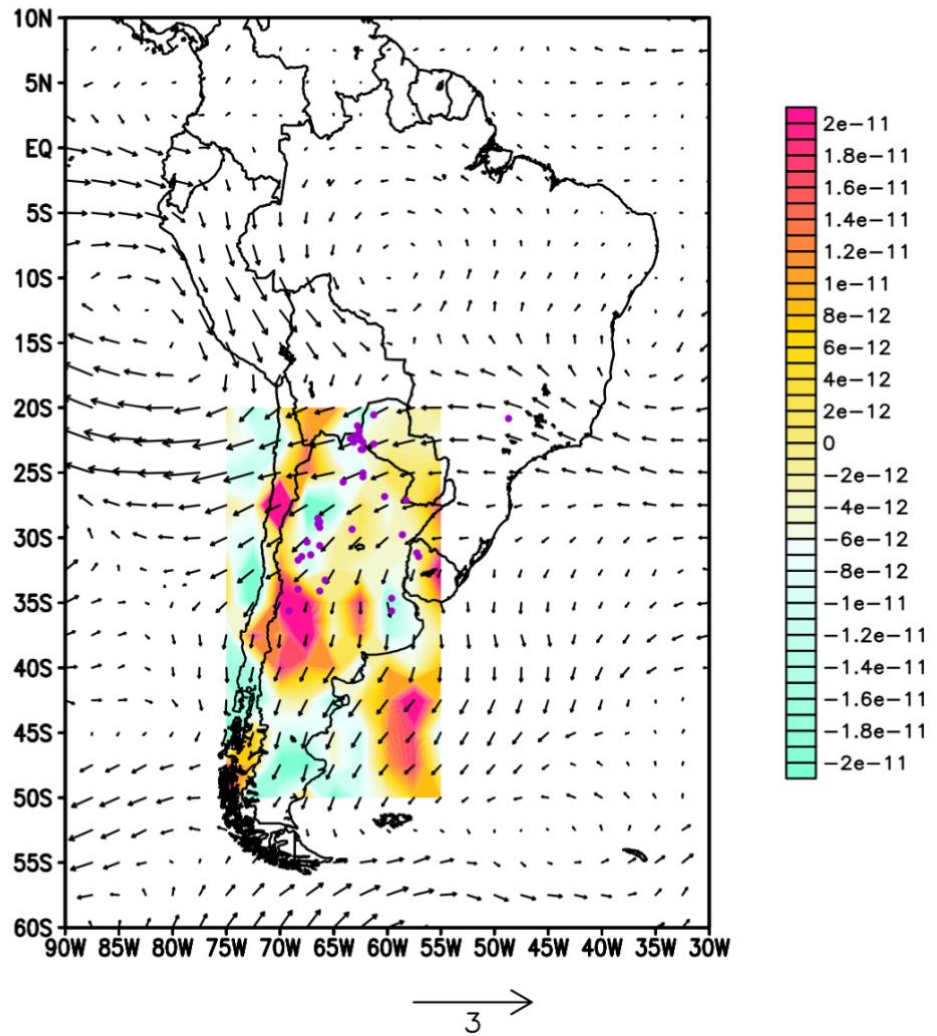
$$\Delta[V, -V \cdot \nabla(f + \zeta)]$$


Figure 48: Cold period analysis for lee cases using vorticity advection averaged for the upper troposphere (500 hPa) across 50°S 20°S with 500 hPa wind vectors.

MJJAS - Lee

$$\int_{850}^{500} \Delta[-f \cdot \nabla V] \, d\rho$$

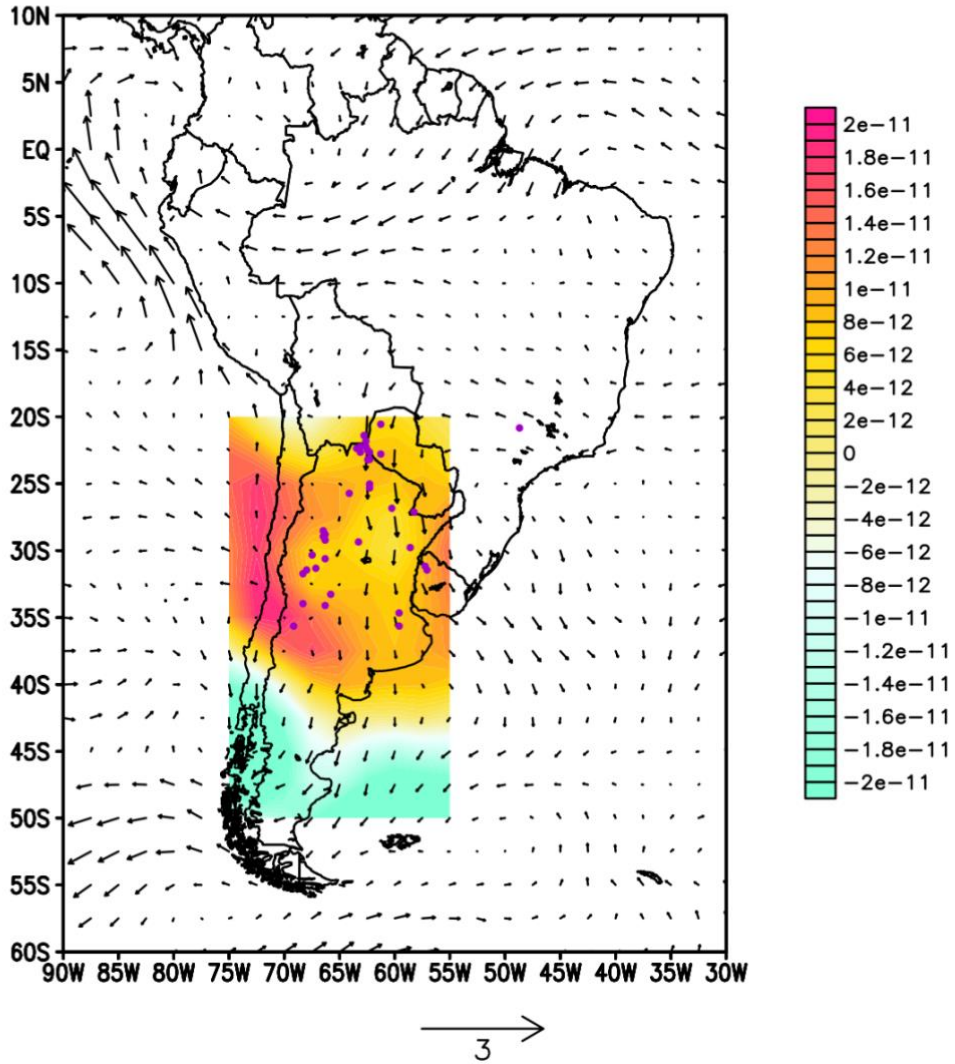


Figure 49: Vortex stretching analysis for the lower troposphere from 850–500 hPa across 50°S 20°S and with 850 hPa wind vectors for lee cases considering cold period analysis

MJJAS - Coastal

$$\Delta[V, -V \cdot \nabla(f + \zeta)]$$

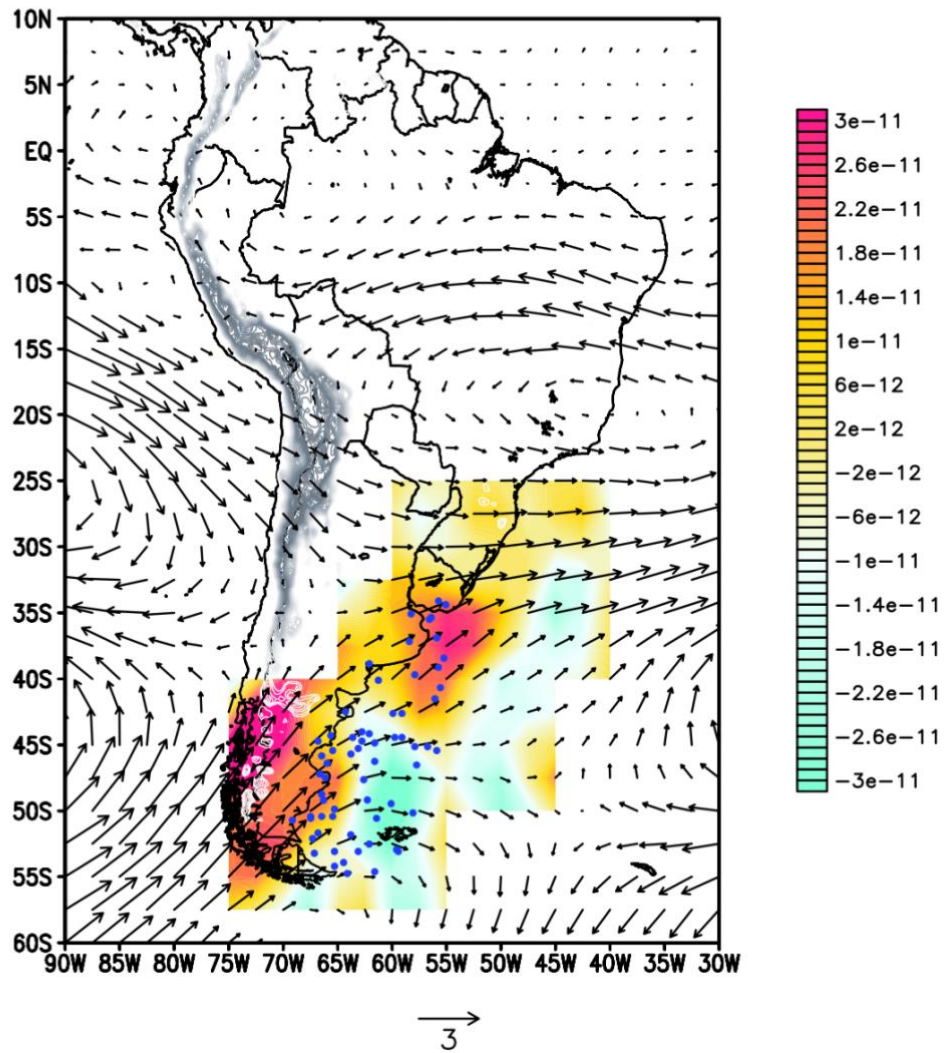


Figure 50: Cold period analysis for coastal cases using vorticity advection averaged for the upper troposphere (500 hPa) across 55°S 25°S with 500 hPa wind vectors.

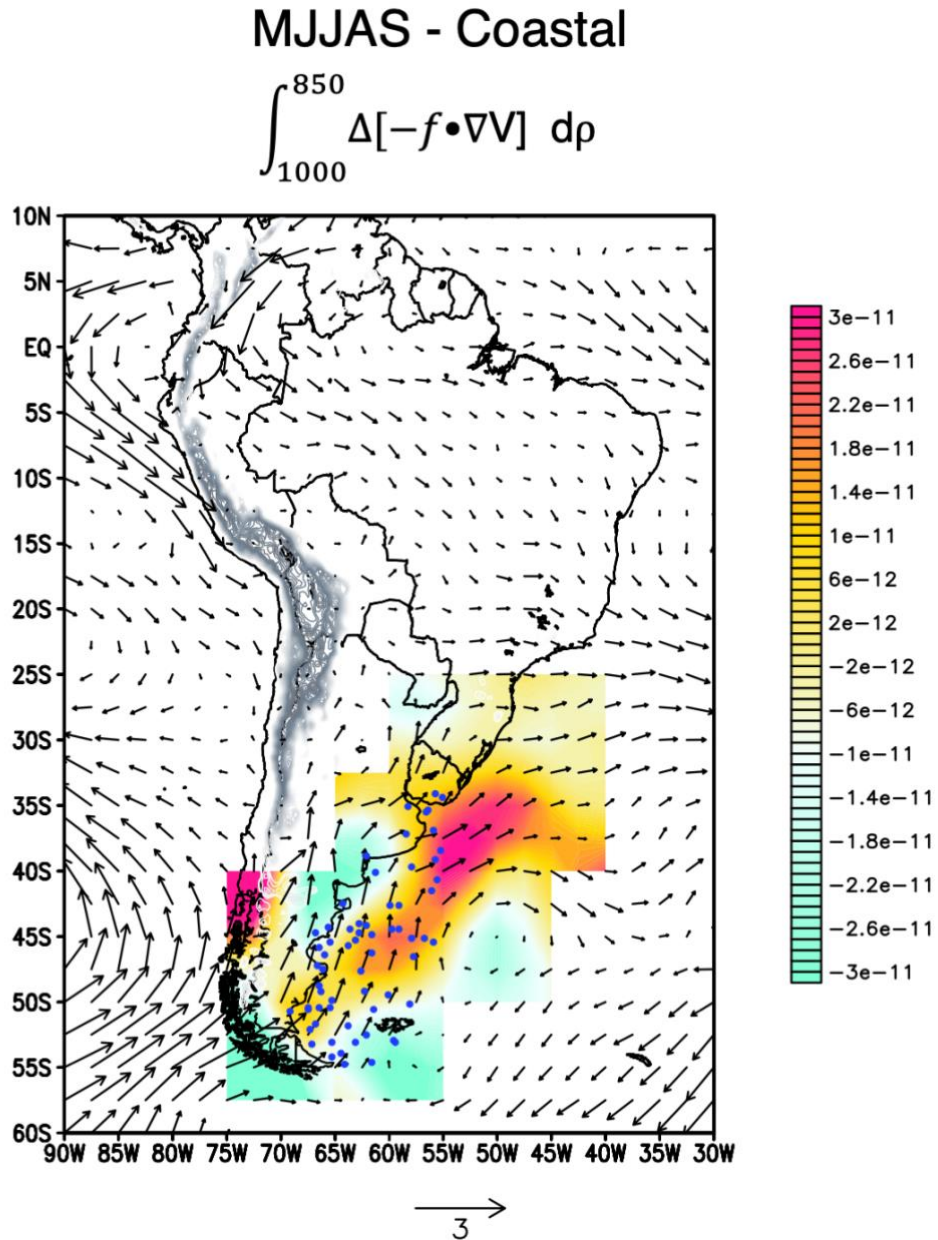


Figure 51: Vortex stretching analysis for the lower troposphere from 1000–850 hPa across 55°S 25°S and with 850 hPa wind vectors for coastal cases considering cold period analysis.

4 DISCUSSION AND CONCLUSIONS

By analyzing a modern, high-resolution reanalysis dataset with comparison to the Navy weather charts, a baseline climatology for South American ECs is provided, and circulation features that preferentially select for cyclogenesis in both lee and coastal cyclogenesis are highlighted. These results support earlier findings that cyclogenesis is

most common in coastal regions (Gan & Rao, 1991), but the ERA5 and MB tracking also shows that cyclogenesis is commonly initiated inland on the lee side of the Andes mountains. While the ERA5 and MB analyses result in somewhat different seasonal climatologies for lee cyclones, the datasets agree that coastal cyclones are more common during the warm season, between November through March, while lee ECs are more prevalent in the cold season. Lee cyclogenesis relies on directional wind shear adjacent to the mountain range, while coastal instability can be generated by either vortex stretching or vorticity advection, or both.

Through this newly constructed EC climatology, we noted an inter-decadal "seesaw" in the frequencies between lee and coast cyclogenesis, a previously undocumented feature. Lee cases seem to have an anticorrelated behavior compared to coastal cases, and SST differences between the Pacific and Atlantic oceans over time may trigger that behavior. In terms of climate variability affecting the ECs, Garreaud & Wallace (1998) have shown that the trough–ridge dipole (as revealed in Figure 6a) centered over the Andes mountains provides the dynamic forcing for these summer instabilities due to directional wind shear. In the wintertime, transient disturbances associated with the Andes topography most commonly result in temperature drops and wind events rather than cyclogenesis due to the lack of surface heating to boost convective potential. While instability generation mechanisms differ across the region, these factors likely contribute to the muted seasonal cycle of ECs over South America (Crespo et al., 2021; Garreaud & Wallace, 1998).

The Andes have long been established as a forcing mechanism for local instability (Funatsu et al., 2004; Gan & Rao, 1994). This study shows that the Andes' influence on instability is heightened due to a trough–ridge dipole which saddles the mountain range. This circulation anomaly induces more directional wind shear, resulting in vortex stretching and positive vorticity generation on the lee side of the range. This atmospheric circulation anomaly is associated with La Niña-like conditions, with negative SST anomalies on the west coast of the continent coupled with warmer south Atlantic water. Coastal cyclones become more frequent under El Niño-like conditions when a broad region of cyclonic circulation settles over the south Atlantic. The vorticity budget analysis shows that both vortex stretching and vorticity advection contribute to cyclogenesis during years with more frequent coastal cyclones; this is the potential cause of the greater

frequency of coastal cyclones in the region, as more atmospheric factors exist near the coast for generating instability.

Due to the difference in circulation features and ENSO phase associated with lee and coastal cyclogenesis, seasonal forecasting of cyclone risk or potential may benefit from considering semi-stationary features such as ENSO or the cross-basin SST difference and the associated trough-ridge dipole in the upper troposphere. The result of this empirical analysis serves as an important baseline for future studies concerned with South American ECs.

REFERENCES

- Andreoli, R. v., Ferreira, S.H.S., Sapucci, L.F., Souza, R.A.F. de, Mendonça, R.W.B., Herdies, D.L., Aaravéquia, J.A., 2008. Contribuição de diversos sistemas de observação na previsão de tempo no CPTEC/INPE. *Revista Brasileira de Meteorologia* 23, 219–238. <https://doi.org/10.1590/S0102-77862008000200009>
- Balaguru, K., Foltz, G.R., Leung, L.R., Kaplan, J., Xu, W., Reul, N., Chapron, B., 2020. Pronounced impact of salinity on rapidly intensifying tropical cyclones. *Bulletin of the American Meteorological Society preprint*, BAMS-D-19-0303.1. <https://doi.org/10.1175/BAMS-D-19-0303.1>
- Banta, R.M., 1986. Daytime Boundary Layer Evolution over Mountainous Terrain. Part II: Numerical Studies of Upslope Flow Duration. *Monthly Weather Review* 114, 1112–1130. [https://doi.org/10.1175/1520-0493\(1986\)114<1112:DBLEOM>2.0.CO;2](https://doi.org/10.1175/1520-0493(1986)114<1112:DBLEOM>2.0.CO;2)
- Banta, R.M., 1984. Daytime Boundary-Layer Evolution over Mountainous Terrain. Part 1: Observations of the Dry Circulations. *Monthly Weather Review* 112, 340–356. [https://doi.org/10.1175/1520-0493\(1984\)112<0340:DBLEOM>2.0.CO;2](https://doi.org/10.1175/1520-0493(1984)112<0340:DBLEOM>2.0.CO;2)
- Bernardino, B.S., Vasconcellos, F.C., Nunes, A.M.B., 2018. Impact of the equatorial Pacific and South Atlantic SST anomalies on extremes in austral summer precipitation over Grande river basin in Southeast Brazil. *International Journal of Climatology* 38, e131–e143. <https://doi.org/10.1002/joc.5358>
- Bjerknes, J., 1919. On the Structure of Moving Cyclones. *Monthly Weather Review* 47, 95–99. [https://doi.org/10.1175/1520-0493\(1919\)47<95:OTSOMC>2.0.CO;2](https://doi.org/10.1175/1520-0493(1919)47<95:OTSOMC>2.0.CO;2)
- Bjerknes, J., Holmboe, J., 1944. On The Theory Of Cyclones. *Journal of Meteorology* 1, 1–22. [https://doi.org/10.1175/1520-0469\(1944\)001<0001:OTTOC>2.0.CO;2](https://doi.org/10.1175/1520-0469(1944)001<0001:OTTOC>2.0.CO;2)
- Bjerknes, J., Solberg, H., 1922. Life cycle of cyclones and the polar front theory of atmospheric circulation. *Geophysisks Publikationer* 3, 16. <https://doi.org/10.1002/qj.49704920609>
- Blender, R., Schubert, M., 2000. Cyclone Tracking in Different Spatial and Temporal Resolutions. *American Meteorological Society* 8. [https://doi.org/10.1175/1520-0493\(2000\)128<0377:CTIDSA>2.0.CO;2](https://doi.org/10.1175/1520-0493(2000)128<0377:CTIDSA>2.0.CO;2)
- Boffi, J.A., 1949. Effect of the Andes Mountains on the General Circulation Over the Southern Part of South America. *Bulletin of the American Meteorological Society* 30, 242–247. <https://doi.org/10.1175/1520-0477-30.7.242>

- Bombardi, R.J., Carvalho, L.M.V., Jones, C., Reboita, M.S., 2014. Precipitation over eastern South America and the South Atlantic Sea surface temperature during neutral ENSO periods. *Climate Dynamics* 42, 1553–1568. <https://doi.org/10.1007/s00382-013-1832-7>
- Brasil, M. do, 2020. Glossário de Termos aplicados à Meteorologia Marinha.
- Brasil, M. do, 2018. CARTA DE SERVIÇOS AO USUÁRIO.
- Caetano Neto, E.S., Innocentini, V., Rocha, R.P. da, 1996. Um sistema de previsão de tempo e de ondas oceânicas para o Atlântico Sul. *Revista Brasileira de Oceanografia* 44, 35–46. <https://doi.org/10.1590/S1413-77391996000100004>
- Campos, E.J.D., Lentini, C.A.D., Miller, J.L., Piola, A.R., 1999. Interannual variability of the sea surface temperature in the South Brazil Bight. *Geophysical Research Letters* 26, 2061–2064. <https://doi.org/10.1029/1999GL900297>
- Campos, E.J.D., Velhote, D., da Silveira, I.C.A., 2000. Shelf break upwelling driven by Brazil Current Cyclonic Meanders. *Geophysical Research Letters* 27, 751–754. <https://doi.org/10.1029/1999GL010502>
- Candella, R.N., 1997. ESTUDO DE CASOS DE ONDAS NO ATLÂNTICO SUL ATRAVÉS DE MODELAGEM NUMÉRICA. Cambridge University Press, Cambridge.
- Carvalho, L.M. v., Jones, C., Liebmann, B., 2002. Extreme Precipitation Events in Southeastern South America and Large-Scale Convective Patterns in the South Atlantic Convergence Zone. *Journal of Climate* 15, 2377–2394. [https://doi.org/10.1175/1520-0442\(2002\)015<2377:EPEISS>2.0.CO;2](https://doi.org/10.1175/1520-0442(2002)015<2377:EPEISS>2.0.CO;2)
- Cataldi, M., Assad, L.P. de F., Torres Junior, A.R., Alves, J.L.D., 2010. Estudo da influência das anomalias da TSM do Atlântico Sul extratropical na região da Confluência Brasil-Malvinas no regime hidrometeorológico de verão do Sul e Sudeste do Brasil. *Revista Brasileira de Meteorologia* 25, 513–524. <https://doi.org/10.1590/S0102-77862010000400010>
- Catto, J.L., Ackerley, D., Booth, J.F., Champion, A.J., Colle, B.A., Pfahl, S., Pinto, J.G., Quinting, J.F., Seiler, C., 2019. The Future of Midlatitude Cyclones. *Current Climate Change Reports* 5, 407–420. <https://doi.org/10.1007/s40641-019-00149-4>
- Cavallo, E.A., Noy, I., 2009. The Economics of Natural Disasters: A Survey. *SSRN Electronic Journal* 86, 1–11. <https://doi.org/10.2139/ssrn.1817217>
- CHAN, J.C.L., DUAN, Y., SHAY, L.K., 2001. Tropical Cyclone Intensity Change from a Simple Ocean – Atmosphere Coupled Model. *JOURNAL OF THE*

- ATMOSPHERIC SCIENCES 58, 154–172. [https://doi.org/10.1175/1520-0469\(2001\)058<0154:TCICFA>2.0.CO;2](https://doi.org/10.1175/1520-0469(2001)058<0154:TCICFA>2.0.CO;2)
- Charney, J.G., 1947. The Dynamics of Long Waves in a Baroclinic Westerly Current. *Journal of Meteorology* 4, 136–162. [https://doi.org/10.1175/1520-0469\(1947\)004<0136:TDOLWI>2.0.CO;2](https://doi.org/10.1175/1520-0469(1947)004<0136:TDOLWI>2.0.CO;2)
- Chelton, D.B., Schlax, M.G., Witter, D.L., Richman, J.G., 1990. Geosat altimeter observations of the surface circulation of the Southern Ocean. *Journal of Geophysical Research* 95, 17877. <https://doi.org/10.1029/JC095iC10p17877>
- Cinco, T.A., de Guzman, R.G., Ortiz, A.M.D., Delfino, R.J.P., Lasco, R.D., Hilario, F.D., Juanillo, E.L., Barba, R., Ares, E.D., 2016. Observed trends and impacts of tropical cyclones in the Philippines. *International Journal of Climatology* 36, 4638–4650. <https://doi.org/10.1002/joc.4659>
- Cirano, M., Mata, M.M., Campos, E.J.D., Deiró, N.F.R., 2006. A circulação oceânica de larga-escala na região oeste do Atlântico Sul com base no modelo de circulação Global OCCAM. *Revista Brasileira de Geofísica* 24, 209–230. <https://doi.org/10.1590/S0102-261X2006000200005>
- Corell, H., Nilsson, J., Döös, K., Broström, G., 2008. Wind sensitivity of the inter-ocean heat exchange. *Tellus A: Dynamic Meteorology and Oceanography* 61, 635–653. <https://doi.org/10.1111/j.1600-0870.2009.00414.x>
- Crespo, N.M., da Rocha, R.P., Sprenger, M., Wernli, H., 2021. A potential vorticity perspective on cyclogenesis over centre-eastern South America. *International Journal of Climatology* 41, 663–678. <https://doi.org/10.1002/joc.6644>
- Dal Piva, E., Moscati, M.C. de L., Gan, M.A., 2008. Papel dos fluxos de calor latente e sensível em superfície associado a um caso de ciclogênese na Costa Leste da América do Sul. *Revista Brasileira de Meteorologia* 23, 450–476. <https://doi.org/10.1590/S0102-77862008000400006>
- Dereczynski, C.P., Menezes, W.F., 2015. *Meteorologia Da Bacia De Campos, Meteorologia e Oceanografia*. Elsevier Editora Ltda. <https://doi.org/10.1016/b978-85-352-6208-7.50008-8>
- Dong, S., Garzoli, S., Baringer, M., 2011. The Role of Interocean Exchanges on Decadal Variations of the Meridional Heat Transport in the South Atlantic. *Journal of Physical Oceanography* 41, 1498–1511. <https://doi.org/10.1175/2011JPO4549.1>
- Doong, D.J., Chuang, L.Z.H., Wu, L.C., Fan, Y.M., Kao, C.C., Wang, J.H., 2012. Development of an operational coastal flooding early warning system. *Natural*

- Hazards and Earth System Science 12, 379–390. <https://doi.org/10.5194/nhess-12-379-2012>
- Eady, E.T., 1949. Long Waves and Cyclone Waves. *Tellus* 1, 33–52. <https://doi.org/10.3402/tellusa.v1i3.8507>
- Esteban, M., Webersik, C., Shibayama, T., 2010. Methodology for the estimation of the increase in time loss due to future increase in tropical cyclone intensity in Japan. *Climatic Change* 102, 555–578. <https://doi.org/10.1007/s10584-009-9725-9>
- Evans, J.L., Braun, A., 2012. A Climatology of Subtropical Cyclones in the South Atlantic. *Journal of Climate* 25, 7328–7340. <https://doi.org/10.1175/JCLI-D-11-00212.1>
- Falco, M., Li, L.Z.X., Menéndez, C.G., Carril, A.F., 2019. The influence of South American regional climate on the simulation of the Southern Hemisphere extratropical circulation. *Climate Dynamics* 53, 6469–6488. <https://doi.org/10.1007/s00382-019-04940-9>
- Farber, S., 1987. The value of coastal wetlands for protection of property against hurricane wind damage. *Journal of Environmental Economics and Management* 14, 143–151. [https://doi.org/10.1016/0095-0696\(87\)90012-X](https://doi.org/10.1016/0095-0696(87)90012-X)
- Ferreira, R.N., Rickenbach, T.M., Herdies, D.L., Carvalho, L.M. v., 2003. Variability of South American Convective Cloud Systems and Tropospheric Circulation during January–March 1998 and 1999. *Monthly Weather Review* 131, 961–973. [https://doi.org/10.1175/1520-0493\(2003\)131<0961:VOSACC>2.0.CO;2](https://doi.org/10.1175/1520-0493(2003)131<0961:VOSACC>2.0.CO;2)
- Forget, G., Ferreira, D., 2019. Global ocean heat transport dominated by heat export from the tropical Pacific. *Nature Geoscience* 12, 351–354. <https://doi.org/10.1038/s41561-019-0333-7>
- Fortune, M. a., Kousky, V.E., 1983. Two Severe Freezes in Brazil: Precursors and Synoptic Evolution. *Monthly Weather Review*. [https://doi.org/10.1175/1520-0493\(1983\)111<0181:TSFIBP>2.0.CO;2](https://doi.org/10.1175/1520-0493(1983)111<0181:TSFIBP>2.0.CO;2)
- Frank, N.L., Husain, S.A., 1971. The Deadliest Tropical Cyclone in History. *Bulletin of the American Meteorological Society* 52, 438–445. [https://doi.org/10.1175/1520-0477\(1971\)052<0438:tdtcih>2.0.co;2](https://doi.org/10.1175/1520-0477(1971)052<0438:tdtcih>2.0.co;2)
- Fuentes, E.V., Bitencourt, D.P., Fuentes, M.V., 2013. ANÁLISE DA VELOCIDADE DO VENTO E ALTURA DE ONDA EM INCIDENTES DE NAUFRÁGIO NA COSTA BRASILEIRA ENTRE OS ESTADOS DO SERGIPE E DO RIO

- GRANDE DO SUL. *Revista Brasileira de Meteorologia* 28, 257–266.
<https://doi.org/10.1590/S0102-77862013000300003>
- Fujita, T., 1955. Results of Detailed Synoptic Studies of Squall Lines. *Tellus* 7, 405–436.
<https://doi.org/10.3402/tellusa.v7i4.8920>
- Funatsu, B.M., Gan, M.A., Caetano, E., 2004. A case study of orographic cyclogenesis over South America. *Atmosfera* 17, 91–113.
- Gan, M.A., 1992. Ciclogênese e Ciclones sobre a América do Sul.
- Gan, M.A., Ferreira, S.H., Costa, K.R. da, Reboita, M.S., Piva, E.D., 2020. Ciclones em Superfície nas Latitudes Austrais. Parte III: Energética. *Revista Brasileira de Meteorologia* 35, 281–300. <https://doi.org/10.1590/0102-7786352011>
- Gan, M.A., Rao, V.B., 1999. Energetics of the high frequency disturbances over South America. *Revista Brasileira de Geofísica* 17, 20–28. <https://doi.org/10.1590/S0102-261X1999000100003>
- Gan, M.A., Rao, V.B., 1996. Case studies of cyclogenesis over South America. *Meteorological Applications* 3, 359–367. <https://doi.org/10.1002/met.5060030410>
- Gan, Manuel Alonso, Rao, V.B., 1994. The influence of the Andes Cordillera on transient disturbances. *Monthly Weather Review*. [https://doi.org/10.1175/1520-0493\(1994\)122<1141:TIOTAC>2.0.CO;2](https://doi.org/10.1175/1520-0493(1994)122<1141:TIOTAC>2.0.CO;2)
- Gan, Manoel Alonso, Rao, V.B., 1994. The Influence of the Andes Cordillera on Transient Disturbances. *Monthly Weather Review* 122, 1141–1157. [https://doi.org/10.1175/1520-0493\(1994\)122<1141:TIOTAC>2.0.CO;2](https://doi.org/10.1175/1520-0493(1994)122<1141:TIOTAC>2.0.CO;2)
- Gan, M.A., Rao, V.B., 1991a. Surface Cyclogenesis over South America. *Monthly Weather Review*. [https://doi.org/10.1175/1520-0493\(1991\)119<1293:scosa>2.0.co;2](https://doi.org/10.1175/1520-0493(1991)119<1293:scosa>2.0.co;2)
- Gan, M.A., Rao, V.B., 1991b. Surface Cyclogenesis over South America. *Monthly Weather Review* 119, 1293–1302. [https://doi.org/10.1175/1520-0493\(1991\)119<1293:SCOSA>2.0.CO;2](https://doi.org/10.1175/1520-0493(1991)119<1293:SCOSA>2.0.CO;2)
- Gan, M.A., Rao, V.B., 1991c. Surface Cyclogenesis over South America. *Monthly Weather Review* 119, 1293–1302. [https://doi.org/10.1175/1520-0493\(1991\)119<1293:SCOSA>2.0.CO;2](https://doi.org/10.1175/1520-0493(1991)119<1293:SCOSA>2.0.CO;2)
- Garreaud, R.D., Wallace, J.M., 1998. Summertime incursions of midlatitude air into subtropical and tropical South America. *Monthly Weather Review* 126, 2713–2733. [https://doi.org/10.1175/1520-0493\(1998\)126<2713:SIOMAI>2.0.CO;2](https://doi.org/10.1175/1520-0493(1998)126<2713:SIOMAI>2.0.CO;2)

- Garzoli, S., Simionato, C., 1990a. Baroclinic instabilities and forced oscillations in the Brazil/Malvinas confluence front. *Deep Sea Research Part A. Oceanographic Research Papers* 37, 1053–1074. [https://doi.org/10.1016/0198-0149\(90\)90110-H](https://doi.org/10.1016/0198-0149(90)90110-H)
- Garzoli, S., Simionato, C., 1990b. Baroclinic instabilities and forced oscillations in the Brazil/Malvinas confluence front. *Deep Sea Research Part A. Oceanographic Research Papers* 37, 1053–1074. [https://doi.org/10.1016/0198-0149\(90\)90110-H](https://doi.org/10.1016/0198-0149(90)90110-H)
- Gozzo, L.F., da Rocha, R.P., Gimeno, L., Drumond, A., 2017. Climatology and numerical case study of moisture sources associated with subtropical cyclogenesis over the southwestern Atlantic Ocean. *Journal of Geophysical Research* 122, 5636–5653. <https://doi.org/10.1002/2016JD025764>
- Gozzo, L.F., da Rocha, R.P., Reboita, M.S., Sugahara, S., 2014. Subtropical Cyclones over the Southwestern South Atlantic: Climatological Aspects and Case Study. *Journal of Climate* 27, 8543–8562. <https://doi.org/10.1175/JCLI-D-14-00149.1>
- Gramscianinov, C.B., Hodges, K.I., Camargo, R., 2019a. The properties and genesis environments of South Atlantic cyclones. *Climate Dynamics* 53, 4115–4140. <https://doi.org/10.1007/s00382-019-04778-1>
- Gramscianinov, C.B., Hodges, K.I., Camargo, R., 2019b. The properties and genesis environments of South Atlantic cyclones. *Climate Dynamics* 53, 4115–4140. <https://doi.org/10.1007/s00382-019-04778-1>
- Gray, W.M., 1982. Tropical Cyclone Genesis and Intensification, in: *Intense Atmospheric Vortices*. Springer Berlin Heidelberg, Berlin, Heidelberg, pp. 3–20. https://doi.org/10.1007/978-3-642-81866-0_1
- Grimm, A.M., 2003. The El Niño impact on the summer monsoon in Brazil: Regional processes versus remote influences. *Journal of Climate* 16, 263–280. [https://doi.org/10.1175/1520-0442\(2003\)016<0263:TENIOT>2.0.CO;2](https://doi.org/10.1175/1520-0442(2003)016<0263:TENIOT>2.0.CO;2)
- Heinen, A., Khadan, J., Strobl, E., 2019. The Price Impact of Extreme Weather in Developing Countries. *The Economic Journal* 129, 1327–1342. <https://doi.org/10.1111/eoj.12581>
- Hersbach, H., Bell, B., Berrisford, P., Hirahara, S., Horányi, A., Muñoz-Sabater, J., Nicolas, J., Peubey, C., Radu, R., Schepers, D., Simmons, A., Soci, C., Abdalla, S., Abellan, X., Balsamo, G., Bechtold, P., Biavati, G., Bidlot, J., Bonavita, M., de Chiara, G., Dahlgren, P., Dee, D., Diamantakis, M., Dragani, R., Flemming, J., Forbes, R., Fuentes, M., Geer, A., Haimberger, L., Healy, S., Hogan, R.J., Hólm, E., Janisková, M., Keeley, S., Laloyaux, P., Lopez, P., Lupu, C., Radnoti, G., de Rosnay,

- P., Rozum, I., Vamborg, F., Villaume, S., Thépaut, J.N., 2020. The ERA5 global reanalysis. *Quarterly Journal of the Royal Meteorological Society* 146, 1999–2049. <https://doi.org/10.1002/qj.3803>
- Hodges, K.I., 1999. Adaptive Constraints for Feature Tracking. *Monthly Weather Review* 127, 1362–1373. [https://doi.org/10.1175/1520-0493\(1999\)127<1362:ACFFT>2.0.CO;2](https://doi.org/10.1175/1520-0493(1999)127<1362:ACFFT>2.0.CO;2)
- Hodges, K.I., 1995. Feature Tracking on the Unit Sphere. *Monthly Weather Review* 123, 3458–3465. [https://doi.org/10.1175/1520-0493\(1995\)123<3458:FTOTUS>2.0.CO;2](https://doi.org/10.1175/1520-0493(1995)123<3458:FTOTUS>2.0.CO;2)
- Holland, G.J., Lynch, A.H., Leslie, L.M., 1987. Australian East-Coast Cyclones. Part I: Synoptic Overview and Case Study. *Monthly Weather Review* 115, 3024–3036. [https://doi.org/10.1175/1520-0493\(1987\)115<3024:AECCPI>2.0.CO;2](https://doi.org/10.1175/1520-0493(1987)115<3024:AECCPI>2.0.CO;2)
- Hoskins, B.J., Hodges, K.I., 2005. A New Perspective on Southern Hemisphere Storm Tracks. *Journal of Climate* 18, 4108–4129. <https://doi.org/10.1175/JCLI3570.1>
- Hurrell, J.W., Deser, C., 2009. North Atlantic climate variability: The role of the North Atlantic Oscillation. *Journal of Marine Systems* 78, 28–41. <https://doi.org/10.1016/j.jmarsys.2008.11.026>
- Innocentini, V., Caetano Neto, E.D.S., 1996. A Case Study of the 9 August 1988 South Atlantic Storm: Numerical Simulations of the Wave Activity. *Weather and Forecasting* 11, 78–88. [https://doi.org/10.1175/1520-0434\(1996\)011<0078:ACSOTA>2.0.CO;2](https://doi.org/10.1175/1520-0434(1996)011<0078:ACSOTA>2.0.CO;2)
- Irish, J.L., Resio, D.T., 2010. A hydrodynamics-based surge scale for hurricanes. *Ocean Engineering* 37, 69–81. <https://doi.org/10.1016/j.oceaneng.2009.07.012>
- Jones, D.A., Simmonds, I., 1993. A climatology of Southern Hemisphere extratropical cyclones. *Climate Dynamics* 9, 131–145. <https://doi.org/10.1007/BF00209750>
- Koszalka, I.M., Stramma, L., 2019. Current Systems in the Atlantic Ocean, in: *Encyclopedia of Ocean Sciences*. Elsevier, pp. 204–211. <https://doi.org/10.1016/B978-0-12-409548-9.11291-6>
- Kousky, V.E., 1979. Frontal Influences on Northeast Brazil. *Monthly Weather Review* 107, 1140–1153. [https://doi.org/10.1175/1520-0493\(1979\)107<1140:FIONB>2.0.CO;2](https://doi.org/10.1175/1520-0493(1979)107<1140:FIONB>2.0.CO;2)
- Kousky, V.E., Gan, M.A., 1981. Upper tropospheric cyclonic vortices in the tropical South Atlantic. *Tellus* 33, 538–551. <https://doi.org/10.3402/tellusa.v33i6.10775>

- Liebmann, B., Kiladis, G.N., Vera, C.S., Saulo, A.C., Carvalho, L.M. v., 2004. Subseasonal Variations of Rainfall in South America in the Vicinity of the Low-Level Jet East of the Andes and Comparison to Those in the South Atlantic Convergence Zone. *Journal of Climate* 17, 3829–3842. [https://doi.org/10.1175/1520-0442\(2004\)017<3829:SVORIS>2.0.CO;2](https://doi.org/10.1175/1520-0442(2004)017<3829:SVORIS>2.0.CO;2)
- Lionello, P., Trigo, I.F., Gil, V., Liberato, M.M.L., Nissen, K.M., 2016. An analysis of consensus and disagreement among different cyclone tracking methods on the climatology of cyclones in the Mediterranean region 18, 11461.
- Lutgens, F.K., Tarbuck, E.J., 2016. *The atmosphere: an introduction to meteorology*. Pearson.
- Marengo, J.A., 2009. Impactos de extremos relacionados com o tempo e o clima - Impactos sociais e econômicos. *Boletim do Grupo de Pesquisa em Mudanças Climáticas - GPMC* 13, 1–5.
- Marengo, J.A., 2002. The South American low-level jet east of the Andes during the 1999 LBA-TRMM and LBA-WET AMC campaign. *Journal of Geophysical Research* 107, 8079. <https://doi.org/10.1029/2001JD001188>
- Marengo, J.A., Soares, W.R., Saulo, C., Nicolini, M., 2004. Climatology of the Low-Level Jet East of the Andes as Derived from the NCEP–NCAR Reanalyses: Characteristics and Temporal Variability. *Journal of Climate* 17, 2261–2280. [https://doi.org/10.1175/1520-0442\(2004\)017<2261:COTLJE>2.0.CO;2](https://doi.org/10.1175/1520-0442(2004)017<2261:COTLJE>2.0.CO;2)
- Mayhorn, C.B., McLaughlin, A.C., 2014. Warning the world of extreme events: A global perspective on risk communication for natural and technological disaster. *Safety Science* 61, 43–50. <https://doi.org/10.1016/j.ssci.2012.04.014>
- McDonald, W.F., 1935. The Hurricane of August 31 to September 6, 1935. *Monthly Weather Review* 63, 269–271. [https://doi.org/10.1175/1520-0493\(1935\)63<269:THOATS>2.0.CO;2](https://doi.org/10.1175/1520-0493(1935)63<269:THOATS>2.0.CO;2)
- McTaggart-Cowan, R., Bosart, L.F., Davis, C.A., Atallah, E.H., Gyakum, J.R., Emanuel, K.A., 2006. Analysis of Hurricane Catarina (2004). *Monthly Weather Review* 134, 3029–3053. <https://doi.org/10.1175/MWR3330.1>
- Mendes, D., Souza, E.P., Trigo, I.F., Miranda, P.M.A., 2007. On precursors of South American cyclogenesis. *Tellus A: Dynamic Meteorology and Oceanography* 59, 114–121. <https://doi.org/10.1111/j.1600-0870.2006.00215.x>

- Minor, J.E., 1983. Construction tradition for housing determines disaster potential from severe tropical cyclones. *Journal of Wind Engineering and Industrial Aerodynamics* 14, 55–66. [https://doi.org/10.1016/0167-6105\(83\)90010-7](https://doi.org/10.1016/0167-6105(83)90010-7)
- Morrow, B.H., Lazo, J.K., Rhome, J., Feyen, J., 2015. Improving storm surge risk communication: Stakeholder perspectives. *Bulletin of the American Meteorological Society* 96, 35–48. <https://doi.org/10.1175/BAMS-D-13-00197.1>
- Morss, R.E., Demuth, J.L., Lazo, J.K., 2008. Communicating uncertainty in weather forecasts: A survey of the U.S. public. *Weather and Forecasting* 23, 974–991. <https://doi.org/10.1175/2008WAF2007088.1>
- Morss, R.E., Demuth, J.L., Lazrus, H., Palen, L., Barton, C.M., Davis, C.A., Snyder, C., Wilhelmi, O. v., Anderson, K.M., Ahijevych, D.A., Anderson, J., Bica, M., Fossell, K.R., Henderson, J., Kogan, M., Stowe, K., Watts, J., 2017. Hazardous weather prediction and communication in the modern information environment. *Bulletin of the American Meteorological Society* 98, 2653–2674. <https://doi.org/10.1175/BAMS-D-16-0058.1>
- Morss, R.E., Wilhelmi, O. v., Downton, M.W., Grunfest, E., 2005. Flood Risk, Uncertainty, and Scientific Information for Decision Making: Lessons from an Interdisciplinary Project. *Bulletin of the American Meteorological Society* 86, 1593–1602. <https://doi.org/10.1175/BAMS-86-11-1593>
- Murray, R.J., Simmonds, I., 1991a. A numerical scheme for tracking cyclone centres from digital data. Part I: Development and operation of the scheme. *Australian Meteorological Magazine*. <https://doi.org/10.1175/JCLI4203.1>
- Murray, R.J., Simmonds, I., 1991b. A numerical scheme for tracking cyclone centres from digital data. Part II: application to January and July general circulation model simulations. *Australian Meteorological Magazine*.
- Nielsen, D.M., Cataldi, M., Belém, A.L., Albuquerque, A.L.S., 2016. Local indices for the South American monsoon system and its impacts on Southeast Brazilian precipitation patterns. *Natural Hazards* 83, 909–928. <https://doi.org/10.1007/s11069-016-2355-4>
- Nobre, P., Shukla, J., 1996. Variations of Sea Surface Temperature, Wind Stress, and Rainfall over the Tropical Atlantic and South America. *Journal of Climate* 9, 2464–2479. [https://doi.org/https://doi.org/10.1175/1520-0442\(1996\)009<2464:VOSSTW>2.0.CO;2](https://doi.org/https://doi.org/10.1175/1520-0442(1996)009<2464:VOSSTW>2.0.CO;2)

- Nobre, P., Srukla, J., 1996. Variations of Sea Surface Temperature, Wind Stress, and Rainfall over the Tropical Atlantic and South America. *Journal of Climate* 9, 2464–2479. [https://doi.org/10.1175/1520-0442\(1996\)009<2464:VOSSTW>2.0.CO;2](https://doi.org/10.1175/1520-0442(1996)009<2464:VOSSTW>2.0.CO;2)
- Orlanski, I., Katzfey, J., 1991. The Life Cycle of a Cyclone Wave in the Southern Hemisphere. Part I: Eddy Energy Budget. *Journal of the Atmospheric Sciences* 48, 1972–1998. [https://doi.org/10.1175/1520-0469\(1991\)048<1972:TLCOAC>2.0.CO;2](https://doi.org/10.1175/1520-0469(1991)048<1972:TLCOAC>2.0.CO;2)
- Palmeira, A.C.P. de A., Camargo, R. de, Palmeira, R.M. de J., 2015. RELAÇÃO ENTRE A TEMPERATURA DA SUPERFÍCIE DO MAR E A CAMADA DE MISTURA OCEÂNICA SOB A PASSAGEM DE CICLONES EXTRATROPICAIS NO ATLÂNTICO SUDOESTE. *Revista Brasileira de Meteorologia* 30, 89–100. <https://doi.org/10.1590/0102-778620130679>
- Peterson, R.G., Stramma, L., 1991. Upper-level circulation in the South Atlantic Ocean. *Progress in Oceanography* 26, 1–73. [https://doi.org/10.1016/0079-6611\(91\)90006-8](https://doi.org/10.1016/0079-6611(91)90006-8)
- Petterssen, S., Dunn, G.E., Means, L.L., 1955. REPORT OF AN EXPERIMENT IN FORECASTING OF CYCLONE DEVELOPMENT. *Journal of Meteorology* 12, 58–67. [https://doi.org/10.1175/1520-0469\(1955\)012<0058:ROAEIF>2.0.CO;2](https://doi.org/10.1175/1520-0469(1955)012<0058:ROAEIF>2.0.CO;2)
- Petterssen, S., Smebye, S.J., 1971. On the development of extratropical cyclones. *Quarterly Journal of the Royal Meteorological Society* 97, 457–482. <https://doi.org/10.1002/qj.49709741407>
- Pezza, A.B., Ambrizzi, T., 2003a. Variability of Southern Hemisphere Cyclone and Anticyclone Behavior: Further Analysis. *Journal of Climate* 16, 1075–1083. [https://doi.org/10.1175/1520-0442\(2003\)016<1075:VOSHCA>2.0.CO;2](https://doi.org/10.1175/1520-0442(2003)016<1075:VOSHCA>2.0.CO;2)
- Pezza, A.B., Ambrizzi, T., 2003b. Variability of Southern Hemisphere cyclone and anticyclone behavior: Further analysis. *Journal of Climate* 16, 1075–1083. [https://doi.org/10.1175/1520-0442\(2003\)016<1075:VOSHCA>2.0.CO;2](https://doi.org/10.1175/1520-0442(2003)016<1075:VOSHCA>2.0.CO;2)
- Pezza, A.B., Ambrizzi, T., 2000. Propagação de Ondas de Frio na América do Sul e as Trajetórias de Ciclones e Anticiclones Extratropicais. *Anais do XI-CBMET* 3107–3117.
- Pezza, A.B., Simmonds, I., 2005. The first South Atlantic hurricane: Unprecedented blocking, low shear and climate change. *Geophysical Research Letters* 32. <https://doi.org/10.1029/2005GL023390>
- Pezza, A.B., Simmonds, I., Renwick, J.A., 2007. Southern Hemisphere cyclones and anticyclones: Recent trends and links with decadal variability in the Pacific Ocean.

- International Journal of Climatology 1419, 1403–1419.
<https://doi.org/10.1002/joc.1477>
- Pezzi, L.P., Souza, R.B. de, Quadro, M.F.L., 2016. Uma Revisão dos Processos de Interação Oceano-Atmosfera em Regiões de Intenso Gradiente Termal do Oceano Atlântico Sul Baseada em Dados Observacionais. *Revista Brasileira de Meteorologia* 31, 428–453. <https://doi.org/10.1590/0102-778631231420150032>
- Physick, W.L., 1981. Winter depression tracks and climatological jet streams in the Southern Hemisphere during the FGGE year. *Quarterly Journal of the Royal Meteorological Society* 107, 883–898. <https://doi.org/10.1002/qj.49710745409>
- Pianca, C., Mazzini, P.L.F., Siegle, E., 2010. Brazilian offshore wave climate based on NWW3 reanalysis. *Brazilian Journal of Oceanography* 58, 53–70. <https://doi.org/10.1590/S1679-87592010000100006>
- Pinto, J.G., Ulbrich, S., Economou, T., Stephenson, D.B., Karremann, M.K., Shaffrey, L.C., 2016. Robustness of serial clustering of extratropical cyclones to the choice of tracking method. *Tellus, Series A: Dynamic Meteorology and Oceanography* 68. <https://doi.org/10.3402/tellusa.v68.32204>
- Pinto, J.R.D., Reboita, M.S., da Rocha, R.P., 2013. Synoptic and dynamical analysis of subtropical cyclone Anita (2010) and its potential for tropical transition over the South Atlantic Ocean. *Journal of Geophysical Research: Atmospheres* 118, 10,870–10,883. <https://doi.org/10.1002/jgrd.50830>
- Radinovic, D., 1986. On the development of orographic cyclones. *Quarterly Journal of the Royal Meteorological Society* 112, 927–951. <https://doi.org/10.1002/qj.49711247403>
- Ramón-Valencia, J.A., Palacios-González, J.R., Santos-Granados, G.R., Ramón-Valencia, J.D., 2019. Early warning system on extreme weather events for disaster risk reduction. *Revista Facultad de Ingeniería Universidad de Antioquia* 80–87. <https://doi.org/10.17533/udea.redin.20190628>
- Rappaport, E.N., 2000. Loss of Life in the United States Associated with Recent Atlantic Tropical Cyclones. *Bulletin of the American Meteorological Society* 81, 2065–2073. [https://doi.org/10.1175/1520-0477\(2000\)081<2065:LOLITU>2.3.CO;2](https://doi.org/10.1175/1520-0477(2000)081<2065:LOLITU>2.3.CO;2)
- Reboita, M.S., 2008. Ciclones Extratropicais sobre o Atlântico Sul: Simulação Climática e Experimentos de Sensibilidade.

- Reboita, M.S., Ambrizzi, T., Rocha, R.P. da, 2009. Relationship between the southern annular mode and southern hemisphere atmospheric systems. *Revista Brasileira de Meteorologia* 24, 48–55. <https://doi.org/10.1590/S0102-77862009000100005>
- Reboita, M.S., da Rocha, R.P., Ambrizzi, T., Caetano, E., 2010a. An assessment of the latent and sensible heat flux on the simulated regional climate over Southwestern South Atlantic Ocean. *Climate Dynamics* 34, 873–889. <https://doi.org/10.1007/s00382-009-0681-x>
- Reboita, M.S., da Rocha, R.P., Ambrizzi, T., Sugahara, S., 2010b. South Atlantic Ocean cyclogenesis climatology simulated by regional climate model (RegCM3). *Climate Dynamics* 35, 1331–1347. <https://doi.org/10.1007/s00382-009-0668-7>
- Reboita, Michelle Simões, da Rocha, R.P., de Oliveira, D.M., 2018. Key features and adverse weather of the named subtropical cyclones over the southwestern South Atlantic Ocean. *Atmosphere* 10. <https://doi.org/10.3390/atmos10010006>
- Reboita, Michelle S., da Rocha, R.P., de Souza, M.R., Llopart, M., 2018a. Extratropical cyclones over the southwestern South Atlantic Ocean: HadGEM2-ES and RegCM4 projections. *International Journal of Climatology* 38, 2866–2879. <https://doi.org/10.1002/joc.5468>
- Reboita, Michelle S., da Rocha, R.P., de Souza, M.R., Llopart, M., 2018b. Extratropical cyclones over the southwestern South Atlantic Ocean: HadGEM2-ES and RegCM4 projections. *International Journal of Climatology* 38, 2866–2879. <https://doi.org/10.1002/joc.5468>
- Reboita, M.S., Oliveira, D.M., Rocha, R.P., Dutra, L.M.M., 2019. Subtropical Cyclone Anita's Potential to Tropical Transition Under Warmer Sea Surface Temperature Scenarios. *Geophysical Research Letters* 46, 8484–8489. <https://doi.org/10.1029/2019GL083415>
- Redfield, W.C., 1841. VI. Remarks relating to the tornado which visited New Brunswick in the State of New Jersey, June 18, 1835, with a plan and schedule of the prostrations observed on a section of its track. *The London, Edinburgh, and Dublin Philosophical Magazine and Journal of Science* 18, 20–29. <https://doi.org/10.1080/14786444108650237>
- Rehbein, A., Dutra, L.M.M., Ambrizzi, T., da Rocha, R.P., Reboita, M.S., da Silva, G.A.M., Gozzo, L.F., Tomaziello, A.C.N., Campos, J.L.P.S., Mayta, V.R.C., Crespo, N.M., Bueno, P.G., Aliaga Nestares, V.J., Machado, L.T., de Jesus, E.M., Pampuch, L.A., Custódio, M.D.S., Carpenedo, C.B., 2018. Severe Weather Events

- over Southeastern Brazil during the 2016 Dry Season. *Advances in Meteorology* 2018, 1–15. <https://doi.org/10.1155/2018/4878503>
- Resio, D.T., Irish, J.L., 2015. Tropical Cyclone Storm Surge Risk. *Current Climate Change Reports* 1, 74–84. <https://doi.org/10.1007/s40641-015-0011-9>
- Ribeiro, B.Z., Seluchi, M.E., Chou, S.C., 2016. Synoptic climatology of warm fronts in Southeastern South America. *International Journal of Climatology* 36, 644–655. <https://doi.org/10.1002/joc.4373>
- Robertson, F.R., Smith, P.J., 1980. The kinetic energy budgets of two severe storm producing extratropical cyclones. *Monthly Weather Review*. [https://doi.org/10.1175/1520-0493\(1980\)108<0127:TKEBOT>2.0.CO;2](https://doi.org/10.1175/1520-0493(1980)108<0127:TKEBOT>2.0.CO;2)
- Rocha, F.P. da, Aravéquia, J.A., Ribeiro, B.Z., 2016. Estudo de Ciclones e de Padrões de Circulação Atmosférica no Oceano Atlântico Sul Próximo à Costa das Regiões Sul e Sudeste do Brasil Usando Dados da Reanálise do Era-Interim. *Revista Brasileira de Meteorologia* 31, 141–156. <https://doi.org/10.1590/0102-778631220140151>
- Rodrigues, R.R., Woollings, T., 2017. Impact of Atmospheric Blocking on South America in Austral Summer. *Journal of Climate* 30, 1821–1837. <https://doi.org/10.1175/JCLI-D-16-0493.1>
- Rogers, D., Tsirkunov, V., 2010. Coastal and benefits of early warning systems.
- Sahani, J., Kumar, P., Debele, S., Spyrou, C., Loupis, M., Aragão, L., Porcù, F., Shah, M.A.R., di Sabatino, S., 2019. Hydro-meteorological risk assessment methods and management by nature-based solutions. *Science of The Total Environment* 696, 133936. <https://doi.org/10.1016/j.scitotenv.2019.133936>
- SATYAMURTY, P., FERREIRA, C.D.A.C., GAN, M.A., 1990. Cyclonic vortices over South America. *Tellus A* 42, 194–201. <https://doi.org/10.1034/j.1600-0870.1990.00016.x>
- Seluchi, M.E., Garreaud, R.D., 2012. Campos médios e processos físicos associados ao ciclo de vida da Baixa do Chaco. *Revista Brasileira de Meteorologia* 27, 447–462. <https://doi.org/10.1590/S0102-77862012000400008>
- Seluchi, M.E., Marengo, J.A., 2000. Tropical-midlatitude exchange of air masses during summer and winter in South America: climatic aspects and examples of intense events. *International Journal of Climatology* 20, 1167–1190. [https://doi.org/10.1002/1097-0088\(200008\)20:10<1167::AID-JOC526>3.0.CO;2-T](https://doi.org/10.1002/1097-0088(200008)20:10<1167::AID-JOC526>3.0.CO;2-T)

- Seluchi, M.E., Saulo, A.C., 2012. Baixa do Noroeste Argentino e Baixa do Chaco: características, diferenças e semelhanças. *Revista Brasileira de Meteorologia* 27, 49–60. <https://doi.org/10.1590/S0102-77862012000100006>
- Shapiro, M.A., Keyser, D., 1990. Fronts, Jet Streams and the Tropopause, in: *Extratropical Cyclones*. American Meteorological Society, Boston, MA, pp. 167–191. https://doi.org/10.1007/978-1-944970-33-8_10
- Silveira, I.C.A. da, Schmidt, A.C.K., Campos, E.J.D., Godoi, S.S. de, Ikeda, Y., 2000. A corrente do Brasil ao largo da costa leste brasileira. *Brazilian Journal of Oceanography* 48, 171–183. <https://doi.org/10.1590/S1679-87592000000200008>
- Simmonds, I., Key, K., Bye, J.A.T., 2012. Identification and climatology of Southern Hemisphere mobile fronts in a modern reanalysis. *Journal of Climate* 25, 1945–1962. <https://doi.org/10.1175/JCLI-D-11-00100.1>
- Sinclair, M.R., 1996a. A Climatology of Anticyclones and Blocking for the Southern Hemisphere. *Monthly Weather Review* 124, 245–264. [https://doi.org/10.1175/1520-0493\(1996\)124<0245:ACOAAB>2.0.CO;2](https://doi.org/10.1175/1520-0493(1996)124<0245:ACOAAB>2.0.CO;2)
- Sinclair, M.R., 1996b. A Climatology of Anticyclones and Blocking for the Southern Hemisphere. *Monthly Weather Review* 124, 245–264. [https://doi.org/10.1175/1520-0493\(1996\)124<0245:ACOAAB>2.0.CO;2](https://doi.org/10.1175/1520-0493(1996)124<0245:ACOAAB>2.0.CO;2)
- Sinclair, M.R., 1994a. An objective cyclone climatology for the Southern Hemisphere. *Monthly Weather Review*. [https://doi.org/10.1175/1520-0493\(1994\)122<2239:AOCFT>2.0.CO;2](https://doi.org/10.1175/1520-0493(1994)122<2239:AOCFT>2.0.CO;2)
- Sinclair, M.R., 1994b. An objective cyclone climatology for the Southern Hemisphere. *Monthly Weather Review*. [https://doi.org/10.1175/1520-0493\(1994\)122<2239:AOCFT>2.0.CO;2](https://doi.org/10.1175/1520-0493(1994)122<2239:AOCFT>2.0.CO;2)
- Sinclair, M.R., Renwick, J.A., Kidson, J.W., 1997. Low-Frequency Variability of Southern Hemisphere Sea Level Pressure and Weather System Activity. *Monthly Weather Review* 125, 2531–2543. [https://doi.org/10.1175/1520-0493\(1997\)125<2531:LFVOSH>2.0.CO;2](https://doi.org/10.1175/1520-0493(1997)125<2531:LFVOSH>2.0.CO;2)
- Sterl, A., Hazeleger, W., 2003. Coupled variability and air-sea interaction in the South Atlantic Ocean. *Climate Dynamics* 21, 559–571. <https://doi.org/10.1007/s00382-003-0348-y>
- Sutcliffe, R.C., 1947. A contribution to the problem of development. *Quarterly Journal of the Royal Meteorological Society* 73, 370–383. <https://doi.org/10.1002/qj.49707331710>

- SUTIL, U.A., PEZZI, L.P., ALVES, R.C.M., NUNES, A.B., 2019. Ocean-Atmosphere Interactions in an Extratropical Cyclone in the Southwest Atlantic. *Anuário do Instituto de Geociências - UFRJ* 42, 525–535. https://doi.org/10.11137/2019_1_525_535
- Taljaard, J.J., 1967. Development, Distribution and Movement of Cyclones and Anticyclones in the Southern Hemisphere During the IGY. *Journal of Applied Meteorology*. [https://doi.org/10.1175/1520-0450\(1967\)006<0973:ddamoc>2.0.co;2](https://doi.org/10.1175/1520-0450(1967)006<0973:ddamoc>2.0.co;2)
- Trenberth, K.E., 1991. Storm Tracks in the Southern Hemisphere. *Journal of the Atmospheric Sciences* 48, 2159–2178. [https://doi.org/10.1175/1520-0469\(1991\)048<2159:STITSH>2.0.CO;2](https://doi.org/10.1175/1520-0469(1991)048<2159:STITSH>2.0.CO;2)
- Troup, A.J., Streten, N.A., 1972. Satellite-Observed Southern Hemisphere Cloud Vortices in Relation to Conventional Observations. *Journal of Applied Meteorology*. [https://doi.org/10.1175/1520-0450\(1972\)011<0909:soshcv>2.0.co;2](https://doi.org/10.1175/1520-0450(1972)011<0909:soshcv>2.0.co;2)
- Ulbrich, U., Leckebusch, G.C., Pinto, J.G., 2009. Extra-tropical cyclones in the present and future climate: A review. *Theoretical and Applied Climatology* 96, 117–131. <https://doi.org/10.1007/s00704-008-0083-8>
- Venegas, S.A., Mysak, L.A., Straub, D.N., 1996. Evidence for interannual and interdecadal climate variability in the South Atlantic. *Geophysical Research Letters* 23, 2673–2676. <https://doi.org/https://doi.org/10.1029/96GL02373>
- Wang, S.-Y., Chen, T.-C., Takle, E.S., 2011. Climatology of summer midtropospheric perturbations in the US northern plains. Part II: large-scale effects of the Rocky Mountains on genesis. *Climate Dynamics* 36, 1221–1237. <https://doi.org/10.1007/s00382-010-0765-7>
- WHO, W.H.O., WMO, W.M.O., 2012. Atlas of Health and climate. World Health Organization (WHO).
- Woollings, T., Barnes, E., Hoskins, B., Kwon, Y.O., Lee, R.W., Li, C., Madonna, E., McGraw, M., Parker, T., Rodrigues, R., Spensberger, C., Williams, K., 2018a. Daily to decadal modulation of jet variability. *Journal of Climate* 31, 1297–1314. <https://doi.org/10.1175/JCLI-D-17-0286.1>
- Woollings, T., Barnes, E., Hoskins, B., Kwon, Y.O., Lee, R.W., Li, C., Madonna, E., McGraw, M., Parker, T., Rodrigues, R., Spensberger, C., Williams, K., 2018b. Daily to decadal modulation of jet variability. *Journal of Climate* 31, 1297–1314. <https://doi.org/10.1175/JCLI-D-17-0286.1>

